GREEN SYNTHESIS OF ZINC OXIDE NANOPARTICLES USING DIFFERENT PLANT EXTRACTS AND ITS ANTIBACTERIAL ACTIVITY

ABARA, UZOMA CHIDOZIE, BSc (IMSU)
20184142028

A THESIS SUBMITTED TO THEPOST GRADUATE SCHOOL
FEDERAL UNIVERSITY OF TECHNOLOGY, OWERRI

IN PARTIAL FUFILMENT OF THE REQUIREMENTS FOR THE
AWARD OF MASTER OF SCIENCE (MSc) DEGREE IN ENVIRONMENTAL MICROBIOLOGY

MAY, 2021

CERTIFICATION

This is to certify that work **GREEN SYNTHESIS OF ZINC OXIDE NANOPARTICLES USING DIFFERENT PLANT EXTRACTS AND ITS ANTIBACTERIAL ACTIVITY** was carried out by **ABARA, UZOMA CHIDOZIE (20184142028)** in partial fulfillment for the award of an MS_C degree in Environment Microbiology in the department of Microbiology, federal University of technology, Owerri.

.....	23-03-23 .....
Prof. J.N. OGBULIE	**DATE**
(Principal supervisor)	
.....	04-04-23 .....
DR. MRS. E.E. MIKE-ANOSIKE	
(Co-Supervisor)	**DATE**
.....	04/04/2023 .....
Prof. I.E. ADIEZE	**DATE**
(HOD)	
.....	08/05/23 .....
Prof. C.S. ALISI	**DATE**
(Dean, school of biological science)	
.....	.....
PROF. B.O. ESONU	**DATE**
(Dean Post Graduate School)	
.....	5/10/2023 .....
(EXTERNAL EXAMINER)	**DATE**

DEDICATION

I dedicate this work to God almighty, the maker of Heaven and Earth and to my parents Mr. Abara Vincent Obioma and Mrs. Abara Lucy Ngozi and my siblings Abara Ifeanyi, Abara Uchechukwu, Abara Chioma (Blessed Memory), Abara Ugochukwu, Abara Emmanuel and Abara Joseph Onyebuchi.

ACKNOWLEDGMENTS

With sincere gratitude in my heart I would like to thank in a special way my God the impossibility specialist. I want to thank my supervisor Prof. J.N. Ogbulie and Co msupervisor, Dr. Mrs. E.E. Mike-Anosike who never relented in guiding me, and having continual patience throughout the work also for always motivating me in the course of the work. Special thanks to the head of department Prof I.E. Adieze, the post graduate coordinator in the department Prof CambelAkujiobi and all lecturers in the department prof

(mrs) R.N. Nwabueze, prof E.S. Amadi, Prof S.I. Okorondu, Prof C.O. Nwaeke, Prof C.E. Nwanyanwu, Prof W. Braide, Prof I.E. Adieze, Dr. Mrs. C.I. Chikwendu, Dr C.C. Opurum, Dr E. Chinakwe, Dr I.N. Nwachukwu, Dr. Mrs. Mejeha My loving lecturers who have all including the administrative staff who shown immense support in the course of my program.

In a special way I want to thank my lovely parents Mr. Abara Vincent Obioma and Mrs. Abara Lucy Ngozi and my loving brothers Ifeanyi, Uche, Ugochukwu, Emmanuel and Onyebuchi, for their support, prayers and patience, guidance and unending believe in me.

I also want to sincerely appreciate my colleagues and friends for their support, God bless you all.

TABLE OF CONTENTS

Chapter Three

Chapter Four

Chapter Five

LIST OF TABLES

LIST OF FIGURES/CHARTS

ABSTRACT

Nanotechnology is the understanding and control of matter in the 1-100 nm range. Nanomaterials have unique physiochemical properties, such as ultra-small size, large surface area to mass ratio and high reactivity which are different from bulk materials of the same composition. The synthesis of metal oxide nanoparticles with the use of plant extracts is a promising alternative to conventional chemical methods. Zincoxide nanoparticles have received considerable attention due to their unique antibacterial, antifungal and UV filtering properties, high catalytic and photochemical activity. Green synthesis of zincoxide nanoparticles using aqueous plant leaf extracts of Neem *(Azadirachtaindica L*), Bitter leaf (*Vernonia amygdalina L*), Scent leaf (*Ocimumgratissimum L*), Moringa leaf (*Moringaoliefera L*), Ginger lilly (*Costusafer L*) and the antimicrobial activity of green synthesized zincoxide nanoparticles were carried out in this study. Standard top-down method of green synthesis was carried out using the fresh leaves which were pulverised to powdered form ,boiled and finally filtered to get the aqueous extract which was eventually mixed with 1M of zinc nitrate hexahydrate in a 1:1 ratio. The resultant solution was mixed thoroughly with a magnetic stirrer and was further centrifuged, washed and calcinised at 420ºC. Characterization was done using UV-Visible spectroscopy, Fourier Transform infrared spectroscopy (FTIR), X-ray Diffractometer, Scanning Electron Microscopy (SEM) and Energy Dispersive X-ray spectroscopy (EDX) to ascertain the physico-chemical and morphological properties of the zinc oxide nanoparticles. The antimicrobial activity of the ZnO nanoparticle were tested using clinical isolates of *Staphylococcus aureus, Staphylococous epidermidis, Escherichia coli, Klebisiella* species*, Proteus* species and *Pseudomonas aerugenosa*. The UV-Visible spectrum of colloidal solutions had absorbance peaks at 356-369 nm. The Fourier Transform infrared spectroscopy (FTIR) gave band peaks which were characteristic to specific functional groups. The Energy Dispersive X-ray spectroscopy (EDX) showed that the zinc oxide nanoparticles of the five samples contain higher amount of Zn both in atomic concentration, weight concentration and few other elements which showed high rate of purity of the samples, while the SEM and XRD revealed clustered flake-like crystal arrangement of nanorod-like structures. The antibacterial activity revealed zone of clearance on some and little or none zone of clearance on others. *Escherichia coli, Klebisiella* species and *Pseudomonas aerugenosa* recorded higher zones of inhibition. This study reveals another application of the use of nanoparticles in the control of bacterial diseases and could be very suitable for those in animal husbandry and livestock management to reduce drastically the ever growing rate of antibiotic resistance.

Keywords: nanoparticles, green synthesis, ZnO nanoparticle, characterization, antibacterial.

CHAPTER ONE

1.0 INTRODUCTION

1.1 Background of the study

The world suffers from a lot of problems (Setbacks) and one of the major aspects that disturbs the world economy is plant and animal disease. This aspect has led to the loss of plant harvest produce, loss of cash crops, poor form of human life and also loss of human life (Wilkinson *et al*., 2011). It has also affected animals, especially farm animals. These losses can be attributed to poor lifestyle and emergence and re-emergence of plant and animal disease. (Wilkinson *et al*., 2011).

In underdeveloped and developing countries for example Nigeria, the incidence of plant and animal diseases is at an abnormal rise yearly and this can be attributed to poor form of life of the inhabitants. They lack basic amenities like good drinking water, proper health care and also funds for the poor farmers to take proper care of their farm produce. It is also attributed to poor state of farmers and also their ways of life has led to a rise in the rate of both plants and animal disease (Kumar and kalita, 2017). The poor farming practice is of great importance to this abnormal rate of plant and farm animal diseases and pest .This bad and unhealthy conditions has led to distribution of disease of infested plants and plants produce, dead carcass of disease infected farm animals that are unhealthy for human and animal consumption (Kumar and kalita, 2017).

Treatment of plants and animal disease is of paramount importance because of the health risk associated with the consumption of plants and animals infected with various types of microorganisms. Plant disease attracts public attention because they are disease carriers and this will lead to food poisoning, reduction in yield and harvest produce. Animal disease is of public attention as we have a great deal of farm animal and animal produce that are infected

by all sorts of microorganisms. Human are not left out as the spread of diseases has led to increase in mortality rate and led to low productivity (WHO 2009). This disease is caused by different types of microorganisms ranging from bacteria, fungi, parasites, virus and protozoa (Blessy 2014).

There is need to curtail such predicaments from befalling on humans. There are different ways to treat plant, animal and human disease which include: Cutting down, killing and burning of infected plants and farm animals, treatment with chemical insecticides, pesticide, herbicide and antibiotics (Moabiemand *et al.,* 2013).

These convectional techniques used to treat plant and animal diseases as listed above, have setbacks including the abuse of antibiotics which has led to the emergence of antibiotic resistant strains of various microbes. Antibiotic resistant strain emerge because of the improper use or abuse of antibiotics. The resistant microbes use a number of mechanism to confer resistance on themselves like the possession of efflux pumps that help discharge antibiotics as soon as they enter (Shahram *et al.,* 2021). This factor and other related factors has led to researchers trying to proffer other solutions different from antibiotics application in treatment and management of infections and diseases.

Nanotechnology is the use of nanoparticles to solve man's needs. Nanoparticles are particles in the nanorange structure with unique properties for example optical, magnetic, electrical, thermal properties, high surface area and exhibit quantum effect (Luo *et al*., 2015). Nanotechnology has its numerous application for example in medicines used to produce nano drugs, medical devices and tissue engineering (Zhang *et al.*, 2008), in chemical and cosmetics nanoscale chemicals and compounds, paints, coatings, ceramics (Godwin *et al.,* 2015), in food sciences processing, nutracetical food, nanocapsules (Prakash *et al.,* 2019), in environment and energy water and air purification filters, fuel cells, photovoltaic (Godwin *et*

al., 2015), in military and energy biosensors, weapons, sensory enhancement (Miroslav 2019), in electronics semiconductors chips, memory storage, photonica, optoelectronics (Godwin *et al.,* 2015).

The high surface area-to-volume ratio of nanoparticles is an advantage for their use in plant and animal disease management, compared to other convectional means (Luo *et al*., 2015). There are various means of producing nanoparticles, these include the physical synthesis, chemical synthesis and green synthesis (Singh *et al.,* 2018). Amongst the mentioned ways for producing nanoparticles, green synthesis for the production of nanoparticles, has an added advantage over others because it is environmental friendly, cheaper and safe to synthesize (Khadeeja *et al.,* 2016). The photocatalytic process releases excited electrons that can adhere to the nanoparticle, enter the bacteria, fungi, virus (Plant and animal disease causing microorganism), thereby resulting in disinfection and lysis (Palaniyandi *et al.,* 2016).

Metals synthesized from green synthesis are zinc oxide (ZnO), copper (Cu) and copper oxide (CuO), cerium oxide (CeO_2), cadmium sulphide (CdS), Silver (Au) and gold (Ag) (refrence). But in this study the metallic synthesized element used is zinc oxide (ZnO). zinc oxide (ZnO) is a member of the group 2-4 semiconductor family whose covalence is on the boundary between ionic and covalent semiconductors. The intrinsic properties of zinc oxide (ZnO) such as broad range of high photostability, radiation adsorption and large electrochemical coupling coefficient makes it a candidate of choice for a lot of applications including biomedicine (Matinise *et al*., 2017). After the nanoparticle formation characterization is done, different methods have been employed in nanoparticle characterization and they play their respective roles. These methods include, Scanning Electron microscopy: Scanning electron microscopy (SEM) is giving morphological examination with direct visualization. Scanning Electron microscopy examination clarifies the morphology and size of the resultant Nanoparticles. Atomic force microscopy: Atomic force microscopy (AFM) offers ultra-high resolution in

particle size measurement and is based on a physical scanning of samples at sub-micron level using a probe tip of atomic scale (Muhlen *et al*., 1996). Atomic force microscopy provides the most accurate description of size and size distribution and requires no mathematical treatment. Moreover, particle size obtained by Atomic force microscopy technique provides real picture which helps understand the effect of various biological conditions (Polakovic *et al*., 1999). UV–visible spectroscopy: Arrangement of NPs from UV–visible spectroscopy can be studied due of their surface plasmon reverberation assimilation band because of the consolidated wavering of conduction band electrons on the surface of metal nanoparticles in reverberation with light wave (Sathish *et al.,* 2018) and X-ray diffractograms spectroscopy: X-ray diffractograms of nano-materials give an abundance of data from phase creation to crystallite estimate, from cross section strain to crystallographic introduction, XRD is non-contact and non-destructive, which makes it ideal for in situ studies (Sathish *et al.,* 2018)

1.2 STATEMENT OF PROBLEM:

The abuse of antibiotics is on the rise and this has resulted to the development of highly resistant strains of microorganisms.

AIM

The aim of this study focused on the green synthesis of zinc oxide nanoparticles using different plant extracts and its antibacterial activity on some clinical isolates.

OBECTIVES

The specific objective is to determine the effects of:

i. green synthesized[neem plant (*Azadirachta indica*), Bitter leaf (*Vernonia amygdalina*) ,scent leaf (*Ocimum gratissimum*), moringa leaf (*Moringa oliefera*) and ginger lily (*Costus afer*)] zinc oxide (ZnO) nanoparticle on some bacteria isolates;
ii. determine the characteristics of the green synthesized nanoparticles; and
iii. Evaluate the antibacterial potency of the synthesized nanoparticles on some clinical isolates.

JUSTIFICATION

a) Zinc oxide nanoparticle is antimicrobial and has been used to kill some microorganisms.
b) Green synthesis was carried out because of the ease of use and does not by any chance endanger the environment
c) To use green synthesized ZnO nanoparticle as an alternative to antibiotics due to their unique properties such as small size, large surface area, exhibition of quantum effect and ability to have target effect at shorter time.

CHAPTER TWO

2.0 LITERATURE REVIEW

2.1 Overview of nanotechnology

Nanotechnology as the name implies is derived from two Greek words "Nano" and "νᾶνος" through the Latin "nanus" meaning dwarf and, by virtue of extension, very small. Within the convention of International System of Units (SI) it is used to indicate a reduction factor of 10^9 times. So, the nanosized world is typically measured in nanometers (1nm corresponding to 10^{-9} m) and it encompasses systems whose size is above molecular dimensions and below macroscopic ones (generally > 1 nm and < 100 nm). At this size, atoms and molecules work differently, and provide a variety of surprising and interesting uses. (Shuaixuan *et al.,* 2022)

Nanotechnology represents the design, production and application of materials at atomic, molecular and macromolecular scales, in order to produce new nanosized materials (Hahens *et al*., 2007). Nanotechnology is an important field of modern research dealing with synthesis, strategy and manipulation of particles structure ranging from approximately 1 to 100 nm in size. Richard P Feynman first recognized it in early 20th century. On 29 December 1959, a lecture by Richard P Feynman titled "There's plenty of room at the bottom", at the annual meeting of the American Physical Society, opened up a whole new field, known as 'nanotechnology'. He spoke about manipulating and controlling things on a small scale. Nanotechnology may be able to create many new materials and devices with a vast range of application such as energy production, medicine, environmental management and a lot of industrial application (Zhang *et al.,* 2008; Godwin *et al.,* 2015; Prakash *et al.,* 2019).

These particles may or may not be biodegradable. Any material that has at least one dimension in the nanometric range is known as a nanomaterial. Nanometic range in a simpler term can be seen as dimension that is ten thousand times smaller than a single human hair.

In the case of polycrystalline materials, the grain size is typically of the order 1-100 microns (1 micron=10^{-6} m). Nanocrystaline materials have a grain size of the order 101000 times smaller than conventional grain dimensions. When compared to atom size (0.2-0.4 nm in diameter), nanocrystaline grains are still significantly big.

For example, a nanocrystal of 10 nm size contains over a hundred thousand atoms (assuming a spherical nanograin of 10 nm and atomic diamic of 0.2 nm), large enough to exhibit bulk properties. The scales of materials are iustrated in figure 2.1

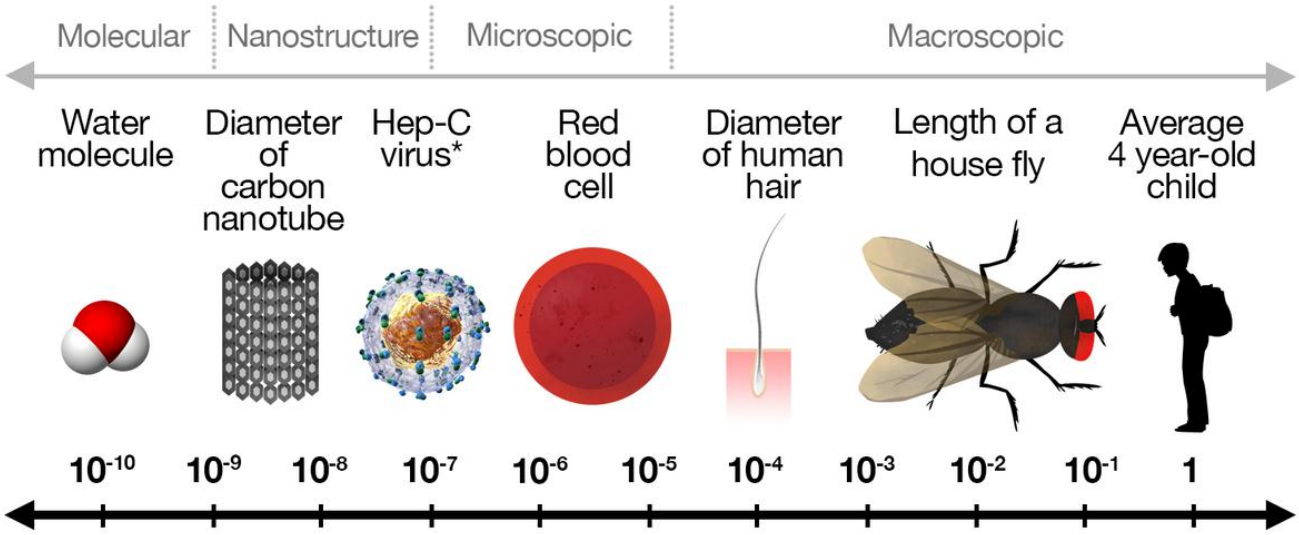

Figure 2.1: Scales of materials.

Source bruceBlaus/wikimedia comons, CC BY-SA 2017

Nanomaterial can be metals, ceramics, polymers, or composites. Nanotechnology is an umbrella term for many areas of research dealing with objects that have one of their dimension in the realm of a few hundreds of nanometers.

2.2 History of Nanotechnology

Norio Taniguchi in 1974 coined the word nanotechnology when he used it to describe simi-conductor process such as thin film deposition and ion beam milling where the features can be controlled at the nanometric level (Hulla *et al.,* 2015). The most widely accepted definition of nanotechnology to date appears on the NASA website. Nanomaterial has been produced and used by humans for as nanostructured is relatively recent. Some ancient glass beautiful red ruby colour paintings is due to gold and silver nanoparticles in Trapped in glass matrix. The decorative glass or metallic film known as "luster" found on some medical pottery contains metallic spherical nanoparticles dispersed in a complex way in the glaze, which gives rise to special optical properties. The technique used to produce there materials were a closely guarded secret and are not completely understood even now (Samer *et al.,* 2020). Carbon black is a nanostructured materials used in car tyres to increase the life of the tyre and impart black colour. This materials was discovered in the 1900's. Fumed silica, a component of silicon rubber, coating, adhesive and sealants, is a nanostructural materials. It became commercially available in 1940's. Steel 1500 years ago is popularly known as wootz this steel was used to make sword and sharp that they could penetrate through a helmet cutting it to pieces. Recently, it was discovered that carbon nanotubes was present in them. It is now believed that the high strength of these steel comes from presence of carbon nanotubes. Based on early application of Nanoparticles, e.g Gold been broken down to its nano form is responsible for the varying colouration in Ancient Roman Lycorus cup (Freestone *et al.,* 2007).

Prominent individuals in Nanoscience or Technology

Richard P. Feynman was first to mention the concept of "Nano" in 1959 lecture (Hulla *et al.,* 2015). Scientist Norio Tainigochi 1974 defined and brought about the term Nanotechnology (Hulla *et al.,* 2015). Eric .K. Drever 1986 published the first book on nanotechnology. Sumio Ijima discovered the carbon nanotubes in 1991 (Hulla *et al.,* 2015). (He was a professor of material science at research centre advanced carbon materials of National institution of advanced industrial science and technology.) Don Eigler 1990 of IBM in almaden and his colleagues used STM to manipulate 35 individual xenon atoms on a nickel surface and formed the letters of the IBM logo (Eigler *et al*., 1990) stodical manipulation of surface atom and the effects on electron of states. Gered Binnig and Heinrinch Rohrer received a noble prize in physics for their design of the STM. This led to the development of atomic force microscope AFM and scanning probe microscope SPM (Binnig *et al*., 1986; Binnig *et al*.,1990) . Richard smalley, Harrold kroto and Robert curl discovered that carbon can also exist in the form of very stable spheres, the fullerenes or buckyballs (Kroto *et al*.,1985). In 1998 Cees Dekker Created a Transistor using carbon nanotubes (Tans *et al.,* 1998). Chad Mirkin 1999 Developed Dip-pen Nanolithography (DPN) (Piner *et al* 1999). In 2004 Andre Geim and Konstantin Novoselov (Discovery of graphene) (Novoselov *et al.,* 2004). In 2009 Nadrian Seeman (DNA structures fold into 3D rhombohedral crystals) (Zheng *et al.,* 2009). In 2010 IBM Developed an ultra-fast lithography to create 3D nano scale textured surface) (Knoll *et al.,* 2010). In 2011 Leonhard Grill (scanning tunneling microscope (STM) describes the electronic and mechanical properties of individual molecules and the polymer chains) (Laerentz *et al.,* 2009) and in 2018 World's smallest tic-tac-toe game board made with DNA (Petersen *et al.,* 2018).

2.3 Methods of nanoparticle synthesis

Nanoparticle synthesis refers to methods for creating nanoparticles. This can be archieved by breaking down larger particles or the accumulation of atoms which are known as top down approach and bottom-up respectively. There are three ways by which nanoparticles can be synthesized they are Physical synthesis, Chemical synthesis (Satyanarayana1 *et al* 2019) and Biological synthesis (Singh *et al.*, 2020)

2.3.1 Physical synthesis: it is the use of physical means to synthesize nanoparticles. It has a lot of approaches as they are listed below;

Pulse laser ablation: this technique involves a high-power pulsed laser beam been focused inside a vacuum chamber to strike a target in the material and plasma is created, which is then converted into a colloidal solution of nanoparticles. Second Harmonic Generation (ND: YAG) type Laser is being used mostly to prepare the nanoparticles. There are many factors that affect the final product such as the type of laser, number of pulses, pulsing time and type of solvent (Satyanarayana1 *et al* 2018).

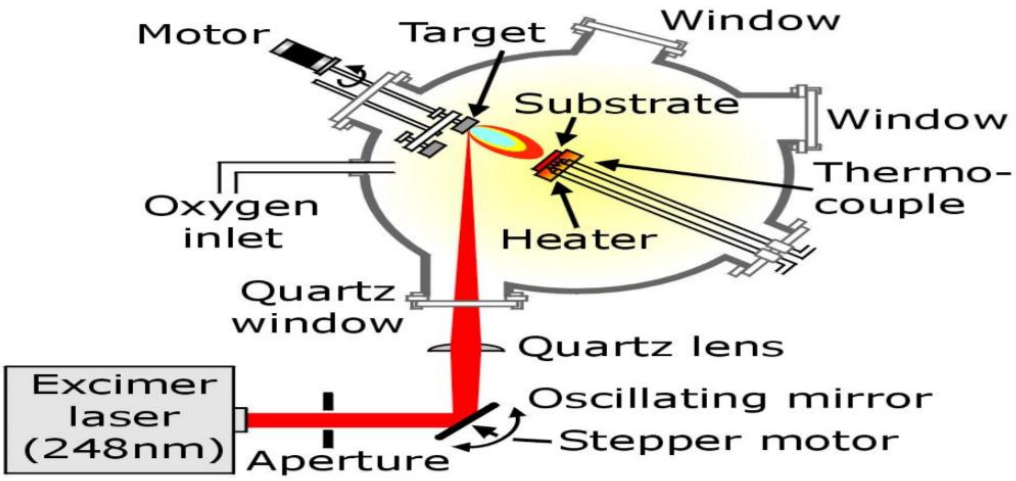

Figure 2.2: A schematic diagram of Pulse laser ablation

Source: Satyanarayana1 *et al.*, 2018.

Mechanical/High ball milling method: This technique was first used by Benjamin for the production of super alloys. Milling is a solid state processing technique for the synthesis of nanoparticles. In the milling process, raw material of micron size is fed to undergo several changes. Different types of mechanical mills are available which are commonly used for the synthesis of nanoparticles. These mills are categorized according to their capacities and applications. Due to mechanical limitations, it is very difficult to produce ultra-fine particles using these techniques or it takes very long time. However, simple operation, low cost of production of nanoparticles and the possibility to scale it to produce large quantities are the main advantages of mechanical milling. The important factors affecting the quality of the final product are the type of mill, milling speed, container, time, temperature, atmosphere, size and size distribution of the grinding medium, process control agent, weight ratio of ball to powder and extent of filling the vial (Satyanarayana1 *et al* 2018).

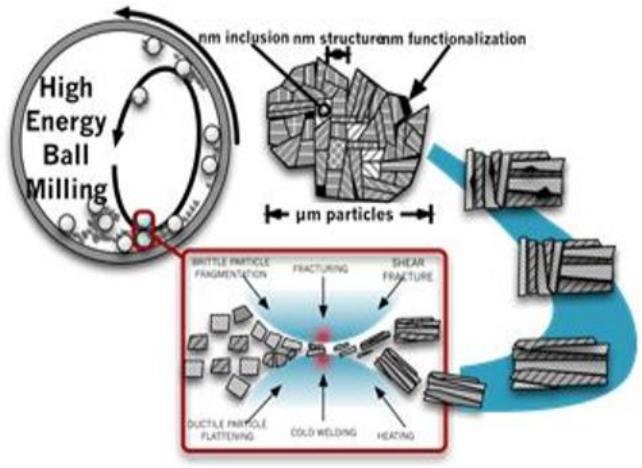

Figure 2.3: A schematic High ball milling method

Source: Source: Satyanarayana1 *et al.*, 2018

Pulsed wire discharge method: Pulsed wire discharge (PWD) is a physical technique used to prepare nanoparticles. Compared to all the other previously mentioned methods, metal nanoparticles synthesis by the Pulsed wire discharge technique follows a completely different mechanism. In Pulsed wire discharge, a metal wire is evaporated by a pulsed current to produce a vapor, which is then cooled by an ambient gas to form nanoparticles. Preparations of metal, oxide and nitride nanoparticles by Pulsed wire discharge has been reported this method have potentially a high production rate and high energy efficiency (Satyanarayana1 *et al* 2018).

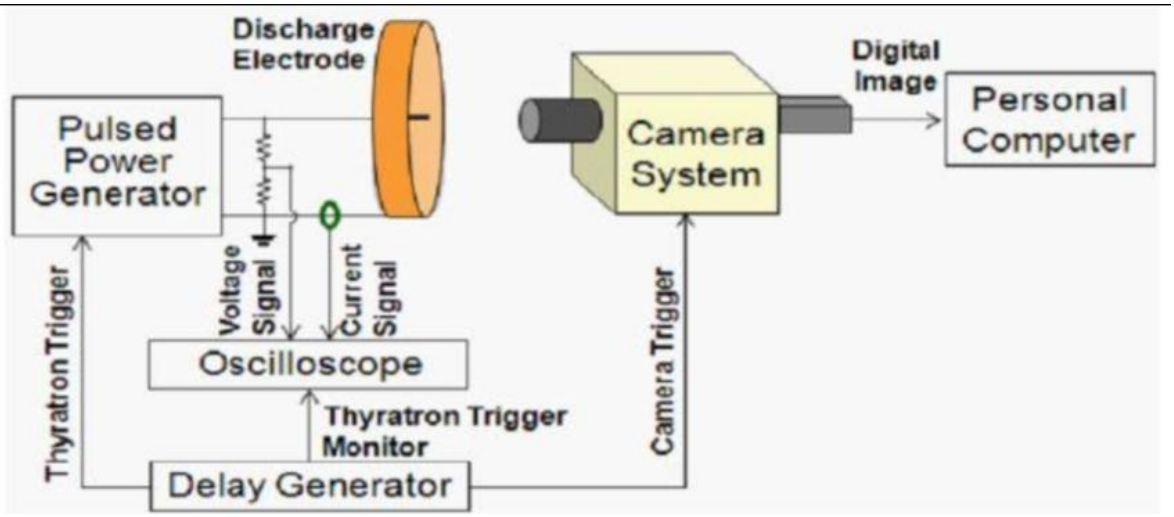

Figure 2.4: A schematic diagram of Pulsed wire discharge.

Source: Source: Satyanarayana1 *et al.*, 2018.

This process is not used conventionally for common industrial purposes because it is very expensive and also impossible to use explicitly for different metals. It is mainly useful for those metals of high electrical conductivity that are easily available in the thin wire form. (Satyanarayana1 *et al* 2018).

2.3.2 Chemical methods

Chemical reduction method: In 1857, Michael Faraday, for the first time reported a systematic study of the synthesis and colors of colloidal gold using chemical reduction route. The chemical reduction of copper salts is the easiest, simplest and the most commonly used synthetic method for copper nanoparticles. In fact, the production of nano sized metal copper particles with good control of morphologies and sizes using chemical reduction of copper salts can be achieved.

Micro emulsion/colloidal method: Hiral et al. (1943) observed that an appropriate amount of water, oil, surfactant and an alcohol or amine-based co-surfactant produced clear and homogeneous solutions that Hirai called Microemulsion. Microemulsion is a technique for the synthesis of nanoparticles in which two immiscible fluids such as water in oil (W/O) or oil in water (O/W) or water in supercritical carbon dioxide (W/Sc. CO_2) become a thermodynamically stable dispersion with the aid of a surfactant. A typical emulsion is a single phase of three components, water, oil and a surfactant. Normally oil and water are immiscible but with the addition of a surfactant, the oil and water become miscible because the surfactant is able to bridge the interfacial tension between the two fluids. Microemulsion consists of surfactant aggregates that are in the ranges of 1 nm to 100 nm. The location of water, oil and surfactant phases affects the geometry of aggregate. The micro-emulsion is said to be oil in water (O/W) if water is the bulk fluid and oil is in less quantity, with small amounts of surfactant. Similarly, the system is said to be water in oil (W/O), if oil is the bulk fluid and water is present in less quantity. The product of oil in water and surfactant (O/W) is

called micelles, which is an aggregate formed to reduce free energy. Hydrophobic surfactants in nanoscale oil and micelles point towards the center of aggregate, whereas the hydrophobic head groups towards water, the bulk solvent. The water in oil Microemulsion carries oil or organic solvent as bulk. The system is thermo dynamically stable and called reverse micelles.(Satyanarayana *et al.,* 2019*)*

Sonochemical method: In this process, powerful ultrasound radiations (20 kHz to 10 MHz) were applied to molecules to enhance the chemical reaction. Acoustic cavitation is a physical phenomenon which is responsible for Sonochemical reaction. This method, initially proposed for the synthesis of iron nanoparticles, nowadays used to synthesize different metals and metal oxides. The main advantages of the Sonochemical method are its simplicity, operating conditions (ambient conditions) and easy control of the size of nanoparticles by using precursors with different concentrations in the solution. Ultrasound power affects the occurring chemical changes due to the cavitation phenomena involving the formation, growth and collapse of bubbles in liquid. The sonolysis technique involves passing sound waves of fixed frequency through a slurry or solution of carefully selected metal complex precursors. In a solvent with vapor pressure of a certain threshold, the alternating waves of expansion and compression cause cavities to form, grow and implode. Sonochemical reactions of volatile organometallics have been exploited as a general approach to the synthesis of various nano phase materials by changing the reaction medium. There are many theories presented by different researchers that have been developed to explain the mechanism of breakup of the chemical bond under 20 KHz ultrasonic radiations. They have explained the sonochemistry process in these theories i.e., how bubble creation, growth and its collapse is formed in the liquid. One of these theories explains the mechanism of breaking of a chemical bond during a bubble collapse. According to one of these theories, bubble collapse occurs at very high temperatures (5000K-25000 K) during the sonochemical process. Upon the collapse of the

bubble, which occurs in less than a nanosecond, the system undergoes a very high cooling rate K/Sec. The organization and crystallization of nano -particles is hindered by this high cooling rate. The creation of amorphous particles is welled fined while the nano structured particles are not clear. The reaction will occur in a 200nm ring surrounding the collapsing bubble if the precursor is a nonvolatile compound. The temperature of the bulk is lower compared to the ring, and temperature of collapsing bubble will be higher than the temperature of the ring. Sonoelectro chemical synthesis employs both electrolytes and ultra - sonic pulses for the production of nanoparticles (Hangxun *et al.*, 2013)

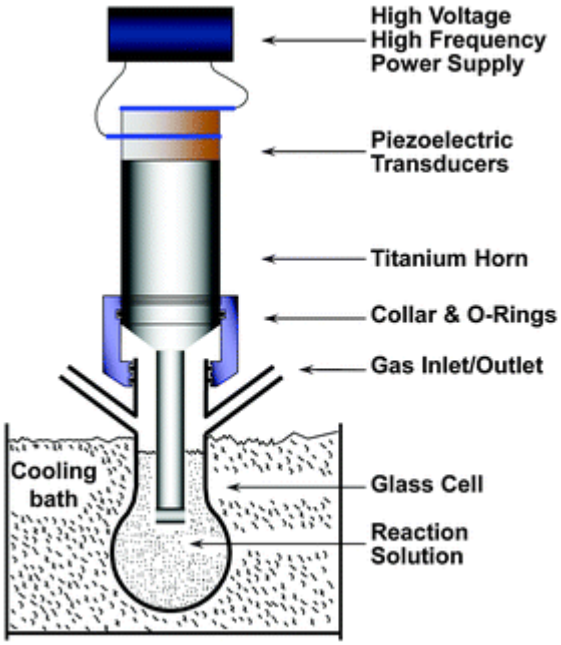

Fig 2.5: A schematic diagram of Sonochemical method.

Source: Hangxun *et al.*, 2013

Electrochemical method: In the electrochemical synthesis method for the production of nanoparticles, electricity is used as the driving or controlling force. Electrochemical synthesis is achieved by passing an electric current between two electrodes separated by an electrolyte. That is, the synthesis takes place at the electrode-electrolyte interface. The main advantages of electro chemical techniques include avoidance of vacuum systems as used in physical techniques, low costs, simple operation, high flexibility, easy availability of equipment and instruments, less contamination (pure product) and environment-friendly process (eco-friendly).Much research work has been done on the electrochemical technique in advancing the basic understanding and industrial applications, but still many aspects of this technique are under study (Garagounis *et al.,* 2014)

Solvothermal decomposition: In the Solvothermal processes, the chemical reaction takes place in a sealed vessel such as autoclave or bomb, where solvents are brought to temperatures that well above their boiling points. When water is used as solvent, it is called a hydrothermal process. There are many advantages in using super critical conditions such as, simplicity, very low grain size, presence of a single phase and synthesis of high purity nanocrystals with high crystallinity and eco friendliness nature (Yuiliang *et al.,* 2017).

2.3.3 Biological synthesis of Nanoparticle

Amongst the above mentioned ways for producing Nanoparticles, green synthesis for the production of Nanoparticles, biological synthesis has an added edge advantage over others because it involves environmental friendly approach.

This method (biological) is preferred over the chemical and physical methods because of the ease of synthesis and also reduction of impurities and better control over size and shape characteristics (Wei *et al.,* 2020). It is also cost friendly. It is divided into 4 parts: namely

nanoparticle synthesis by bacteria, nanoparticle synthesis by fungi, nanoparticle synthesis by algea and nanoparticle synthesis by plants.

Nanoparticle Synthesis by bacteria

Among the vast population of microorganisms, bacteria synthesis of nanoparticle has drawn much attention. Bacteria possess unique ability to reduce heavy metal ions and are among the best candidates for nanoparticle synthesis. For example some bacterial species have developed the ability to resort to specify defense mechanisms to quell stresses like toxicity of heavy metal ions or metals. It was observed that some microorganisms could survive and grow even at high metal ion concentrations (e.g. *Pseudomonas aeruginosa* and *Pseudomonas stutzeri*). Among the great number of natural resources, prokaryotic bacteria have been extensively researched for synthesis of metallic nanoparticles. Because of their relative ease of manipulation "bacterial preference" has been used for nanoparticle synthesis (Slawson *et al*., 1992). Bacteria assisted synthesis of nanoparticles have two routes: extracellular and intracellular approaches. Extracellular synthesis of nanoparticles has advantage over intracellular method in terms of being less time-consuming, since it does not need any downstream process for collection of nanoparticles from the organisms (Singh *et al*., 2016). Bacteria contains reductase enzyme inside the cell that catalyze the reduction of metal ions into metal nanoparticles.

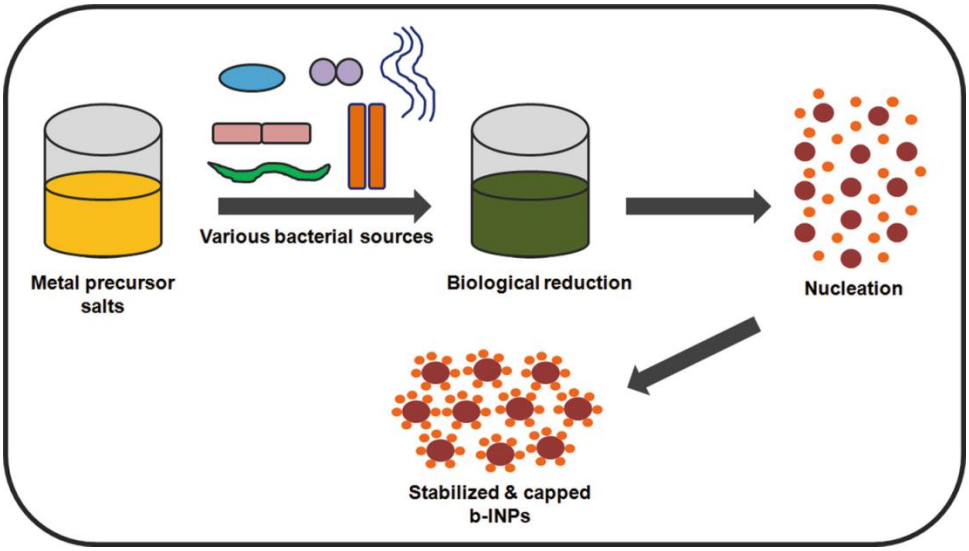

Figure 2.6: bacterial synthesis of metallic nanoparticles

Source: Mukherjee *et al.*, 2019

Naturally, bacteria are frequently exposed to extreme and diverse sometimes environmental situations. To survive in these harsh conditions it depends on their ability to resist the effects of environmental stresses. Natural defense mechanisms exist in bacteria to deal with a variety of stresses e.g toxicity arising from high concentrations of metallic ions in the environment. The major bacterial species used for the synthesis of metallic nanoparticles include *Acinetobacter* sp., *Escherichia coli, Lactobacillus* spp., *Bacillus cereus, Klebsiella pneumoniae*, *Corynebacterium* sp. and *Pseudomonas* sp. (Mohanpuria *et al*., 2008; Prasad *et al.*, 2011; Iravani *et al.*, 2014). Bacteria are known to synthesize metallic nanoparticles by either intracellular or extracellular mechanisms.

Joerger *et al* (2000) reported the first synthesis of silver (Ag) nanoparticles using *Pseudomonas stutzeri* AG259 to synthesize Ag nanoparticles with size less than 200 nm. By 2008, biosynthesis of silver nanocrystals by *B. licheniformis* was studied. Aqueous silver ions were reduced to silver nanoparticles when added to the biomass of *B. licheniformis*. *Pseudomonas stutzeri* AG259 has been reported to fabricate Ag particles (Joerger *et al*., 2000), which are accumulated within the periplasmic space of bacterial cell of 200 nm. Recently studies confirmed that synthesis of Ag can be triggered through liquid mixing process developed in the visible-light spectrum by *Klebsiella pneumoniae* (Mokhtari *et al*., 2009).

Lactobacillus, synthesizes both silver (Ag) and gold (Au) Nanoparticles under standard conditions (Nair *et al*., 2002). Bacteria are also used to synthesize gold nanoparticles. Sharma *et al.,* (2012) reported that novel strain of *Marinobacter pelagius are* applicable for stable formation of, monodisperse gold nanoparticle. Bacterial species like *D. radiodurans* has great antioxidant activity and is highly resistant to radiation and oxidative stress (Li .J. *et al*., 2016). It makes it favourable for use in green synthesis of gold nanoparticles from its ionic

form. The fabricated gold nanoparticles were stable for a longer time and showed better antimicrobial activity. Varshney *et al* (2011) have reported a rapid biological synthesis technique for the synthesis of spherical copper (Cu) nanoparticles using nonpathogenic *Pseudomonas stutzeri*. Prasad *et al* (2007) had reported the use of *Lactobacillus* strains to synthesize the titanium nanoparticles. Sweeney *et al* (2004) demonstrated that *E. coli*, when incubated with cadmium chloride ($CdCl_2$) and sodium sulfide (Na_2S), spontaneously formed cadmium sulfide (CdS) semiconductor nanocrystals. Watson *et al* (1999) demonstrated that sulfate-reducing bacteria synthesize strongly magnetic iron sulfide (FeS) nanoparticles on its surface. , Watson *et al* (1999) demonstrated that sulfate-reducing bacteria synthesize strongly magnetic iron sulfide (FeS) nanoparticles on their surfaces.

Nanoparticle Synthesis by fungi

Fungi can be used to synthesize nanoparticles. The synthesis can be extracellular or intracellular. Fungi are good sources of secondary metabolites and active biomolecules that are of essence for the nanoparticles synthesis. The approach may be bottom up approach or top down approach based on the synthesis. Fungi is an excellent source of various extracellular enzymes. A good number of researchers have chosen fungi over bacteria and plants because of a number of reasons which are: Fungi produce large amounts of protein (enzymes) which catalyze the metal ions hence producing nanoparticles (Rai *et al*., 2009), Isolation and culture is easy as they have simple nutritional requirements. Fungi are easy to manipulate and sustain high flow pressure and agitation. Fungi produce nanoparticles extracellularly. Extracellular synthesis of Ag nanoparticles using *Aspergilus* species has been reported (Gade *et al*., 2008).

There are two strategies for nanoparticle synthesis by fungi

Top down: in this approach nanoscale material is formed from a massive substrate. It involves cutting, etching, grinding by chemical or mechanical methods depending on the basal matter.(Singh *et al*., 2011). Bottom up: in this approach, it involves the construction of structure by self-assembly or possitional assembly into crystals or tubes which is followed by particle synthesis with a nanoscale dimension. Here atoms are gathered/assembled into nanostructure e.g nanotubes (Moghaddam *et al*., 2010). In bottom up approach, there is uniformity and less defects. (Thakkar *et al*., 2010).

The mechanism surrounding the synthesis of nanoparticle using fungi is not generally understood. In the mechanism, heavy metals bind to the fungal cell wall by proteins or present enzymes using the process of electrostatic interactions. The metal ions are reduced by the enzymes that are present in the cell wall. This leads to aggregation of metal ions and thus formation of the nanoparticle (Kashyap *et al*., 2013). A number of researches have been done on the use of fungi (yeast) to synthesize nanoparticles. Silver tolerant yeast strain MKU3 has been used to synthesize Ag nanoparticles which produces nanoparticles in large quantities using the approach of downstream (Kowshik *et al*., 2003). Biosynthesis of gold nanoparticles and silver nanoparticles using the extremophilic yeast strain which was isolated from acid mine drainage as been studied (Mourato *et al*., 2011). The synthesized silver nanoparticles were all well dispersed and also capped by proteins secreted by the yeast. In the biosynthesis of cadmium nanoparticles, *Candida glabrata* and *Schizosacchromyces prome* has been used and reported by Dameroun *et al* (1989). Seshadri *et al* (2011) also reported the biosynthesis of lead sulphide nanoparticles by *Ribosporidium diobovatum* (a lead resistant marine yeast). Of recent Vainshtein *et al* (2014*)* reported that *Sachromyces cerevisiea* and *Cryptococcus humicola* has been harnessed by using them to synthesize magneto sensitive nanoparticles.

Nanoparticle Synthesis by algae: Algae are a diverse group of photoautotrophic, eukaryotic, aquatic, unicellular/multicellular organisms and have been classified on the basis of the pigmentation they release, which includes: brown algae (phaeophytes), red algae (rhodophytes) and green algae (chlorophytes). Algae are commonly used for the biosynthesis of various metallic and metal oxide Nanoparticles, because they grow rapidly, are easy to handle, and their biomass growth. On the average, is ten-times faster than higher plants. Different algal strains have been researched for the green synthesis of different types of Nanoparticles to date.

Brown Algae-Mediated Biosynthesis of Nanoparticles

Brown algae belongs to the order Fucales and family Sargassaceae. The dominant components of Fucales are sterols such as cholesterols, fucosterols, sulfated polysaccharides, and functional groups like glucuroronic acid, muramic acid, alginic acid, and vinyl derivatives which act as reducing as well as capping agents for the synthesis of Nanoparticles. Currently, various metallic (silver and gold) and metal oxide (Zinc oxide and titanium oxide) Nanoparticles have been synthesized from different species of brownalgae (Rajeshkumar *et al*., 2013).

Metallic Nanoparticles such as silver (Ag Nanoparticles), gold (Au Nanoparticles), and copper (Cu Nanoparticles) are some of the most widely synthesized Nanoparticles from brown algae (Azizi *et al.*, 2014; Rajeshkumar *et al*., 2012; Liu *et al*., 2005; Ghodake *et al*., 2011; Rajeshkumar *et al*., 2013). Among different metallic Nanoparticles, more than half of the reported data in literature are about the synthesis of Ag Nanoparticles from different algae strains. This is because the Ag Nanoparticles possess superior physico-chemical characteristics as compared to their bulk forms, thus making them extremely useful in different industries, such as in jewelry, paints, textile, dental alloys, drug-delivery, and

wound-healing .In order to biosynthesize Ag Nanoparticles from brown algae, a variety of species have been reported in literature, such as *Gelidiella acerosa, Turbinaria conoides, Desmarestia menziesii, Sargassum polycystum, Padina pavonica,* and *Cystophora moniliformis* (Azizi *et al*., 2014; Rajeshkumar *et al*., 2012; Liu *et al*., 2005; Ghodake *et al*., 2011; Rajeshkumar *et al*., 2013). In one report, spherical Ag Nanoparticles (96 nm) have been synthesized extracellularly from *T. conoides,* which exhibited tremendous anti-bacterial activity against *Staphylococcus aureus, Staphylococcus epidermis, Escherichia coli, Candida albicans, Aspergillus niger,* and *Pseudomonas aeruginosa* (Rajeshkumar *et al*., 2012). The organic moieties, amines, polyamines, free hydroxyl, and carbonyl groups of Turbinaria species (T. ornate and T. conoides) have been reported to act as reducing agents of precursor silver salts used in the synthesis of Ag Nanoparticles (Khalil *et al*., 2014; Kumar-Krishnan *et al*., 2015).

Among all reported species of brown algae, *T. conoides* is one of the most prominent types that are traditionally used in the generation of Au Nanoparticles. A variety of shapes, like polydispersed, rectangular, spherical, and triangular AuNPs, were generated from T. conoides by extracellular pathway (Khodashenas *et al*., 2019).

Another important species of brown algae, Laminaria japonica, has also been investigated in the green synthesis of Au Nanoparticles. *L. japonica* is a rich source of bio-active components such as polyphenols, peptides, proteins, vitamins, carotenoids, and fibers (Kushnerova *et al*., 2010).

Brown algae have also been reported for biosynthesizing various metal oxide Nanoparticles, such as zinc oxide nanoparticles (ZnO Nanoparticles) and titanium oxide nanoparticles (TiO_2 Nanoparticles) (Sirelkhatim, *et al*., 2015). According to one study, ZnO nanoparticles were synthesized by mixing dried algal powder from S. muticum with distilled water and heated until completely mixed, then zinc acetate salt solution was added, and it was placed on

continuous stirring for hours until the generation of Nanoparticles. The synthesized ZnO nanoparticles were hexagonal in shape, ranging from 35 to 57 nm in size, and were capped by bioactive functional groups like sulfate, amines, hydroxyl, and carbonyl (Azizi *et al*., 2014; Azizi *et al*., 2017).

I. Red Algae-Mediated Biosynthesis of nanoparticles:

Red algae belong to the family Rhodophyta and are primarily used as food in many countries due to their unique flavour and the richness of several important vitamins and proteins. These vitamins and proteins could be the best contenders for reduction and stabilization in algae-mediated biosynthesis of Nanoparticles. However, the synthesis of nanoparticles from seaweed red algae is still in the developmental stages due to of its self-aggregation, slow crystallization growth, and stability issues (Singaravelu *et al*., 2007; Ramakritinan *et al*., 2020). Among various red algae strains, *Porphyra vietnamensis* is one of the most evident species which has been reported numerous times for synthesis of various types of nanoparticles, due to the presence of a strong reducing agent, such as sulfated polysaccharides, that contain anionic disaccharides units, comprised of 3-linked-d-galactosyl residues flashing with 4-linked 3,6-anhydro-l-galactose and 6-sulfate residues (Rao *et al.*, 2007; Venkatpurwar *et al*., 2011). A number of red algae strains have been reported in literature for the biosynthesis of Ag Nanoparticles, such as *Kappaphycus alvarezii, Palmaria decipiens, Gelidiella acerosa, Gracilaria dura, Kappaphycus* spp e.t.c.

II. Blue-green algae Mediated Biosynthesis of nanoparticles:

Blue-green algae belong to the order of Chroococcales, which has two families of Chroococcaceae and Entophysalidaceae. The members of these two families are distinguished by their growth habitat forming colonies (Mosulishvili *et al*., 2007). They grow in dense patterns as parenchymatous cell masses found on moist rocks. Blue-green algae are photoautotrophic in nature, as they use water as an electron donor and contain two photo-

pigments, chlorophyll a and carotene, which help in photosynthesis. On the basis of their morphology, they are also considered counterparts of unicellular bacteria (Khan *et al*., 2019). Unlike brown and red algae, blue-green algae have also been widely exploited for the synthesis of various types of nanoparticles.

The major contributor of Ag Nanoparticles by blue-green algae is *Spirulina platensis*. *S. platensis* is free floating, filamentous cyanobacteria that has multicellular trichomes with one open end and left-handed helix (Mukherjee *et al*., 2002). *S. platensis* has also shown its contribution in the biosynthesis of Au Nanoparticles. Various researchers have reported the *S. platensis*-mediated extracellular synthesis of spherical, octahedral, and cubic Au Nanoparticles, showing the involvement of proteins and peptides as reducing agents (Kalabegishvili, *et al*., 2012; Iravani, *et al*., 2018). Besides monometallic nanoparticles, *S. platensis* has also been reported in the biosynthesis of bimetallic Nanoparticles, such as core shell Ag-Au Nanoparticles and magnetic crystalline-shaped silica-nanoparticles with the help of extracellular proteins (Govindaraju *et al*., 2008; Murugesan *et al*., 2017). Chlamydomonas reinhardtii, another important fresh-water green algae species, was also reported to be involved in the formation of cadmium sulfide bimetallic nanoparticles (CdS Nanoparticles) (Rao *et al*., 2017).

III. Green Micro Algae-Mediated Biosynthesis of nanoparticles

Micro green algae belong to the order Cladophorales and have been extensively used in various industrial, health, and biotechnological applications. They are important source of many essential components, such as phenols, alkaloids, carbohydrates, flavonoids, and functional groups that act as reducing and stabilizing agents in micro-mediated biosynthesis of nanoparticles (Yousefzadi *et al*., 2014). The primarily metabolites involved in the biosynthesis of metallic nanoparticles from green micro algae are proteins, peptides, cyclic

compounds, and carboxylic acids (Castro *et al.*, 2013; Kannan *et al.*, 2013; Beganskien *et al*., 2004).

Silver nanoparticles (Ag Nanoparticles) are the most extensively in-vitro generated nanoparticles from different species of micro green algae. Similar to Silver nanoparticles (Ag Nanoparticles), a number of data have been published in recent years on green micro algae-mediated biosynthesis of gold nanoparticles (Au Nanoparticles). *Pithophora crispa* from higher altitude is one of the most widely exploited species of micro algae involved in the biosynthesis of nanoparticles (Au Nanoparticles). Apart from Ag Nanoparticles and Au Nanoparticles, micro green algae have also been used for the synthesis of Semiconductor Nanoparticles. Many attempts have been done to synthesize silicon nanoparticles from micro green algae.

IV. Green Macro Algae-Mediated Biosynthesis of nanoparticles

Green macro algae are also known as bio-factories for the synthesis of metallic nanoparticles, reason is that they possess numerous valuable compounds which are responsible for reduction and capping of nanoparticles (Singh *et al*., 2013; Priyadharshini, *et al*., 2014). In recent years, various green macro algae strains have been extensively used in the generation of metallic nanoparticles. *Ulva fasciata* is one of most useful green macro algae species, and was utilized to generate nano-sized silver colloids (El-Rafie *et al*., 2013). In another report, *Gracilaria edulis* (rich in amide, carboxylic, and nitro compounds) was used for the synthesis of spherical silver nanparticles (AgNPs) and octahedral zinc oxide (ZnONPs) (Priyadharshini *et al*., 2014; Madhiyazhagan, *et al*., 2017). *Chaetomorpha linum*, another important species of seaweed green macro algae, has been also used for the synthesis of silver nanoparticles (Priyadharshini, *et al* 2014). Besides silver nanoparticles, gold nanoparticles have also been synthesized by green macro algae species such as *Prasiola crispa* and *Rhizoclonium fontinale* (Dhanalakshmi *et al.*, 2012; Parial *et al* 2014).

a) Nanoparticle Synthesis by plants

This is one of the most used approach among the majority of the green synthesizing nanoparticles. Plant assisted synthesis of nanoparticles has more efficiency in terms of obtaining a higher yield than the microbial synthesis. In this approach, leaves, stem, bark, flower or fruit of plants are used for the synthesis. Nanoparticles synthesized from plant sources were found to be much more stable than those formed by microbes and fungus (Singh *et al.,* 2016) Synthesis of Nanoparticles from plant extract is comparatively a cheaper method and it results in higher yield due to presence of larger amount of phytochemicals in plant extract that can either stabilize or reduce the metal ions into metal Nanoparticles (Mohammadinejad *et al.,* 2019). The plant part of interest is first washed after which it is macerated into finer particles and the extract is gotten from the plant after some procedures. The extract from the plant leaf can be obtained very simply to use and has numerous metabolites that act as reducing agents to synthesize nanoparticles (Prathna *et al*., 2010). Different factors such as pH, temperature, contact time, metal salt concentration and phytochemical profile of the plant leaf particles affect the nanoparticles goodness, nanoparticle stabilization, quantity produced, and yield rate. The metal ion reduction in plants is faster than that in fungi and bacteria, as they need a long time for incubation because of the presence of water-soluble phytochemicals (Jha *et al*., 2009).

The plant extract(aqueous/ethanoic) contains a wide range of phytochemicals which act as the primary compounds of plants such as amino acids (Shao *et al*., 2004), citric acid (Yehia *et al*., 2014), flavonoids (Shankar *et al*., 2003), phenolic compounds (Sivaraman *et al*., 2009), terpenoids (Thakkar *et al*., 2010), heterocyclic compounds (Huang *et al*., 2007), enzymes (Narayanan *et al*., 2011), peptides (Tan *et al*., 2010), polysaccharides (Park *et al*.,2011], saponins (Arunachalam *et al*., 2013), and tannis (Huang *et al*., 2011) are responsible for the

metal ion reduction. The whole organs/tissues (Kumar *et al*., 2009; Marchiol *et al*., 2012) or the extracts of the organs/tissues and different parts (e.g., seeds, leaves, barks, roots, and fruits) of the plants are utilized for the green synthesis of nanoparticles and may produce nano-objects with several properties (Rai *et al*., 2008; Kharissova *et al*., 2012).

The numerous phytochemicals present in the plant leaf extracts can be extracted facilely (Thamima *et al*., 2015; Benelli *et al*., 2015), so the plant leaf extracts are considered as a wonderful tool for Metalic nanoparticle synthesis.

The advantage of plant leaf extracts to act as stabilizing agents and reducing agents facilitates the nanoparticle synthesis (Malik *et al*., 2014). Biomedical reducing agents are present at different concentrations in different types of leaf extracts, so the leaf extract composition has a great effect on the nanoparticle synthesis (Mukunthan *et al*., 2012; Li *et al*., 2011). Terpenoids, flavones, ketones, amides, aldehydes, and carboxylic acids are the essential phytochemicals involved in the nanoparticle synthesis (Prathna *et al*., 2010).

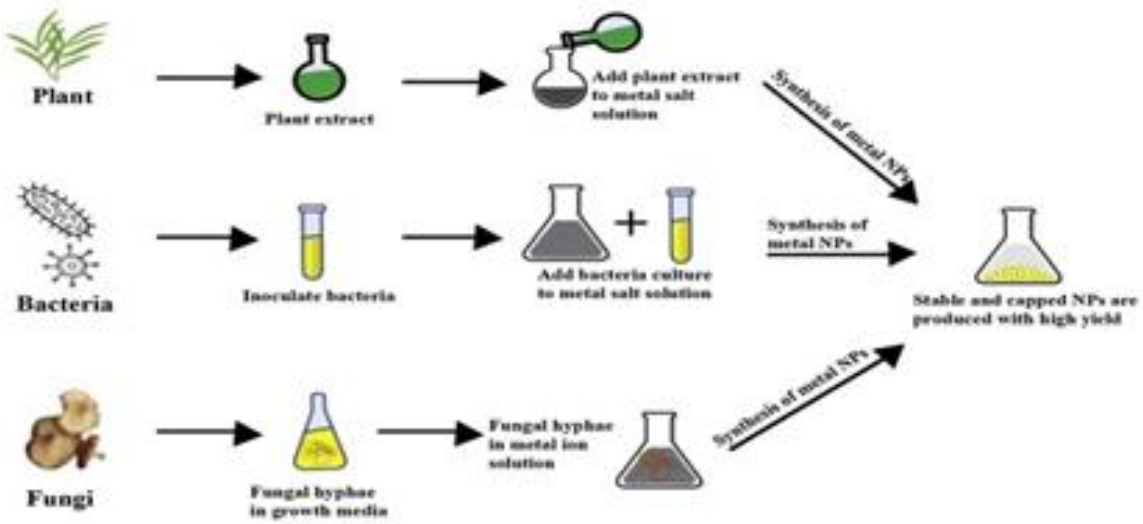

Figure. 2.7. Pictorial representation for green synthesis of metallic nanoparticles from plant, bacteria and fungi.

Source: Singh *et al*., 2020

2.4 Zinc (Zn)

Zinc makes up one of the basic elements that makes up our planet as it makes up about 75ppm(0.0075%) of the earth crust , this alone makes it the 24th most abundant element. zinc is found in all natural waters ,soil and also the atmosphere .it is an important trace element in both animals and the life of plants . it is found in rocks and also in the normal soils in proportion of 20-200mg/kg and 1-30mg/kg respectively . sea water contains 1-27µg/L and uncontaminated fresh water contains <10µg/L. Zinc minerals of commercial importance are listed in the table below.

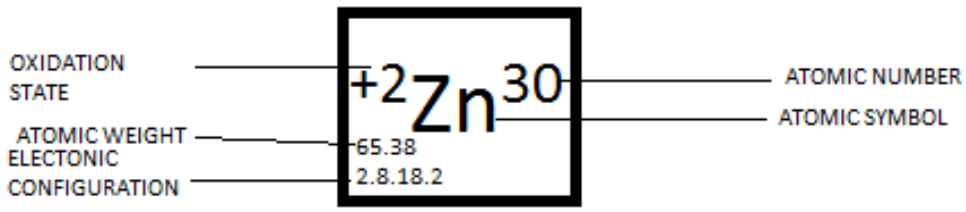

Zn is a group II B of the period table. Zn has an atomic weight of 65.38, atomic number of 30 and electronic configuration of 2-8-18-2. Atomic radius of 11.31^{o}A.

Zinc has five stable isotopes which are Zinc-64, 66, 67, 68 and 70 of which constitute 48.86% 27.62%, 4.12%, 18.71% and 0.69% respectively of the whole. Six radioactive isotopes have so far been identified Zn-62-63-65-69-72 and 73. The most commonly used artificial isotopes are Zn 65 and Zn 69 which have half-lives of about 244 days for the Zn 65, 14 hours for Zn-69 isomer and 58 minutes for Zn-69 itself.

Based on the structure, Zn exhibits a hexagonal close packed lattice. Zinc is a reactive metal which combines readily with non oxidizing acids releasing hydrogen and forming zinc salts. It also dissolves in bases to form Zincate ions $(ZnO_2)_2$. Zinc reacts with oxygen on heating, producing zinc oxide. It also reacts directly with halogens, sulphur and other non-metals. Zinc readily form salts after interacting with other chemicals due to its high reactivity. zinc salts can be divided into inorganic and organic zinc compounds. Inorganic zinc compunds can be further classified into water soluble (zinc sulphate, zinc chloride) and water insoluble (zinc oxide, carbonates, phosphates, silicates and organic complexes). Zinc acetate is used in wood preservation, also as a mordant in dying and also in painting or porcelain. Zinc carbonate is used as nutritive supplement for swine, sheep and poultry. Zinc chloride is used as a mordant in printing and dying textiles also in vulcanizing rubber. Zinc chromate is used as a wood preservative and also on metal surfaces for protection against corrosion. Zinc phosphate is used in dental cement. Zinc phosphide is used in preparation of pesticides e.g rat or mice poison. Zinc sterate is used in tablet manufacture as drying lubricant. Zinc sulphate is used as a mordant in wood preservation. Zinc silicate is used in television screens. Zinc thiocyanate is used in dying.

Medically zinc deficiency leads to loss of appetite, anemia, slow wound healing, skin condition such as acne or eczema, abnormal taste and smell, depressed growth, hair loss, diarrhea and in pregnancy may increase the chance of a difficult or prolonged birth. On the other hand an excess of zinc or high intake of zinc may lead to nausea, vomiting, stomach pains, headache and diarrhea. It may also suppress copper adsorption according to a study in biological trace elements. Research has it that that excess of zinc may also lead to development of kidney stones. (Nazanin *et al.*, 2013)

2.5 ZINC OXIDE

It is an inorganic compound which in powdered form is white in nature, odourless and it is insouluble in water. It has a molar mass of 81.406 g/mol, has a desity of 5.606 g/cm^3. Has a melting point and boiling point of 1974 ^oC, geometry is tetrahedral and a wurtzite crystal structure. Zinc oxide is a simple compound which consists of one atom of oxygen and one atom of zinc respectively. Historically it was first used as a pigment in paint box where it has been cropped up since the mid-1800. Zinc oxide produces a strong, good white pigment which forms the basis of the Chinese white colour and also it gives paper a white bright colour. It is also used in the makeup industry as it forms a bulk basis of the popular mineral makeups.it works better when mixed with other pigment for example lead oxide.

Occurance: zinc oxide occurs naturally in zincate but it is not extractable because of its exixtence in small quantity. Zinc oxide is a mineral that is more likely to form sulphide than oxides because of the chalophile nature, to this reason zinc oxide is produced from sulphide ore. Firstly it is extracted (zinc metal), then it is being vaporized to react with oxygen in the air, this method dates back to the roman times where zinc oxide produced this way was used to react with copper to produce brass. Zinc oxide is mostly used in rubber manufacture, to make durable, it needs to pass through the vulcanization which means adding cross-linkage to the natural polymer chain in the material. The process is done using activators which is zinc oxide or steric acid. Although some rubbers have zinc oxide as the main agent of vulcanization.

Zinc oxide is also used in the cement industry and in ceramic glazing as it helps in crack reduction. Zinc oxide is also used as a way to get dietary zinc into enriched foods e.g. dietary zinc into breakfast cereals, it is also used in cigarette filters and also used in pressurized water nuclear reactors to help reduce corrosion.

2.6 ACTION OF ZINC OXIDE NANOPARTICLE ON MICROBES

The exact mechanism which ZnO nanoparticles employ to cause antimicrobial effect is not yet clearly known and it is still a debated topic. However there are various theories on the action of ZnO Nanoparticles on microbes to cause a microcidal effect. The impact of zinc oxide on biological function depends on its morphorlogy, particle size, exposure time, concentration, pH, and biocompactability (kwaja *et al*., 2011).

It is known that zinc oxide nanoparticles inhibit the growth of microorganisms by permeating into the cell membrane. The oxidative stress initiated by the ZnO nanoparticle damages carbohydrates, lipids, proteins, and DNA (Kelly *et al*., 1998). Lipid peroxidation is crucial because it leads to alteration in cell membrane which results to disruption of vital cellular functions (Rikans *et al*., 1997). It has been reported that the bactericidal effect of Escherichia coli by oxidative stress mechanism involving zinc oxide nanoparticle (Zhang *et al*., 2007). For bulk zinc oxide suspension, external generation of H_2O_2 has been suggested to describe the anti-bacterial properties (Sawai *et al*., 1998). Also, the toxicity of nanoparticles, releasing toxic ions, has been considered. Since zinc oxide is amphoteric in nature, it reacts with both acids and alkalis giving Zn^{2+} ions.

$$ZnO + 2HCl \xrightarrow{\text{acidic medium}} ZnCl_2 + H_2O$$

$$ZnO + 2NaOH \xrightarrow{\text{basic medium}} Na_2ZnO_2 + H_2O$$

$$ZnCl_2 \xrightarrow{\text{aqueous medium}} Zn^{2+} + 2Cl^{-}$$

The free Zn^{2+} ions immediately bind with the biomolecules such as proteins and carbohydrates, and all vital functions of bacteria cease to continue.

Scanning electron microscopy and Transmission electron microscopy images have shown that zinc oxide nanoparticles damage the bacterial cell wall (Zhang *et al*.,2007; Adams *et*

al.,2006) and increase permeability followed by their accumulation in *E. coli* preventing their multiplication (Brayner *et al*., 2006).

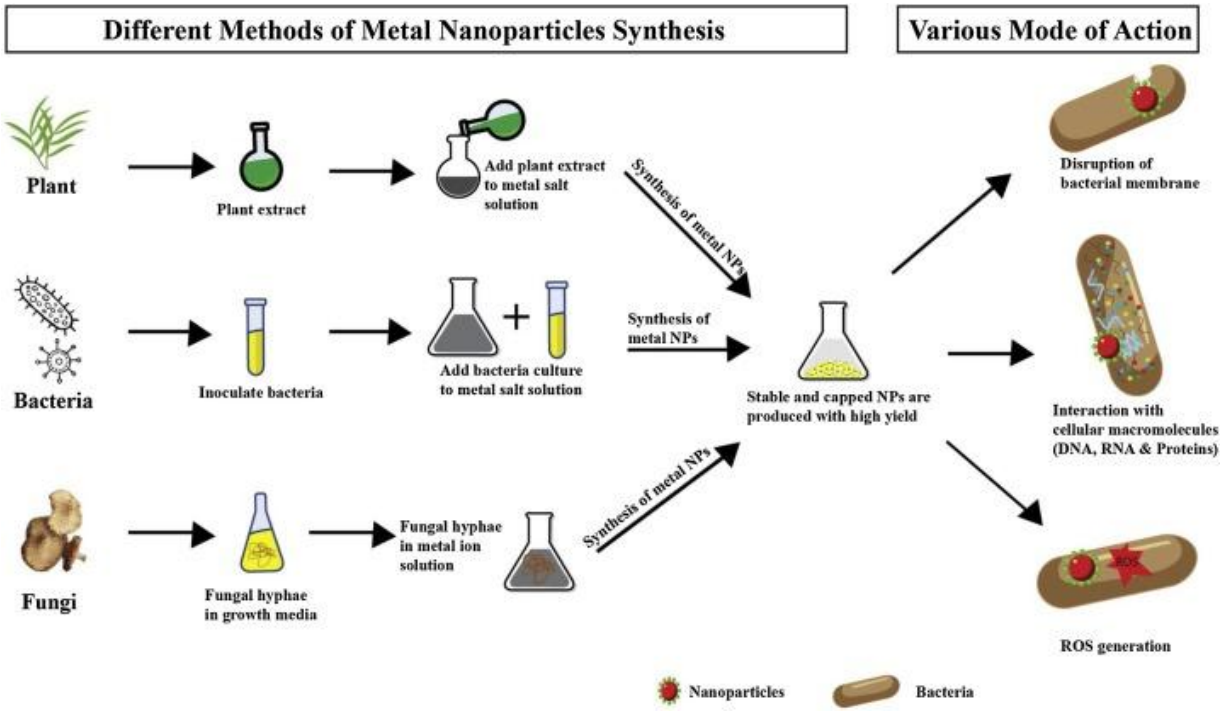

Figure 2.8: various mode of action of nanoparticle on microorganism.

Source : *Singh et al.*, 2020

In the recent past, antibacterial activity of zinc oxide nanoparticle has been investigated against four known gram-positive and gram-negative bacteria, namely *Staphylococcus aureus, E. coli, Salmonella typhimurium*, and *Klebsiella pneumoniae*. It was observed that the growth-inhibiting dose of the zinc oxide nanoparticles was 15 μg/ml, although in the case of *K. pneumoniae*, it was as low as 5 μg/ml (Brayner *et al*., 2006; Stoimenov *et al*., 2002). It has been noticed that with increasing concentration of nanoparticles, growth inhibition of microbes increases. It has been reported that the metal oxide nanoparticles first damage the bacterial cell membrane and then permeate into it (Stoimenov *et al*., 2002). (Premanathan *et al.,* 2011) have reported the toxicity of zinc oxide nanoparticles against prokaryotic and eukaryotic cells. Two mechanisms of action have been proposed for the toxicity of zinc oxide nanoparticles, which are Generation of ROS and Induction of apoptosis.

Metal oxide nanoparticles induce ROS production and put the cells under oxidative stress causing damage to cellular components, i.e., lipids, proteins, and DNA (Lovric *et al*., 2005; Xia *et al*., 2006; Long *et al*., 2006). Zinc oxide nanoparticles, therefore, induce toxicity through apoptosis. They are relatively more toxic to cancer cells than normal cells, although they cannot distinguish between them.

Recently Pati *et al.,* (2014) have shown that zinc oxide nanoparticles disrupt bacterial cell membrane integrity, downregulate the transcription of oxidative stress-resistance genes, and reduces cell surface hydrophobicity in bacteria. They help enhance intracellular bacterial killing by inducing ROS production. These nanoparticles disrupt biofilm formation and inhibit hemolysis by hemolysin toxin produced by pathogens.

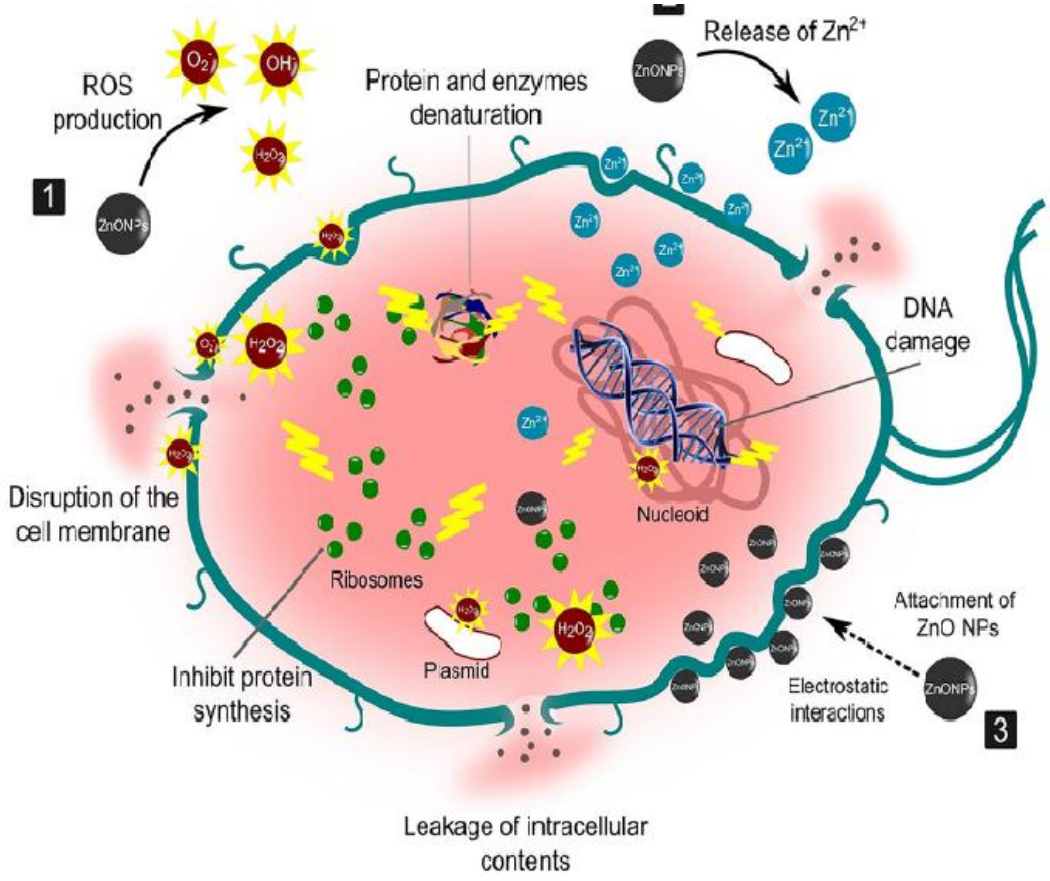

Figure 2.9: Schematic illustration of the antimicrobial mechanism of ZnO NPs against bacterial cells. ZnO NPs act as an antimicrobial agent through the following mechanisms:
(1) the formation of reactive oxygen species (ROS), which induces oxidative stress and membrane and DNA damage,resulting in bacterial death;
(2) dissolution of ZnO NPs into $Zn^{2+,}$ which interferes with enzyme, amino acid, and protein metabolisms in bacterial cells; and
(3) direct interaction between ZnO NPs and cell membrane through electrostatic forces that damages the membrane plasma

Source: Hidayat *et al*., 2019

2.7 TOXICITY OF ZINC NANOPARTICLES

The unique physical and chemical properties of zinc oxide nanoparticles makes them excellent candidates for a number of day to day activities and also the antimicrobial and antiinflamatory properties make them excellent candidates for many purpose in the medical field. However there are reports and studies that suggest that nano zincoxide can allegedly cause adverse effects on humans as well as the environment. zinc oxide is easily absorbed in the body and it results to elevated level of zinc in the human liver, pancrease and adipose tissue(Umrani and Paknikar *et al*., 2014.). In different cell lines it induces different effects:

a) Human bronchial epithelium, normal cell line and alveolar cell line.(BEAS-2B and A549): It initiates intracellular Ca^{2+} flux, loss of membrane intergrity and also a reduction in mitochondrial membrane potential(George *et al*., 2010). Reduced Zn^{2+} dissolution rate and also cytotoxicity occurs on exposure to iron-doped nanoparticles. Zinc oxide nanoparticles alter cytotoxicity, IL-8 generation and AP-1 and NFkB activation in A549 cells (cho *et al.,* 2012). ZnO nanorods are considered as more toxic to cells than the sperical shaped ones (Hsiao and Huang *et al*., 2010). Submerged and air liquid interface ZnO nanoparticles exposure results in altered IL-8 and HO-1 mRNA expression (Lenz *et al*., 2009) in A549 cells.

b) Dermal cell lines

Because of the overuse in sunscreen lotions, it alters p53 and phospho-p38 expressions in human dermal fibroblasts (Meyer *et al*., 2011). It also leads to altered tubular structures in human keratinocytes (Kocbek *et al*., 2010), it also leads to non-activation of inflammasome in primary human keratinocytes (Yazdi *et al.*, 2010).

c) Cells of the immune system

When zinc oxide enters the body, it is ingested by macrophages, monocytes and dentric cells. Increased cytotoxicity and oxidative stress have been reported to occur in the monocytes than the lymphocytes and the severity of the cytotoxicity and the ROS levels depend on the zinc oxide nanoparticle size (Hanley *et al*., 2009). ZnO nanoparticle is reported to induce the production of interferon (IFN)-γ , tumor necrosis factor (TNF)-α and IL-12 in peripheral blood mononuclear cells. it also induces expression of IL-1β and chemokine CXCL9 in murine bone marrow-derived dendritic cells and RAW 264.7 murine macrophages (Palomaki *et al*., 2010). it also involves the loss of membrane intergrity and reduced mitochondrial membrane potential.

d) Colon cell lines

Due to the presence of ZnO in our toothpaste, there is accumulation of zincoxide nanoparticle in the digestive tract, reduced cell viability ,increased H_2O_2/OH , depolarization of the inner mitochondrial membrane, apoptosis and IL-8 release are all reported to occur in L_OV_O human colon carcinoma cells in the presence of zinc oxide nanoparticles (De Berardis *et al*., 2010)

e) In other cell lines

It has been reported to reduce cell viability and contractability in the human airways smooth muscle cells (Bernten *et al.*, 2010)

CHAPTER THREE

3.1 MATERIALS AND METHODS

3.2 Reagents

Fresh plants leaf, zinc nitrate hexahydrate ($ZN_2N0_3.6H_20$), barium chloride (BaCl), sulphuric acid (H_2SO_4), oxoid sensitivity disc nutrent agar.

3.3 Equipment

Centrifuge, magnetic stirrer, hot air oven, incubator, bijou bottles, petri dishes,erlenmeyer flask ,industrial blender, test tubes, wire loop, water bath, fourier transform infared radioscopy machine, ultraviolet–visible spectroscopy, x-ray diffractogram spectroscopy , scanning electron microscopy (SEM) , energy dispersive x-ray spectroscopy (EDX).

3.4 Plants leaf used

Sample 1: neem plant (*Azadirachta indica L*) (Hausa name: Dogon yaro), (Igbo name: Akun shorop), (Youruba name: Dongoyaro),

Sample 2: Bitter leaf (*Vernonia amygdalina L*), (Hausa name: Ganye mai daci), (Chusar doki), (Igbo name: Onugbu, Olugbu, Olibi, Olubu), (Youruba name: Ewuro, Ewuoro jije)

Sample 3: scent leaf (*Ocimum gratissimum L*), (Hausa name: Doddoya), (Igbo name: Nchanwu), (Youruba name: Efirin)

Sample 4: Moringa leaf (*Moringa oliefera L*), (Hausa name: Zogale), (Igbo name: Okwe oyibo), (Youruba name: Igbale, Igi, Iyanu)

Sample 5: Ginger lily (*Costus afer L*), (Hausa name:kakizawa), (Igbo name:Opete, Okpoto), (Youruba name: Tete-egun)

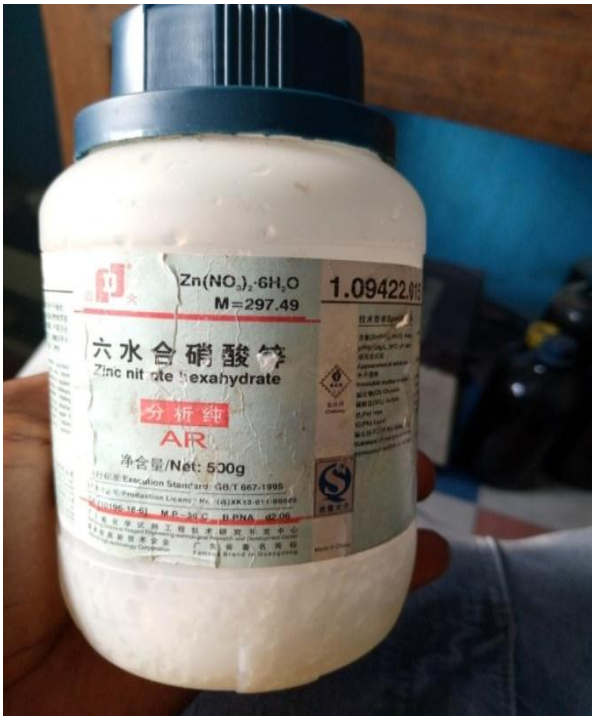

Plate 3.1: Stock zinc nitrate hexahydrate $Zn_2N0_3.6H_20$

Plate 3.2: Dried scent leaf

Plate 3.3: Dried ginger lily

Plate 3.4: Dried moringa leaf

Plate 3.5: Dried bitter leaf

Plate 3.6: Dried neem samples

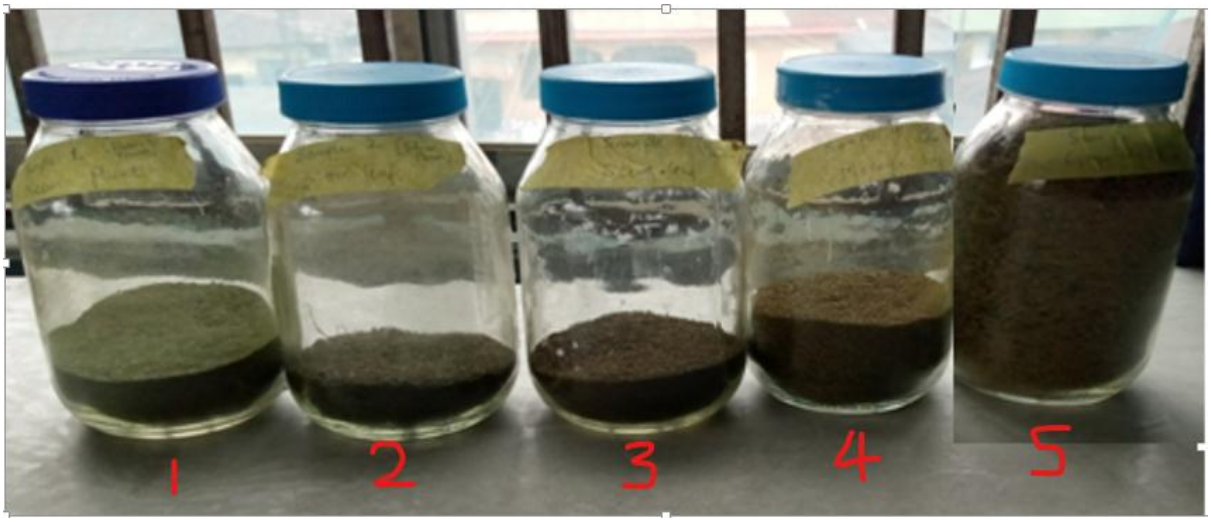

Plate 3.7: From left to right. Dried and grounded

Sample 1: neem plant (*Azadirachta indica L*)

Sample 2: Bitter leaf (*Vernonia amygdalina L*)

Sample 3: scent leaf (*Ocimum gratissimum L*)

Sample 4: Moringa leaf (*Moringa oliefera L*)

Sample 5: ginger lilly (*Costus afer L*)

3.5 Sample collection

Plant leaves were collected at Iheagwa market, Owerri metropolis, Imo state, Nigeria.

3.6 Preparation of plant aqueous extract

Freshly cut leaves were washed thoroughly with running tap water and allowed to dry at room temperature. The dried leaf was blended using a laboratory industry blender to mersh the leaf to powdered form. Then 5 g of the grounded leaf was soaked in 100 ml Erlenmeyer flask (Demissie *et al.,* 2020). The solution was pretreated by boiling it for 15 minutes (Ashwini *et al.,* 2021). The solution was filtered using Whatman No. 1 filter paper and the obtained supernatant solution was used as a plant extract (sample). The leaf extract was allowed to cool to room temperature. (Sharmila *et al.,* 2014)

Plate 3.8: plant leaf aqueous extract

3.7 BIOSYNTHESIS OF ZINC OXIDE

Zinc nitrate hexahydrate was used for the synthesis. A ratio of 1:1 of 1.0 M zinc nitrate hexahydrate $Zn_2N0_3.6H_20$ and plant extracts were mixed in seprate flasks. (50 ml of plant leaf extract was mixed with 50 ml of 1 M zinc nitrate hexahydrate $Zn_2N0_3.6H_20$). The solution was subjected to continuous heating and stirring at 100 rpm for 4 hrs. The resultant solution was purified by centrifugation for 20 mins. The resultant solution was calcinized and the pellets were stored in an amber coloured bottle. (Agakwal *et al.*, 2019)

3.8 COLLECTION AND STANDARDIZATION OF BACTERIA ISOLATES

Pure cultures of the test organisms were collected from Everight laboratory in Owerri metropolis, Imo state in Nigeria and taken to the lab for further standardization. The test isolates includes; *Staphylococcus aureus, Staphylococous epidermidis, Escherichia coli, Klebisiella* species, *Proteus* species, *Pseudomonas aerugenosa*. The test organisms (bacteria) were standardized using McFarland standard 1.5x 10^8 cfu/ml. A McFarland standard is a chemical solution of barium chloride and sulfuric acid. The chemical reaction between these two chemicals results in the production of a fine precipitate of barium sulfate. After shaking well, the turbidity of a McFarland standard was visually comparable to a bacterial suspension of known concentration. McFarland turbidity standards were prepared by mixing various volumes of 1% sulfuric acid and 1% barium chloride to obtain solutions with specific optical densities. by adjusting the volume of these two chemical reagents, McFarland standards of varying degrees of turbidity can be prepared which represent different bacterial density or cell counts. Zero point five (0.5) McFarland turbidity standard provides an optical density comparable to the density of a bacterial suspension with a 1.5 x 10^8 colony forming units (CFU/ml). (Gayathiri *et al.*, 2018). Zero point five (0.5) McFarland standard was prepared by adding 1% BaCl (0.05 ml) in 1% H_2SO_4 (9.95 ml) which result to 1.5x 10^8 cfu/ml

approximately in cell density. Zero point five (0.5) McFarland standard is the most common used standard for antimicrobial susceptibility testing. The test organism was put in a freshly prepared broth and left for 12-18 hours. After which the cloudish broth was put in well labeled tubes and spinned after which it was washed two times (2x) using sterile water. Then the washed organism was compared visually with the McFarland standard visually by adding water until it marches the McFarland standard.

3.7 PREPARING THE NANOPARTICLE STOCK

In preparation of the stock solution of nanoparticle of 5000 µg/ml, 0.1 gram of the green synthesized nanoparticle was dissolved in 20 ml of sterile water (solvent).

It was further reconstituted into different concentrations

1000µg/ml

$x = \frac{1000(\text{given concentration})\text{x}10(\text{ml of test tube})}{5000 \text{ of stock}}$ = 2 ml of stock to be dissolved in 8ml of sterile water

2000µg/ml

$x = \frac{2000(\text{given concentration})\text{x}10(\text{ml of test tube})}{5000 \text{ of stock}}$= 4 ml of stock to be dissolved in 6ml of sterile water

3500µg/ml

$x = \frac{3500(\text{given concentration})\text{x}10(\text{mlof test tube})}{5000 \text{ of stock}}$= 7 ml of stock to be dissolved in 3mls of sterile water.

After achieving the different concentrations, filter paper was cut into circular disc of 6 mm and put into the different tubes containing the different concentrations and allowed to set for 16-24 hours for incoporation of the nanoparticle into the paper disc. Each disc was weighed based on w/v content and it was calculated that 15 µl was incorporated into each disc of various solutions. The discs was allowed to dry and stored in sterile containers till it is ready for use.

3.8 Preparation of media, innoculation of microorganisms and application of the nanoparticle incoporated paper discs.

The media used for the sensitivity testing was nutrient agar and it was prepared in an aseptic environment to avoid contamination. Nutrient agar was prepared according to standard methodology. Application of the paper disc containing the different concentrations of the synthesized nanoparticle follow afterwards. The paper discs are well placed and evenly spread and put in the incubator for 16-24 hours. (ref)

3.9 Chacterization of zinc oxide nanoparticles

3.9.1 Ultraviolet-visible analysis

The Uv analysis spectrometry works basically on the principle of light absorption by the molecules present in sample solution. The UV radiation has a wavelength of range 10–400 nm and the visible region has a wavelength of approximately 400–800 nm (Yang and Legallais, 1954; Rocha *et al*., 2018). On absorption of energy at a range of 200–800 nm, the molecules undergo vibration at its atomic level, and there will be a change in energy in their electronic levels. The boost in energy excites the electron from a ground state to an excited state. (that is $E > E0$), and this absorbed energy is mostly converted into heat and is later

emitted as secondary radiation (Zhang *et al*., 2019). This complete radiation absorption can be obtained as an absorption spectrum.

Thus, the total change in energy can be described as:

$\Delta E = h\upsilon = h(c/\lambda)$

where

ΔE = Change in energy

h = Plank's constant = 6.6256 × 1036 js

c = Speed of light = 3.8×10^8 cm/s

λ = wavelength.

The absorption of the molecules in the solution is measured in optical density (OD). More molecules in the solution more will be the absorption and thus more is the optical density. That is, the solution will appear to be turbid when it has a higher OD, but experimental results vary with the colloidal samples. This is where the molar absorption coefficient comes into play. Molar absorption coefficient is defined as the absorbance of a solution containing 1 mol/L of absorbing particles per centimeter area. It can be calculated by using the BLB law, regression analysis, absorbance values, and isosbestic points. Certain molecules emit fluorescence when energy is absorbed. In such cases, the increase in transmittance due to increased light can be measured by the detector (Sommer, 2012). Generally, to measure the absorption spectra, the algorithm is made based on this formula (Rocha *et al*., 2018).

$\text{Log}A = \text{Log}\, l + \text{Log}\, \varepsilon + \text{Log}\, c$

Based on characterization UV-Visible spectroscopy is used to observe the rate of reduction in metal and further biosynthesis of nanoparticles. Many researchers have used a UV spectrometer as a tool to characterize the novel and synthetic nanoparticles.

Arrangement of nanoparticles from ultraviolet–visible spectroscopy can be studied due of their surface plasmon reverberation assimilation band because of the consolidated wavering of conduction band electrons on the surface of metal Nanoparticles in reverberation with light wave.(ref)

3.9.2 X-Ray Diffractogram spectroscopy

The X-ray diffractograms of nano-materials give an abundance of data from phase creation to crystallite estimate, from cross section strain to crystallographic introduction, XRD is non-contact and non-destructive, which makes it ideal for *in situ* studies. When an electrically charged particle with adequate energy is forced to decelerate, then a shorter wavelength electromagnetic radiation is emitted. These are called X-rays. The XRD is a technique used to resolve the tertiary crystal structures at the atomic level (Sapsford *et al*., 2011). The technique is performed by maintaining high voltage between the electrodes and due to this, the electrons are forced toward metal targets placed in the chamber. Later, after deceleration, the low wavelength X-rays are emitted and radiate in many directions. These rays are collimated together and directed on to the sample, which is already present in the powdered form. These diffracted rays are later observed using the detector. The scan of XRD can be obtained by performing multiple diffractions with varied angles between the sample, source, and detector. The results give information about the element proportions if the sample is in the mixed form. They are helpful in understanding the degree of crystallinity and structure (Epp *et al.,* 2016). The X-ray interacts with the atomic planes to undergo partial beam shift and the rest of them scatter or undergo diffraction. But the scattering occurs only if the X-ray impinges the crystal

lattice. Thus, each element diffracts X-ray in a different way, depending on their size, shape, and atomic arrangement in the lattice (Bragg *et al*., 1913). Bragg's equation explains the angle of diffraction as:

$2dSin\theta = n\lambda$

where

d = Distance between planes

θ = Angle of incidence

n = Integer

λ = Beam wavelength

Debye Scherrer's equation to find the diffraction peak from XRD is

$D = k\lambda/\beta cos\theta$,

where D is the crystallite size (nm);

k is a constant (~0.89);

λ is the wavelength of the X-ray (λ = 0.15406 nm);

Ɵ is Bragg diffraction angle, and

β is the broadening of the diffraction peak measured at half of its maximum intensity (in radians) (Atchudan *et al*., 2019). The diffraction technique uses an X-ray beam and a detector as its major parts where a divergent slit is placed between the beam and sample and another slit between the detector and sample, to limit the scattered radiations while collimating the beam. The X-ray diffraction analysis (XRD) is a technique used to determine the crystallographic structure of the synthesized ZnO nanoparticles. XRD works by irradiating a

material with incident X-rays and then measuring the intensities and scattering angles of the X-rays that leave the nanoparticle. The XRD is used to observe the size, shape, and structure of crystalline materials, but it has low intensity compared to the electron diffraction technique (Epp *et al*., 2016)

3.9.3 Scanning Electron Microscopy (SEM)

In contrast to the light microscope that uses the glass lens and light beam, SEM uses an electromagnetic lens and an electron beam of shorter wavelength. A single electron beam is directed on the specimen, which in turn emits the low energy X-ray light called the cathodoluminescence (Johal *et al*., 2011). Its functions are similar to the transmission electron microscope. The surface of the specimen is scanned by the high voltage beam of electrons using the scanning coils. When the electron hits the specimen, the secondary electrons are either backscattered or emitted. These backscattered secondary electrons are recorded to show the topographic details of the specimen, on the fluorescent screen. Thus, the SEM is used to record images of 10–12 nm. Simply, it helps to identify the size, shape, aggregation, and dispersion of the nanoparticles. Scanning electron microscopy (SEM) gives morphological examination with direct visualization. Scanning electron microscopy examination clarifies the morphology and size of the resultant nanoparticles.

3.9.4 Fourier Transform Infrared Radioscopy Analysis (FTIR)

It is a technique based on the measurement of the absorption of electromagnetic radiation with wavelengths within the mid-infrared region (400–4000 cm^{-1}). If a molecule absorbs IR radiation, the dipole moment is somehow modified and the molecule becomes IR active. A recorded spectrum gives the position of bands related to the strength and nature of bonds, and specific functional groups, providing thus information concerning molecular structures and interactions.

Table 3.1: Selected infrared vibrational assignments for some of the most common groups present on the surface of nanoparticles

Vibrational modes	Frequency (cm^{-1})
Methyl C–H *asym*/*sym* stretch	2970–2950/2880–2860
Methyl C–H *asym*/*sym* bend	1470–1430/1380–1370
C═C alkenyl stretch	1680–1620
Aromatic C–H stretch	3130–3070
O–H hydroxyl group, H-bonded OH stretch	3570–3200 (broad)
C–O stretch, primary alcohol	~1050
N–H aliphatic primary amine, NH stretch	3400–3380, 3345–3325
N–H primary amine, NH bend	1650–1590
C–N, primary amine, CN stretch	1090–1020
Carboxylate	1610–1550/1420–1300
Organic phosphates (P═O stretch)	1350–1250
Aliphatic phosphates (P–O–C stretch)	1050–990
Sulfonates	1365–1340/1200–1100
Organic siloxane or silicone (Si–O–Si)	1095–1075/1055–1020
Organic siloxane or silicone (Si–O–C)	1100–1080
Thiols (S–H stretch)	2600–2550
Thiol or thioether, CH_2–S– (C–S stretch)	710–685
Aliphatic chloro-compounds, C–Cl stretch	800–700
Ammonium ion	3300–3030/1430–1390

Source: (Coates *et al.*, 2006)

3.9.5 Energy Dispersive X-Ray (EDX)

Energy dispersive X-ray spectroscopy (EDX) is an analytical technique used for the elemental analysis or chemical characterization of a sample. It is one of the variants of X-ray fluorescence spectroscopy which relies on the investigation of a sample through interactions between electromagnetic radiation and matter, analyzing X-rays emitted by the matter in response by hitting the charged particles. Its ability to characterize are due in large part to the fundamental principle that each element has a unique atomic structure allowing X-rays that are characteristic of an element's atomic structure to be identified uniquely from one another. To stimulate the emission of characteristic X-rays from a specimen, a high-energy beam of charged particles such as electrons or protons or a beam of X-rays is focused onto the sample being studied (Sathish *et al.,* 2018). At rest, an atom within the sample contains ground state (or unexcited) electrons in discrete energy levels or electron shells bound to the nucleus. The number and energy of the X-rays emitted from a specimen can be measured by an energy dispersive spectrometer. As the energy of the X-rays are characteristic of the difference in energy between the two shells, and of the atomic structure of the element from which they were emitted. This allows the elemental composition of the specimen to be measured (Sathish *et al.,* 2018).

3.10 Estimation of zone of clearance

The disc diffusion method was used. Generally, the reservoir is a filter paper disc, which is placed on top of an agar source which has already been inoculated with a loop full of microorganism isolate that in turn has been standardized. The nanoparticle bactericidal activity was measured using a meter rule around the filter paper disc if there is any visible zone of clearance. The diameter of the zone of inhibition is measured in millimeters (mm). This describes the antimicrobial potency of the nanoparticle solution.

CHAPTER FOUR

RESULTS

4.1 Characterization

4.1.1 Fourier Transform Infrared Radioscopy Analysis (FTIR)

A recorded spectrum gives the position of bands related to the strength and nature of bonds, and specific functional groups, providing the information concerning molecular structures and interactions The IR spectral for the ZnO nanoparticles is presented in Figures 4.1 – 4.5, while the data and assignment are presented in Table 4.1.

Table 4.1 shows the IR spectra for the different plant leaves synthesize ZnO nanoparticles. The peaks at > 3100 cm^{-1} are related to OH species with co-adsorbed H_2O on ZnO surfaces. The characteristics bands at 2109.7 to 2117.1 cm^{-1} and at 1006.4 to 1051.1 cm^{-1} were attributed to the C-N vibrations. Aromatic C-H bending vibrations were observed at 1992.9 cm^{-1}, 1982.9 cm^{-1}, 1990.4 cm^{-1} and 1990.4 cm^{-1} for ZnO nanoparticles from neem, bitter leaf, moringa and ginger lily plant extracts respectively. At the characteristics band ranging from 1608.5 to 1671.1 cm^{-1} were attributed to the stretching vibration mode of C=O residues. This band however was absent in the ZnO nanoparticles from ginger lily plant extracts. The characteristics peak at around 1576.7 and 1599 cm^{-1} is due to the C-C stretching aromatic ring, and the strong intensity at 1408.9 cm^{-1} and 1412.8 cm^{-1} are due to α-CH_2 bending vibrations of aldehydes and ketones. The peak in the region of less than 900 cm^{-1} is assigned to Zn-O stretching vibration.

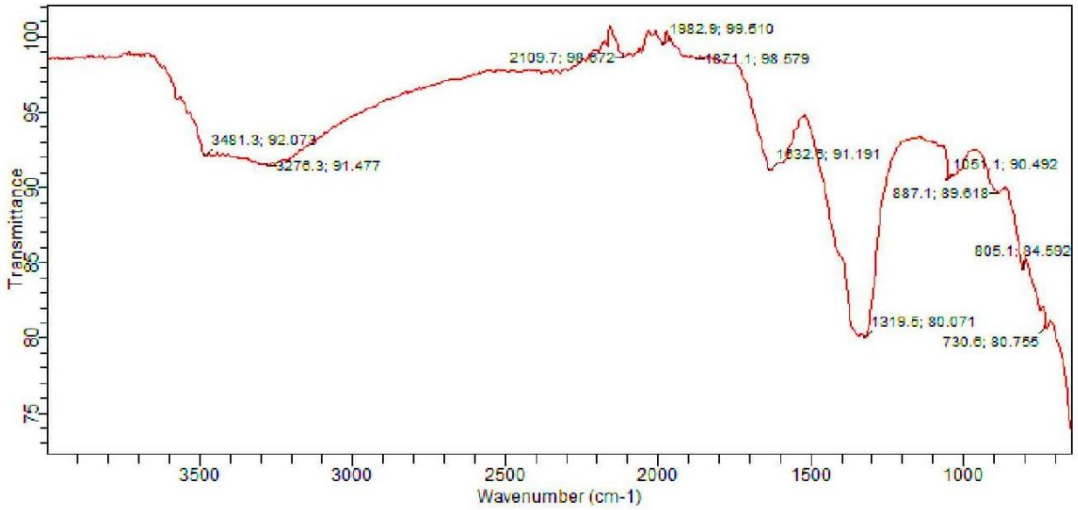

Figure 4.1: IR spectra for ZnO nanoparticle from neem plant

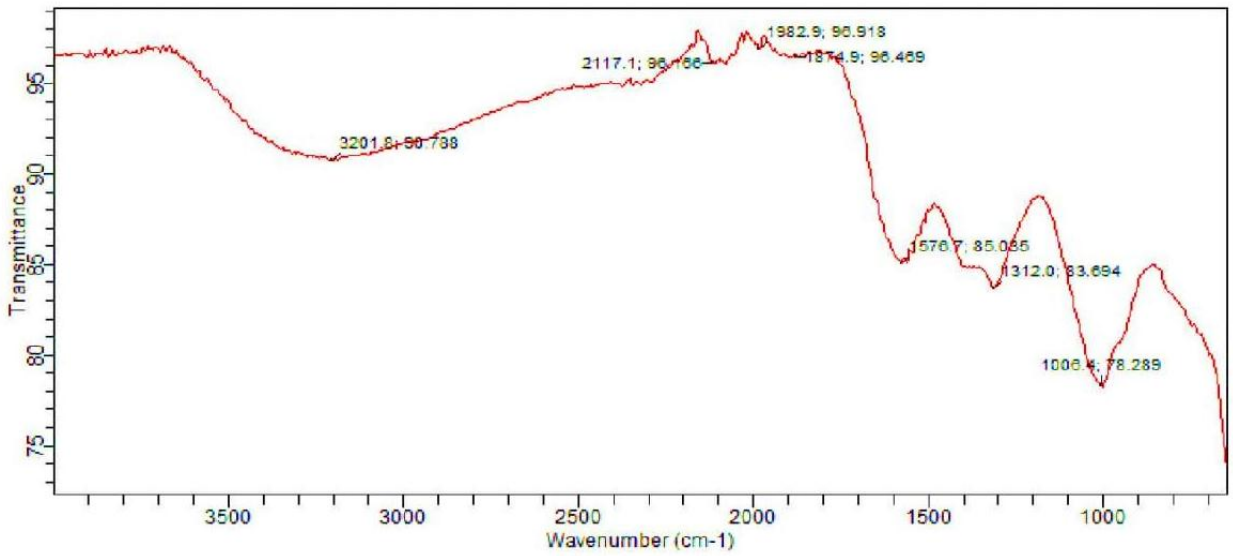

Figure 4.2: IR spectra for ZnO nanoparticle from bitter leaf

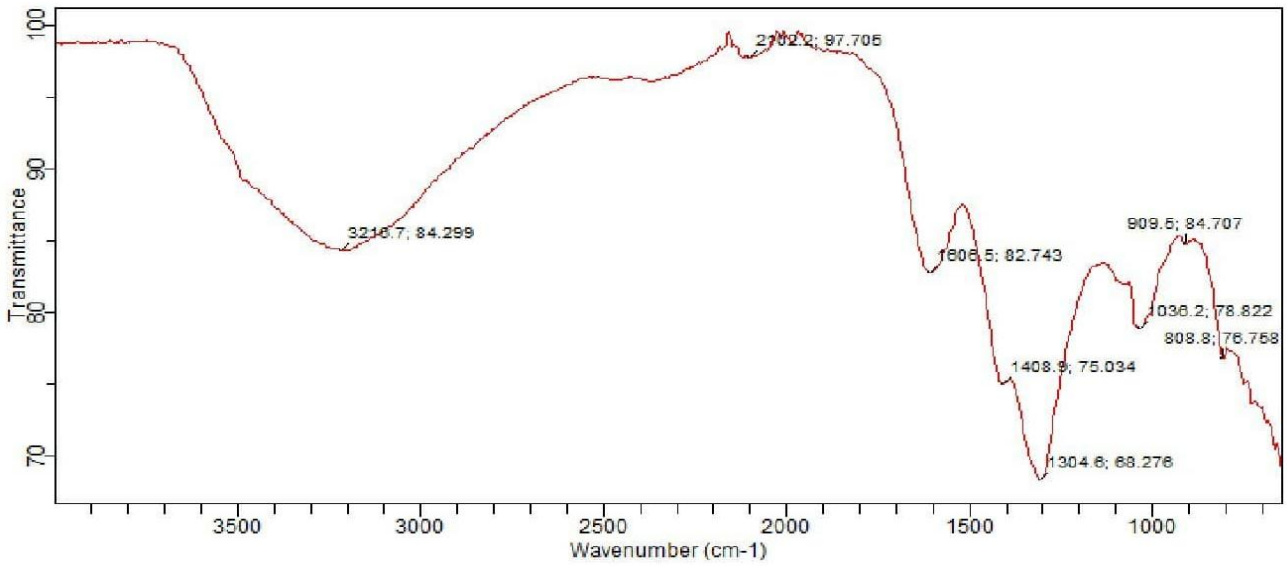

Figure 4.3: IR spectra for ZnO nanoparticle from scent leaf

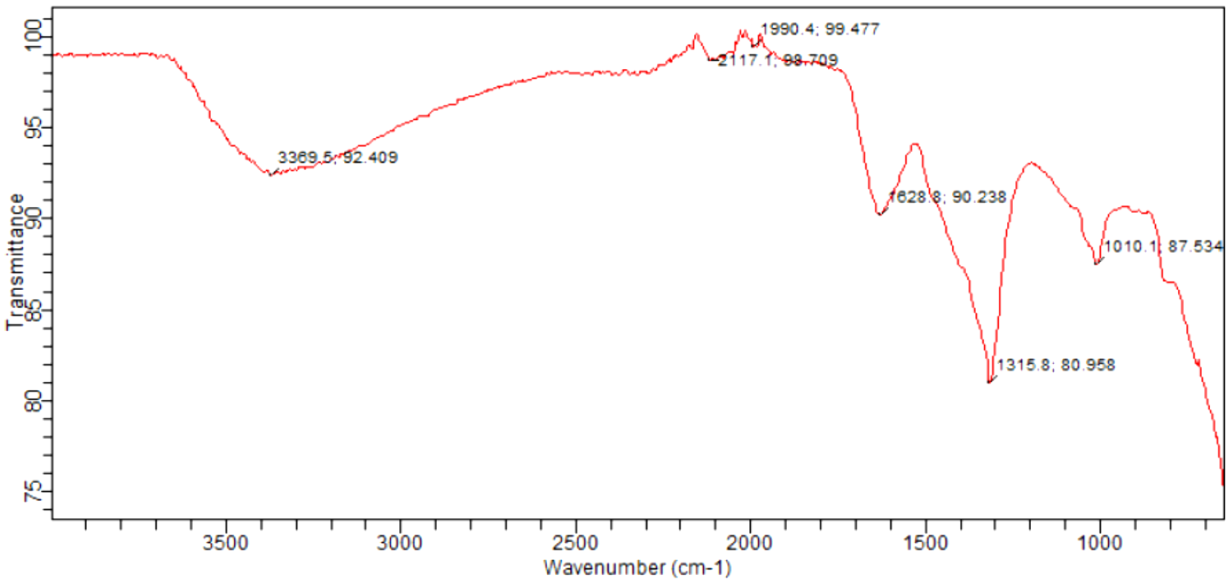

Figure 4.4: IR spectra for ZnO nanoparticle from moringa leaf

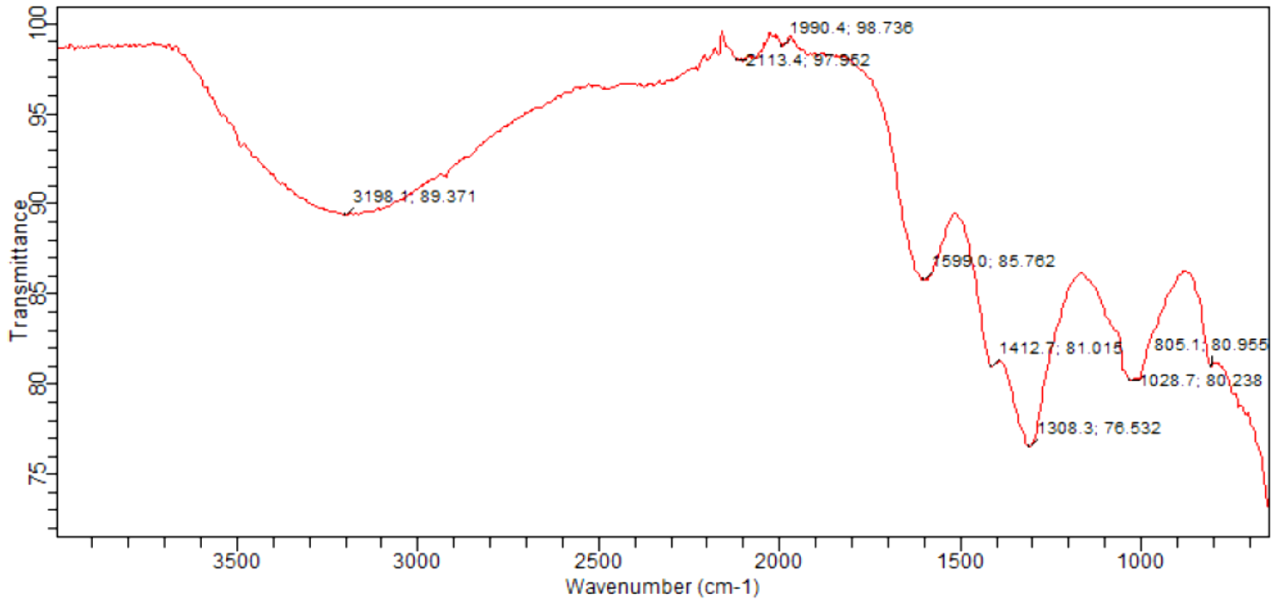

Figure 4.5: IR spectra for ZnO nanoparticle from ginger lilly

Table 4.1: IR spectral data for the different ZnO nanoparticle

Assignment	**Plant extract frequency (cm^{-1})**				
	Neem	**Bitter leaf**	**Scent leaf**	**Moringa leaf**	**Ginger lilly**
ZnO	730.6-887.1	630.2-889.2	808.8-909.5	634	805.1
C-N stretching	1051.1	1006.4	1036.2	1010.1	1028.7
vO-H bending	1319.5	1312.0	1304.6	1315.8	1308.3
CH_2	-	-	1408.9	-	1412.7
C-C stretching	-	1576.7	-	-	1599.0
vC=O	1632.6	-	-	-	-
vC=O	1671.1	-	1608.5	1628.8	-
vC-H bending (aromatic)	-	1874.9	-	-	-
vC-H bending (aromatic)	1992.9	1982.9	-	1990.4	1990.4
vC=N stretching	2109.7	2117.1	-	2117.1	2113.4
C-H bending	-	-	2712.2	-	-
vO-H	3276.3	-	3216.7	3369.5	3198.1
vO-H	3481.3	3201.6	-	-	-

4.2.2 SEM-EDX

The surface morphologies of biosynthesized ZnO nanoparticles were studied by using SEM, and the results are presented in Figures 4.6 to 4.10. The SEM for the ZnO nanoparticle produced from neem plant (Figure 4.6) and moringa leaf (Figure 4.9) extracts showed both nanorod and flake-type shapes in aggregated form. To gain further insight into the features of the biosynthesized ZnO Nanoparticles, the analysis of the sample was performed using EDX techniques.. The weight concentration of Zn in the different ZnO nanoparticles were 85.97, 70.84, 82.49, 87.53 and 76.89 % for neem, bitter leaf, scent leaf, moringa leaf and ginger lilly respectively.

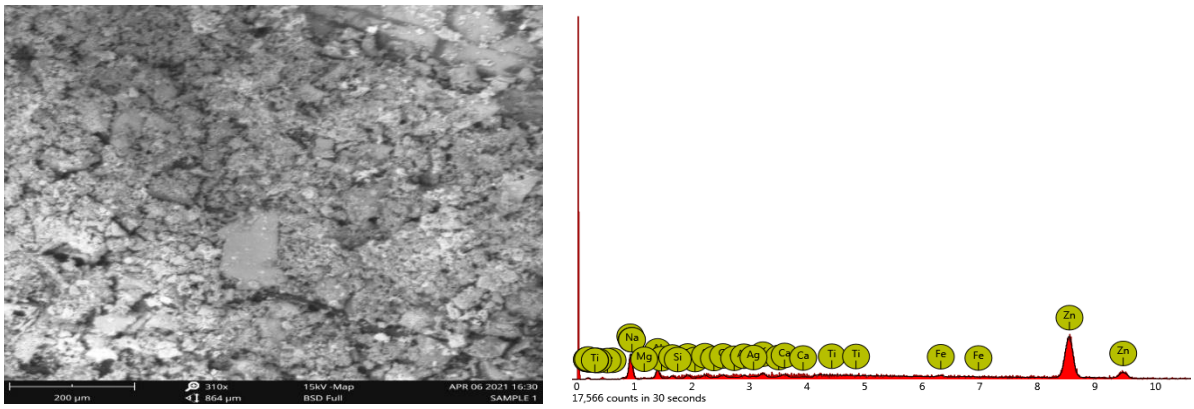

Figure 4.6: SEM-EDX for ZnO nanoparticle from neem plant extract

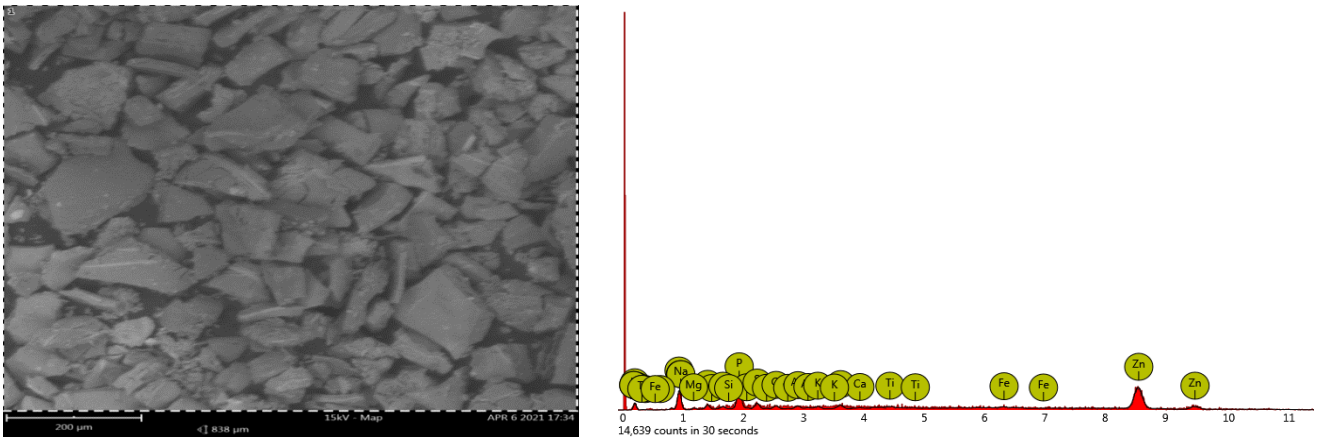

Figure 4.7: SEM-EDX for ZnO Nanoparticle from bitter leaf extract

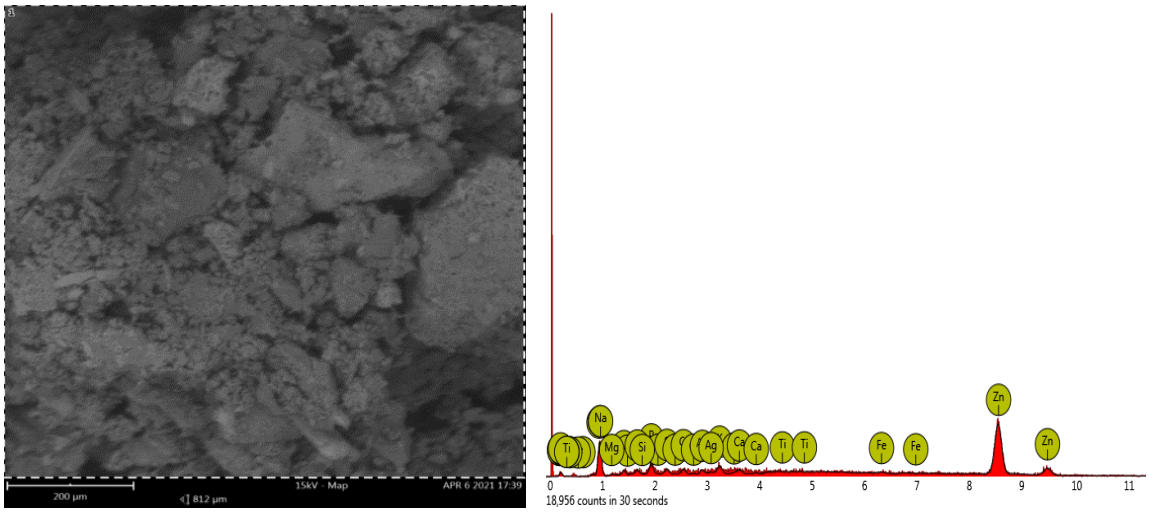

Figure 4.8: SEM-EDX for ZnO nanoparticle from scent leaf extract

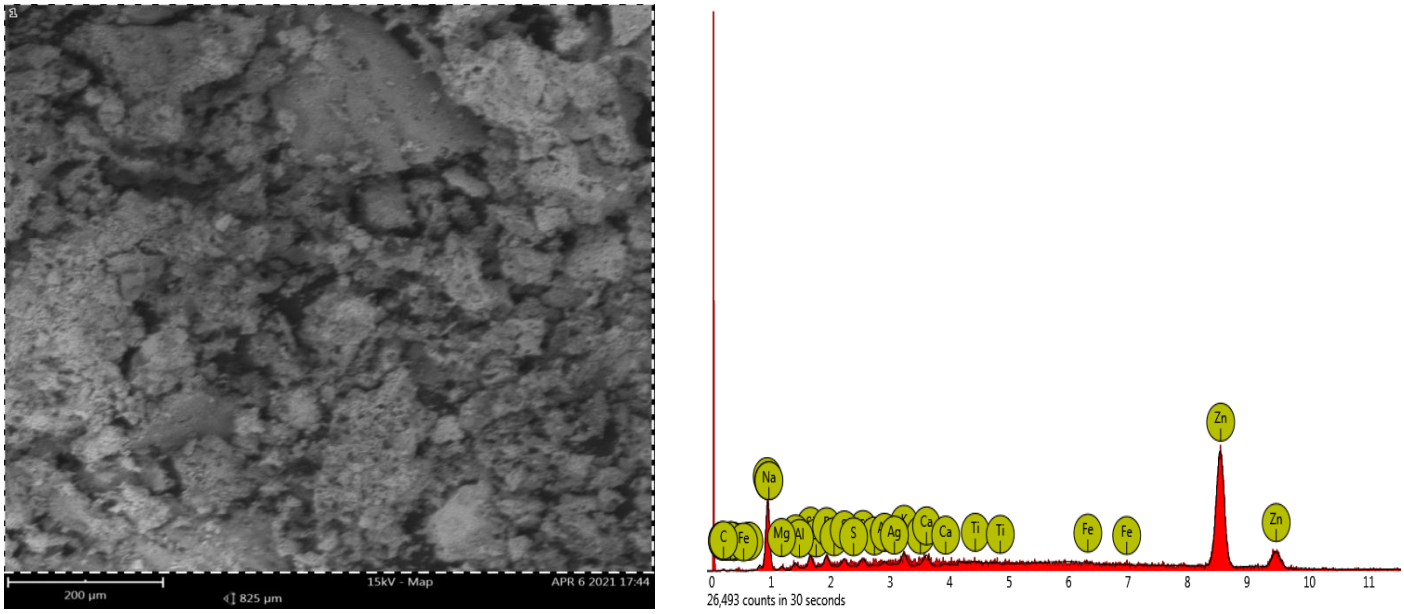

Figure 4.9: SEM-EDX for ZnO nanoparticle from moringa leaf extract

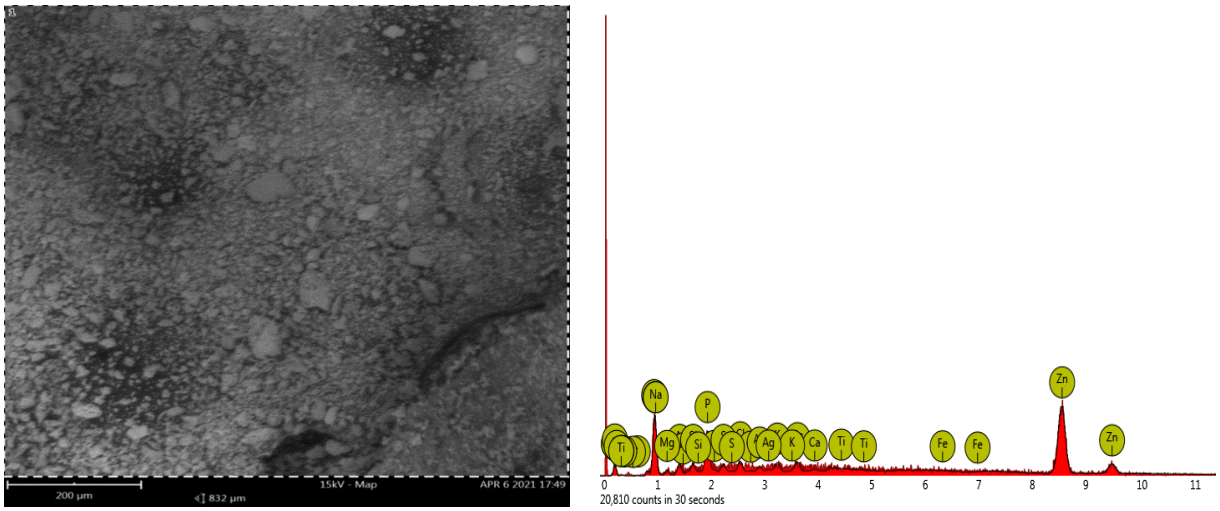

Figure 4.10: SEM-EDX for ZnO nanoparticle from ginger lilly leaf extract

4.2.3 X-ray diffraction analysis (XRD)

The XRD spectral for the different synthesized ZnO nanoparticles are presented in Figures 4.11 to 4.15. from table 4.2 For the synthesized ZnO nanoparticle from neem plant extract, the diffraction peaks appeared at a 2θ value of ≈ 34.2476 °, 38.0201 °, 44.2292 °, 64.3849 °, 68.8340 ° and 72.3879° corresponding to (002), (101), (111), (103), (201) and (220) crystal planes respectively. For the synthesized ZnO nanoparticle from bitter leaf extract, the diffraction peaks appeared at a 2θ value of ≈ 34.2071 °, 37.9973 °, 44.2230 ° and 64.5315 ° corresponding to (002), (101), (111) and (103) crystal planes respectively. For the synthesized ZnO nanoparticle from scent leaf extract, the diffraction peaks appeared at a 2θ value of ≈ 38.0403 ° and 44.3144° corresponding to (101) and (111) crystal planes respectively. For the synthesized ZnO nanoparticle from moringa leaf extract, the diffraction peaks appeared at a 2θ value of ≈ 31.8768 °, 34.4572 °, 36.2915 °, 38.0277 °, 44.1381 °, 56.6470 ° and 31.8768 ° corresponding to (100), (002), (101), (101), (111), (110) and (100) crystal planes respectively while from the ginger lily extract, the diffraction peaks appeared at a 2θ value of ≈ 34.2549 °, 38.0217 °, 44.2366 °, 64.4946 °, and 68.8222 ° corresponding to (100), (101), (111), (103) and (201) crystal planes respectively. The sharpness of the diffraction peaks related to the ZnO structure indicates a good polycrystalline nature of the nanoparticle. Furthermore, XRD spectra also showed that all the diffraction peaks fit well with the hexagonal wurtzite structure of ZnO nanoparticles . Values for θ and β can be found in Table 4.2. The results for average crystallite size of the synthesized ZnO nanoparticles are presented in Table 4.2. The sizes were 661.55 nm, 449.80 nm, 357.74 nm, 206.15 nm and 591.96 nm for ZnO nanoparticles synthesized from neem plant, bitter leaf scent leaf, moringa leaf and ginger lily extracts respectively.

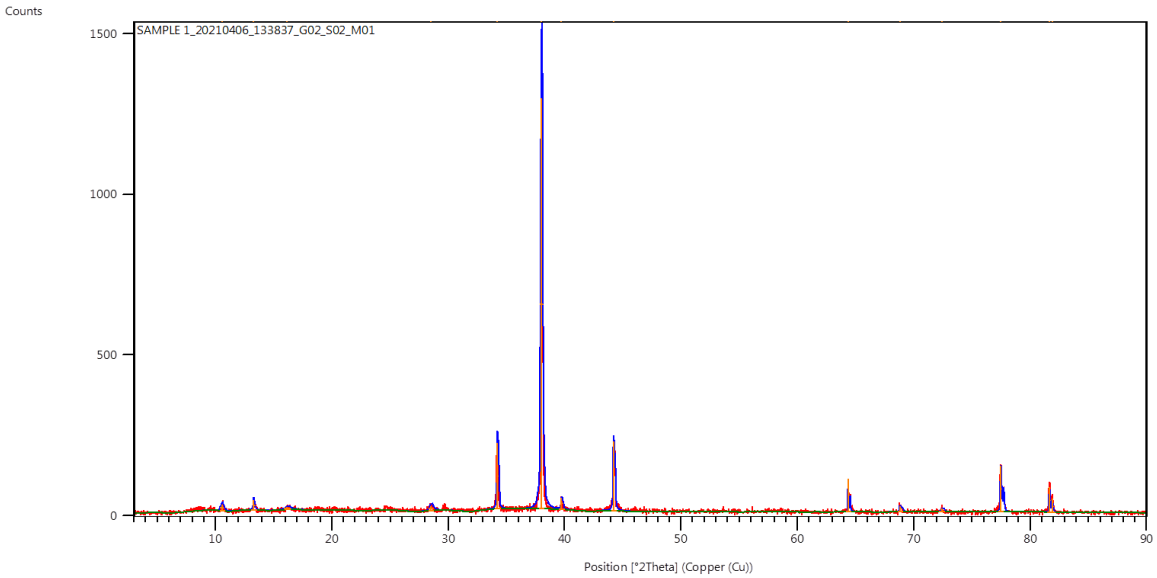

Figure 4.11: XRD spectra for ZnO nanoparticle from neem plant extract

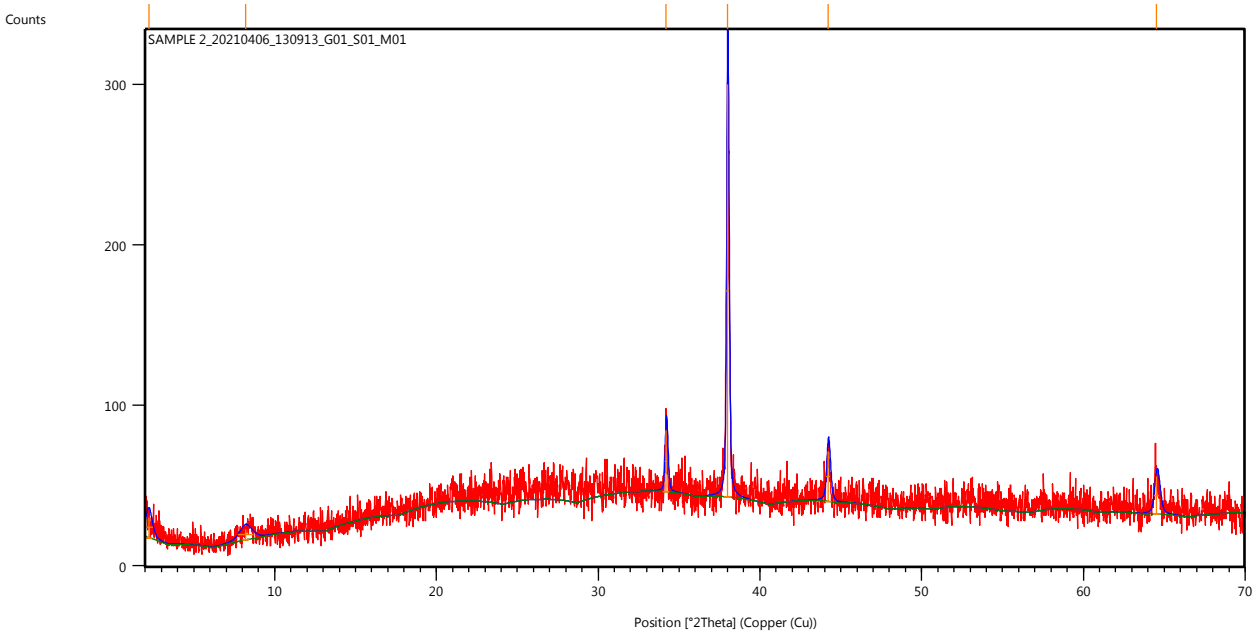

Figure 4.12: XRD spectra for ZnO nanoparticle from bitter leaf extract

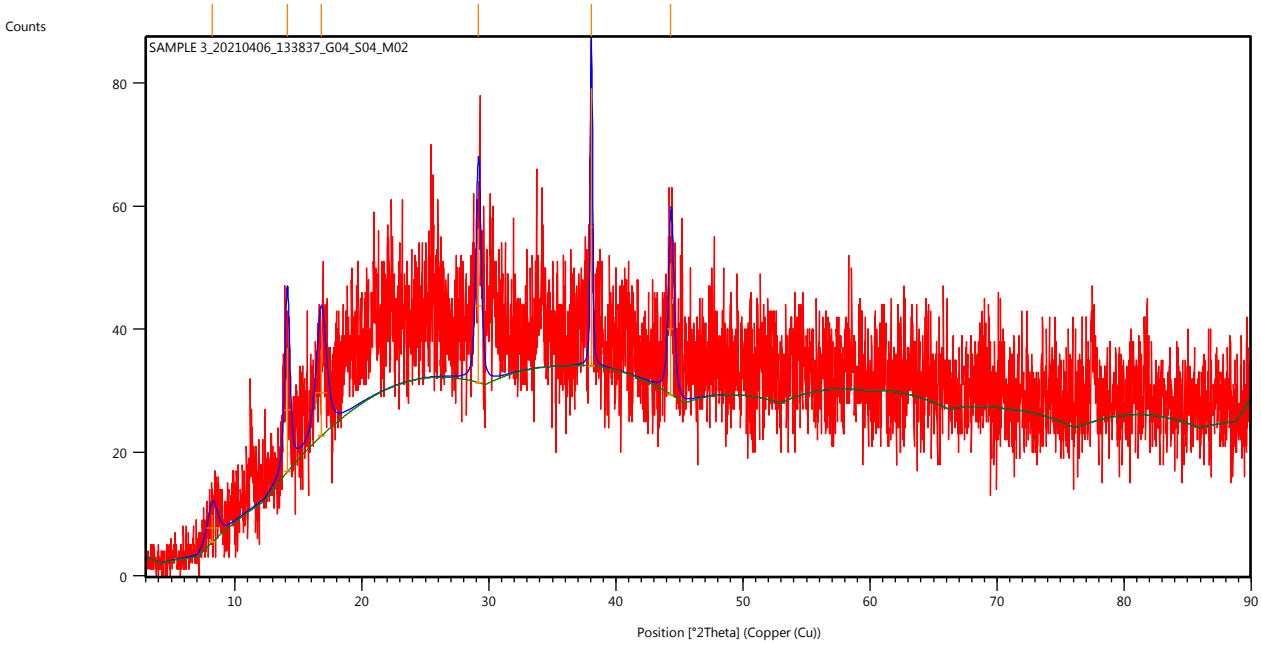

Figure 4.13: XRD spectra for ZnO nanoparticle from scent leaf extract

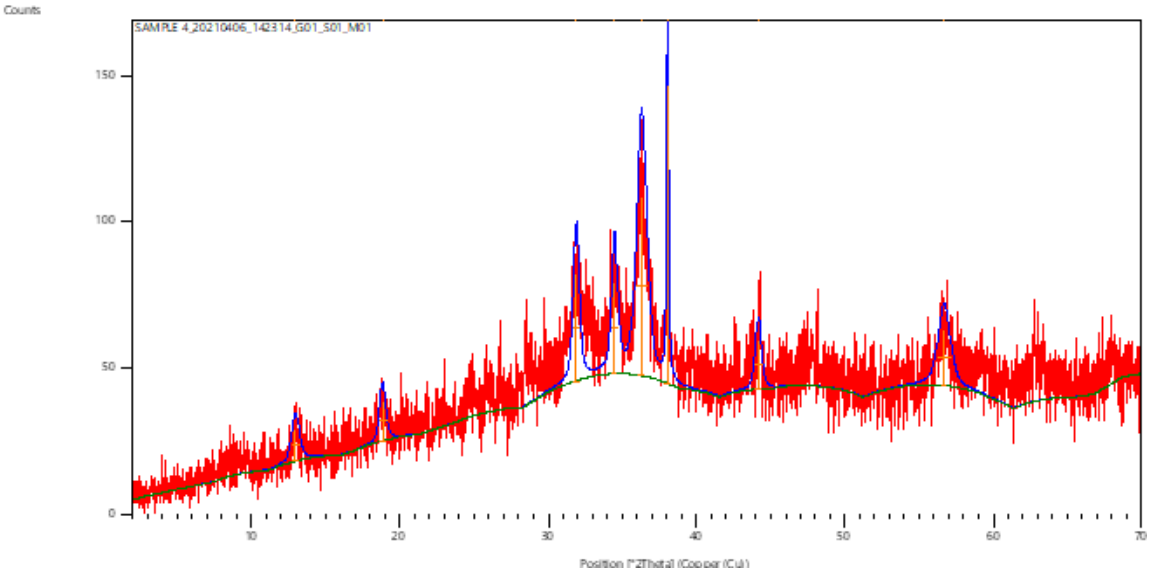

Figure 4.14: XRD spectra for ZnO nanoparticle from moringa leaf extract

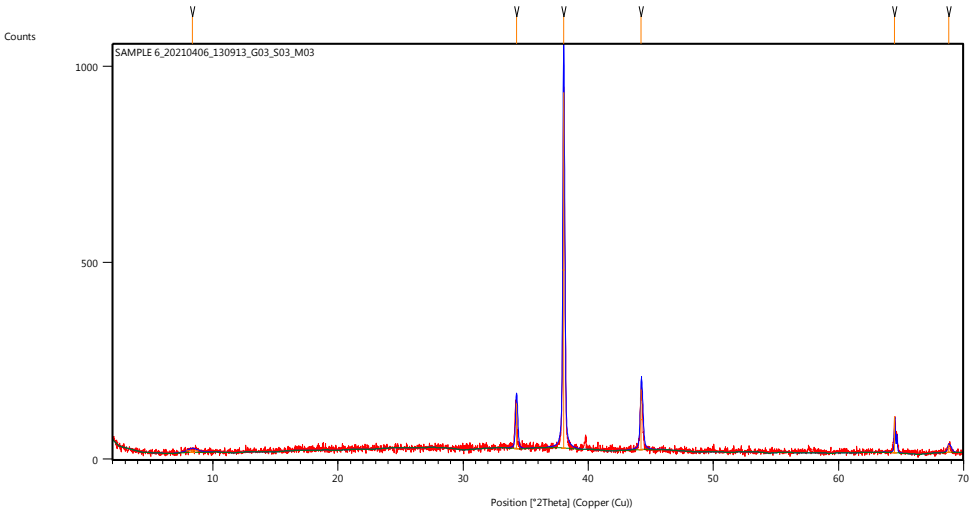

Figure 4.15: XRD spectra for ZnO nanoparticle from ginger lily leaf extract

All the diffraction peaks were properly assigned using the JCPDS file card No. 0361451 and the results are presented in Table 4.2.

Table 4.2: FWHM values, average crystallite sizes calculated using Scherrer's formula, d-spacing, and Bragg's diffraction degree of ZnO NPs synthesized

h k l	Bragg's diffraction [°2Ɵ]	Full width at half maximum (FWHM) (degrees)	d-spacing [Å]
Neem plant extract			
0 0 2	34.2476	0.1378	2.61834
1 0 1	38.0201	0.1574	2.36677
1 1 1	44.2292	0.1378	2.04786
1 0 3	64.3849	0.0720	1.44585
2 0 1	68.8340	0.1968	1.36398
2 2 0	72.3879	0.2362	1.30552
Average crystallite size = 661.55 nm			
Bitter leaf extract			
0 0 2	34.2071	0.1574	2.62135
1 0 1	37.9973	0.1378	2.36813
1 1 1	44.2230	0.2362	2.04813
1 0 3	64.5315	0.3149	1.44412
Average crystallite size = 449.80 nm			
Scent leaf extract			
1 0 1	38.0403	0.1574	2.36556
1 1 1	44.3144	0.4723	2.04412
Average crystallite size = 357.74 nm			

Moringa leaf extract

1 0 0	31.8768	0.4723	2.80745
0 0 2	34.4572	0.4723	2.60289
1 0 1	36.2915	0.7872	2.47543
1 0 1	38.0277	0.1574	2.36632
1 1 1	44.1381	0.4723	2.05187
1 1 0	56.6470	0.9446	1.62491
1 0 0	31.8768	0.4723	2.80745

Average crystallite size = 206.15 nm

Ginger lily extract

1 0 0	34.2549	0.1574	2.61780
1 0 1	38.0217	0.1378	2.36667
1 1 1	44.2366	0.1968	2.04753
1 0 3	64.4946	0.0960	1.44366
2 0 1	68.8222	0.2362	1.36418

Average crystallite size = 591.96 nm

4.2.4 Ultra Violet-Visual analysis spectra of biosynthesied ZnO nanoparticles

The UV-Vis analysis was used to determine the electronic transition in the synthesized ZnO nanoparticles. The energy absorbed in the ultraviolet/ visible region produced changes in the electronic energy of the compound resulting from transition of valence electrons in the ZnO nanoparticles. These transitions consist of the excitation of an electron from a filled molecular orbital (usually a non-bonding (n) or a bonding $\pi \rightarrow \pi^*$ molecular orbital of an unfilled molecular orbital. The UV-Vis spectra for the synthesized ZnO nanoparticles are presented in Figures 16 to 20. Strong absorbance was observed at 356 nm, 368 nm, 368 nm, 368 nm and 369 nm for ZnO nanoparticles synthesized from neem plant, bitter leaf, scent leaf, moringa leaf and ginger lily extracts respectively.

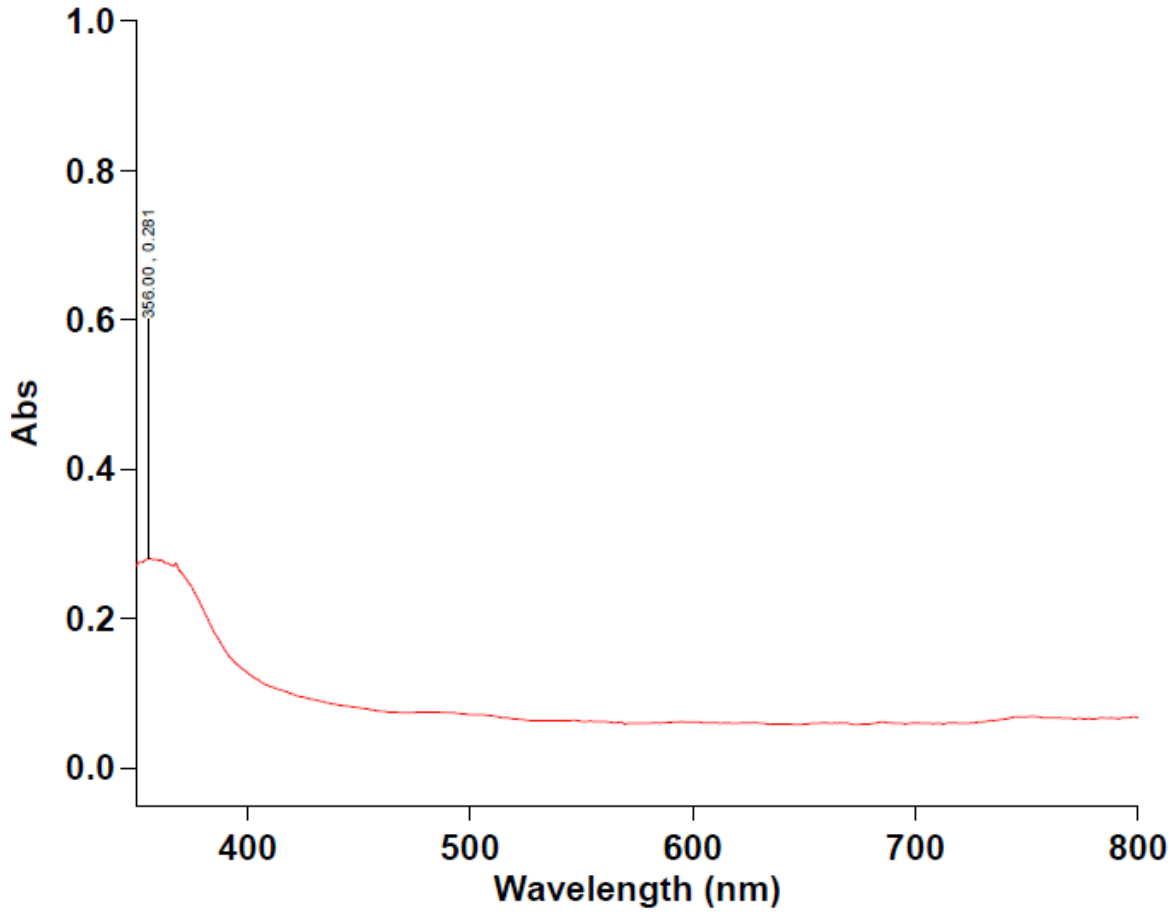

Figure 4.16: UV-Vis spectra for ZnO nanoparticle from neem plant extract

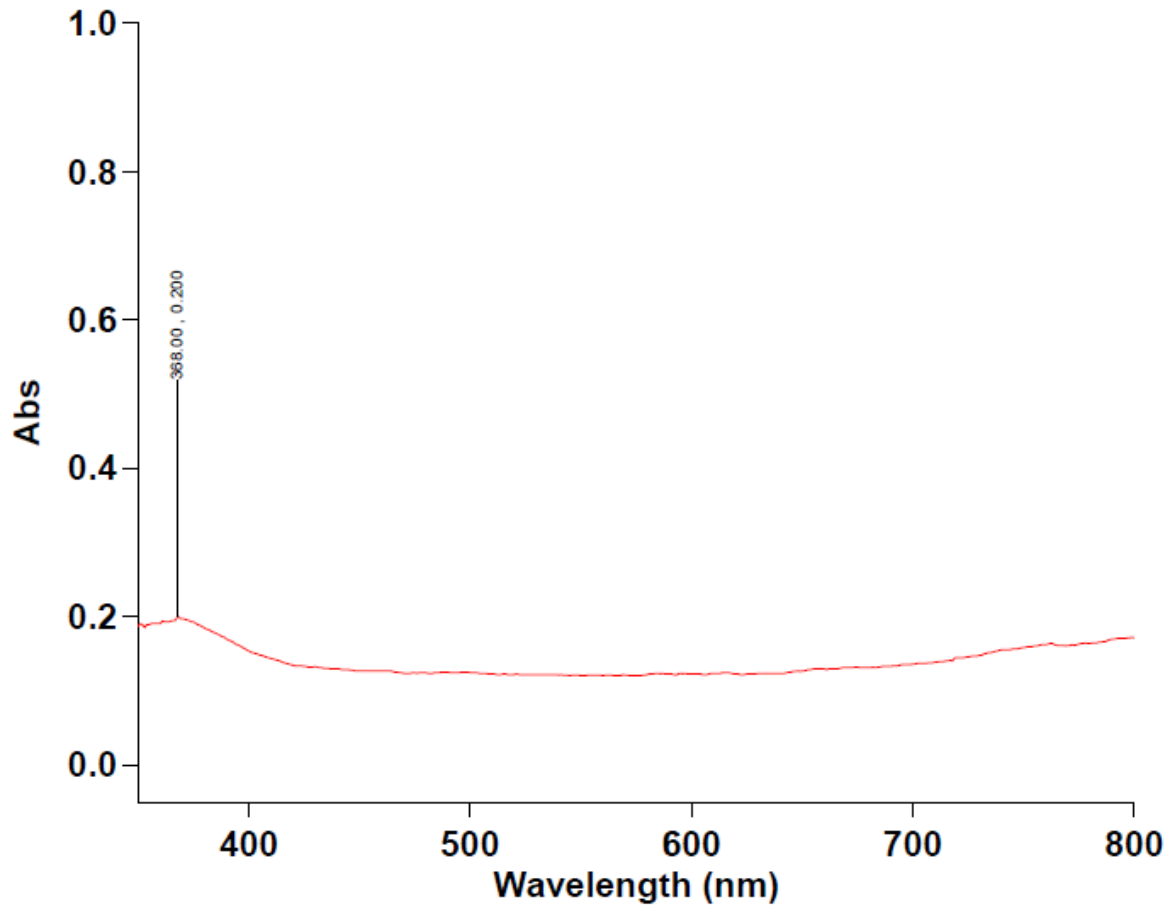

Figure 4.17: UV-Vis spectra for ZnO nanoparticle from bitter leaf extract

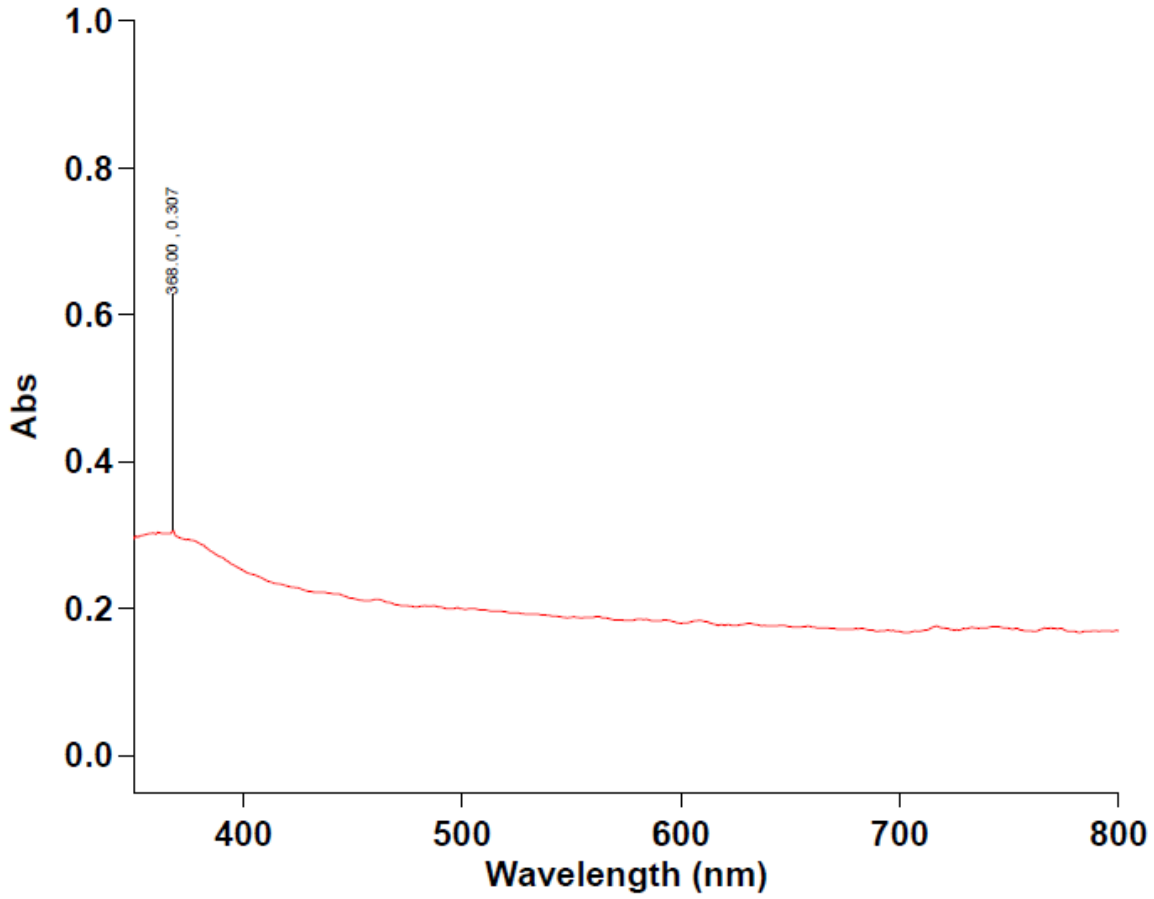

Figure 4.18: UV-Vis spectra for ZnO nanoparticle from scent leaf extract

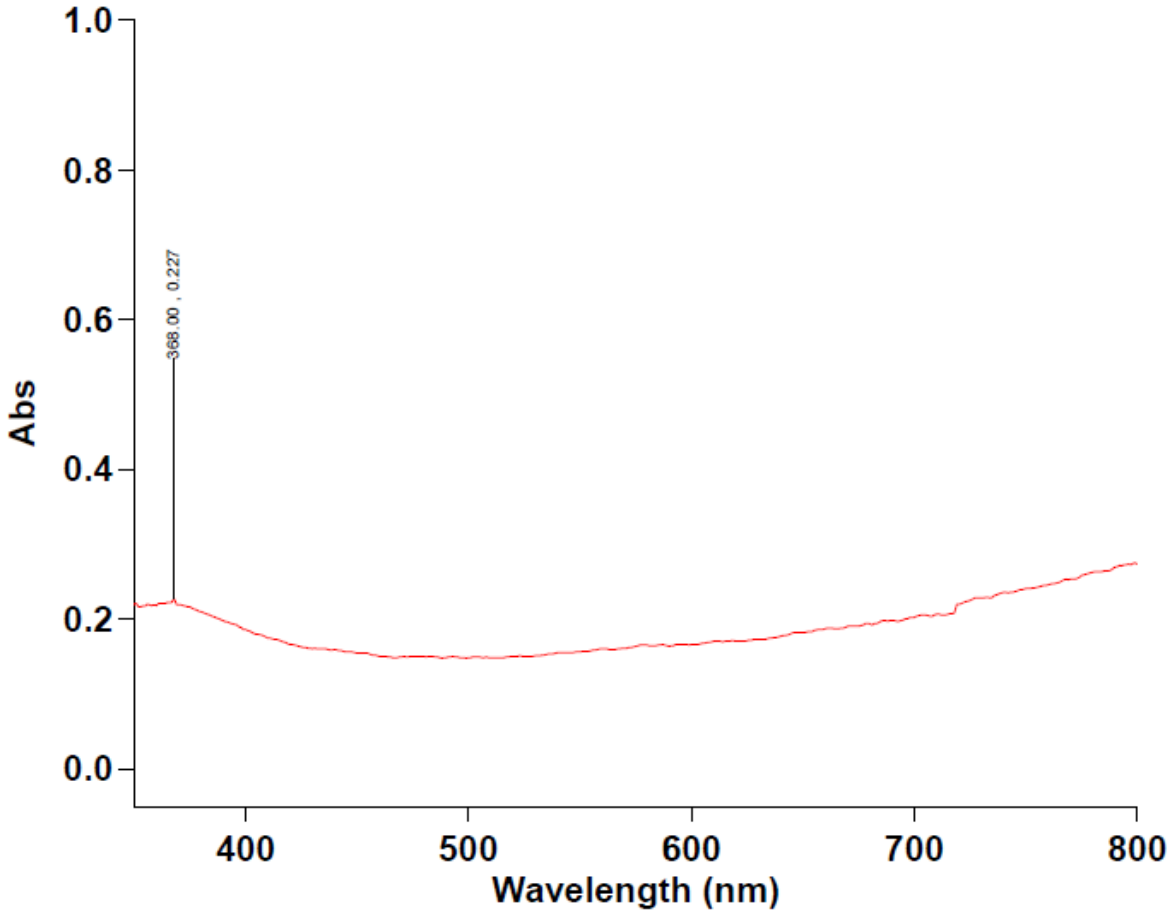

Figure 4.19: UV-Vis spectra for ZnO nanoparticle from moringa leaf extract

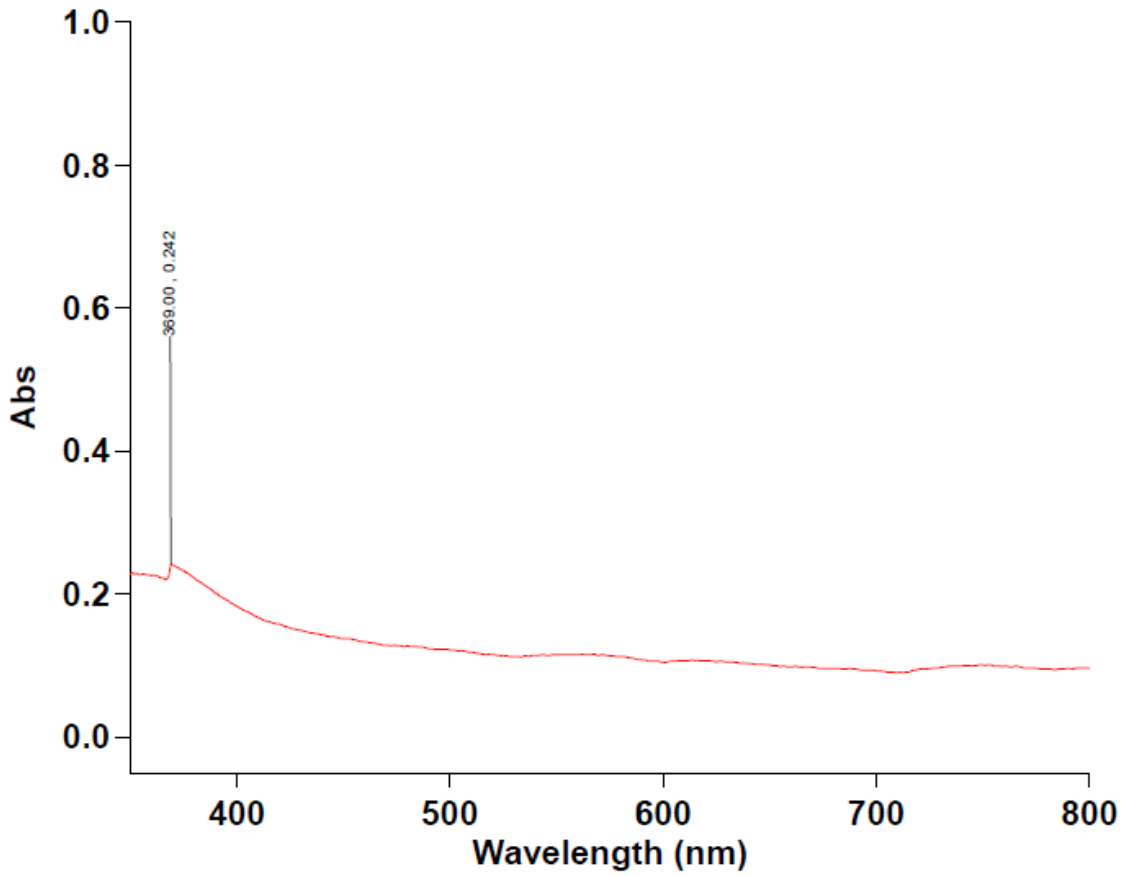

Figure 4.20: UV-Vis spectra for ZnO nanoparticle from ginger lily leaf extract

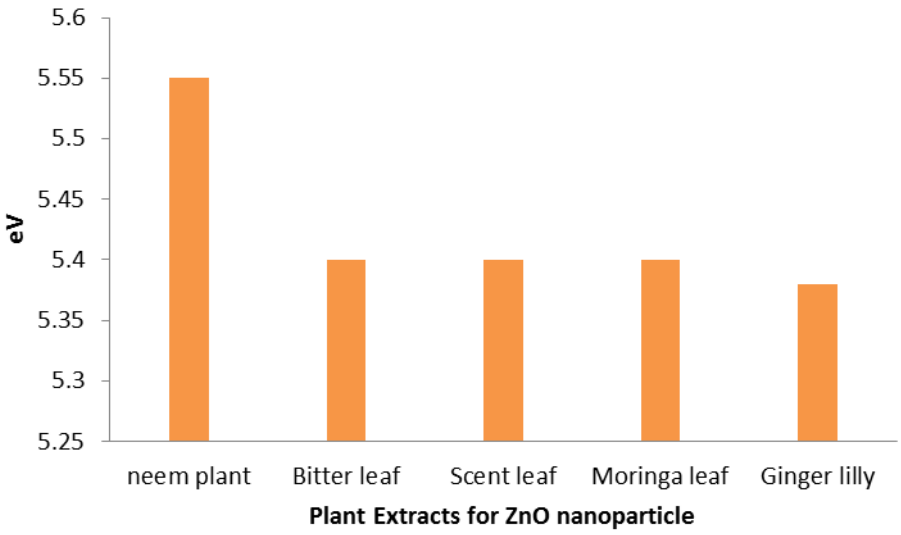

Figure 4.21: Band energies for biosynthesized ZnO nanoparticles

4.2 Antibacterial activity of biosynthesized ZnO nanoparticles

The antibacterial activity of the zinc oxide nanoparticle was measured using a meter rule and measured on all visibly clear zone of clearance around the paper disc.

Figure 4.22 shows the antibacterial activity of various green synthesized nanoparticles on *Staphylococcus aureus*. The standard levofloxacin sensitivity disc showed the highest zone of clearance at 13.4 mm which was followed by 3500 µg/ml of zinc oxide particles synthesized by moringa leaf (*Moringa oliefera L*) at 8.5 mm. The lowest zone of inhibition was noticed at 7.6 mm by 1000µg/ml Zinc oxide nanoparticles synthesized by scent leaf (*Ocimum gratissimum L*). Figure 4.23 shows the antibacterial activity of various green synthesized nanoparticles on *Staphylococcus aureus*. The standard levofloxacin sensitivity disc showed the highest zone of clearance at 14.9 mm which was followed by 3500 µg/ml of ZnO nanoparticles synthesized by ginger lily (Costus afer) at 11.0 mm and Zinc oxide particles synthesized by Bitter leaf (Vernonia amygdalina) at 9.0 mm. The lowest zone of inhibition was noticed at 7.5 mm by 1000 µg/ml of zinc oxide nanoparticles synthesized by Scent leaf (*Ocimum gratissimum L*). Figure 4.24 shows the antibacterial activity of various green synthesized nanoparticles on *Escherichia coli*. The standard levofloxacin sensitivity disc showed the highest zone of clearance at 13.0 mm which was followed by 3500 µg/ml of ZnO nanoparticles synthesized by scent leaf (*Ocimum gratissimum L*) and zinc oxide nanoparticles synthesized by Moringa leaf (*Moringa oliefera L*) at 9.0 mm each. The lowest zone of inhibition was noticed at 7.5 mm by 1000µg/ml Zinc oxide nanoparticles synthesized by Scent leaf (*Ocimum gratissimum*). Figure 4.25 shows the antibacterial activity of various green synthesized nanoparticles on *Klebsiella* spp. The standard levofloxacin sensitivity disc showed the highest zone of clearance at 15.0 mm which was followed by 3500µg/ml of ZnO nanoparticles synthesized by scent leaf (*Ocimum gratissimum L*) at 9.0 mm followed closely by zinc oxide nanoparticles synthesized by ginger lily (*Costus afer L*) at 8.9 mm. The lowest

zone of inhibition was noticed at 6.5 mm by 1000 µg/ml zinc oxide nanoparticles synthesized by bitter leaf (*Vernonia amygdalina*). Figure 4.26 shows the antibacterial activity of various green synthesized nanoparticles on *Pseudomonas* spp. The standard levofloxacin sensitivity disc showed the highest zone of clearance at 13.7 mm which was followed by 3500µg/ml of moringa leaf (*Moringa oliefera L*) ZnO nanoparticles at 10.2 mm, bitter leaf (*Vernonia amygdalina L*) ZnO nanoparticles at 10 mm neem plant (*Azadirachta indica L*) ZnO nanoparticles at 9.7 mm. the lowest zone of inhibition was noticed at ZnO nanoparticles synthesized by Scent leaf (*Ocimum gratissimum L*)

Table 4.3: Antibacterial activity of the green synthesized ZnO nanoparticles and levofloxacin against *S. epidermidis*, *S. aureus*, *E. coli*, *Klebsiella* spp, *Pseudo* spp *and Proteus* spp

	S.epidermidis				***S.aureus***				***E.coli***				***Klebsiella* spp**				***Pseudo* spp**				***Proteus* spp**			
Sam	**A**	**B**	**C**	**D**	**A**	**B**	**C**	**D**	**A**	**B**	**C**	**D**	**A**	**B**	**C**	**D**	**A**	**B**	**C**	**D**	**A**	**B**	**C**	**D**
1	NZ	NZ	8.2	13.	NZ	NZ	8.0	14.9	NZ	8.1	8.5	13.0	NZ	NZ	8.0	15	NZ	9.0	9.7	13.7	NZ	NZ	NZ	4.7
2	NZ	NZ	NZ	4	NZ	8.0	9.0		NZ	8.0	8.9		6.5	7.9	8.0		NZ	8.9	10.0		NZ	NZ	NZ	
3	7.6	8.0	8.1		7.5	7.9	8.0		7.5	8.0	9.0		8.0	8.1	9.0		NZ	8.9	10.2		NZ	NZ	NZ	
4	NZ	NZ	8.5		NZ	NZ	8.1		NZ	8.5	9.0		NZ	7.9	8.5		NZ	NZ	10.0		NZ	NZ	NZ	
5	NZ	NZ	8.0		NZ	10.5	11.0		7.7	8.0	8.1		NZ	7.4	8.9		NZ	7.0	7.1		NZ	NZ	NZ	

Key: 1:Zinc oxide nanoparticles synthesized by neem plant (*Azadirachta indica L*)

2:Zinc oxide nanoparticles synthesized by bitter leaf (*Vernonia amygdalina L*)

3:Zinc oxide nanoparticles synthesized by scent leaf (*Ocimum gratissimum L*)

4:Zinc oxide nanoparticles synthesized by moringa leaf (*Moringa oliefera L*)

5:Zinc oxide particles synthesized by ginger lily (*Costus afer L*)

a: 1000 μg/ml ZnO Nanoparticle impregnated disc

b: 2000 μg/ml ZnO Nanoparticle impregnated disc

c: 3500 μg/ml ZnO Nanoparticle impregnated disc

d: standard levofloxacin sensitivity disc

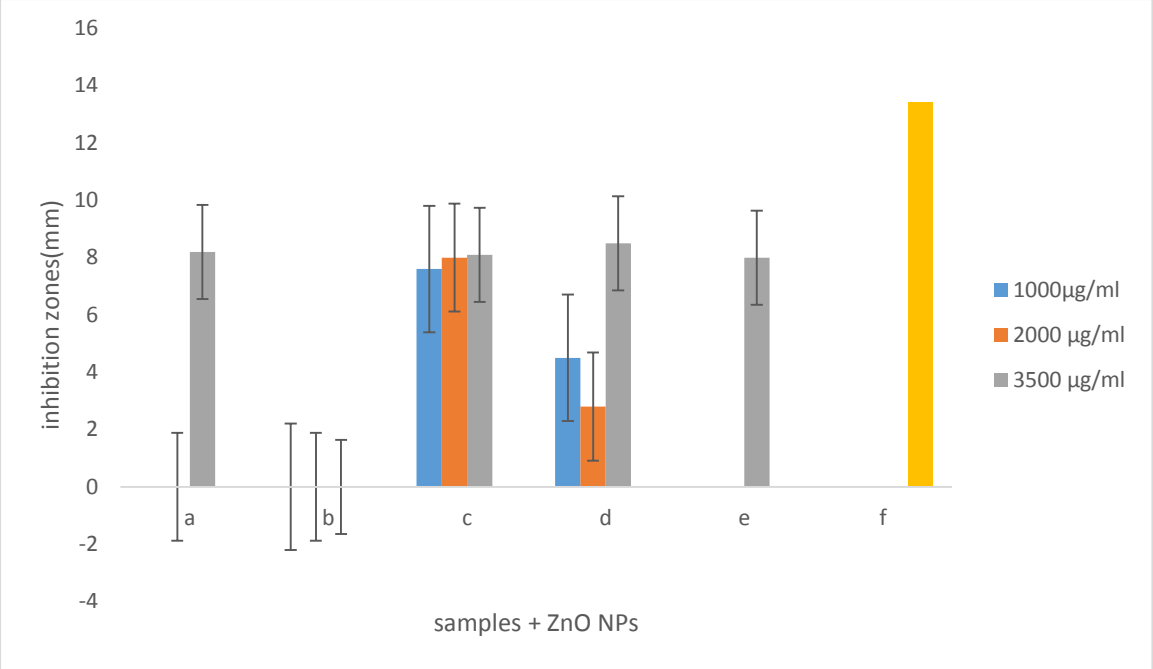

Figure 4.22: Antibacterial activity of zinc oxide nanoparticle against strain of *Staph epidermidis*

A:Zinc oxide particles synthesized by neem plant (*Azadirachta indica*)

B:Zinc oxide particles synthesized by Bitter leaf (*Vernonia amygdalina*)

C:Zinc oxide particles synthesized by Scent leaf (*Ocimum gratissimum*)

D:Zinc oxide particles synthesized by Moringa leaf (*Moringa oliefera*)

E:Zinc oxide particles synthesized by Ginger lily (*Costus afer*)

F:Standard levofloxacin sensitivity disc

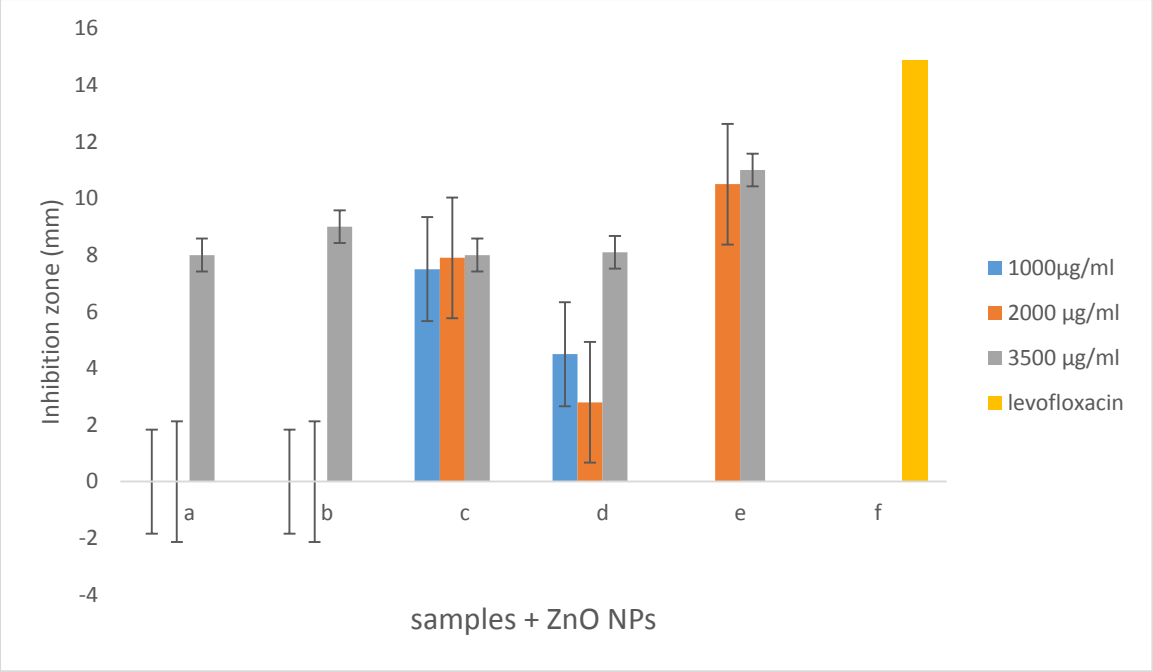

Figure 4.23: Antibacterial activity of zinc oxide nanoparticle against strain of *Staphylococcus aureus*

A: Zinc oxide particles synthesized by Neem plant (*Azadirachta indica*)

B:Zinc oxide particles synthesized by Bitter leaf (*Vernonia amygdalina*)

C:Zinc oxide particles synthesized by Scent leaf (*Ocimum gratissimum*)

D:Zinc oxide particles synthesized by Moringa leaf (*Moringa oliefera*)

E:Zinc oxide particles synthesized by Ginger lily (*Costus afer*)

F: Standard levofloxacin sensitivity disc

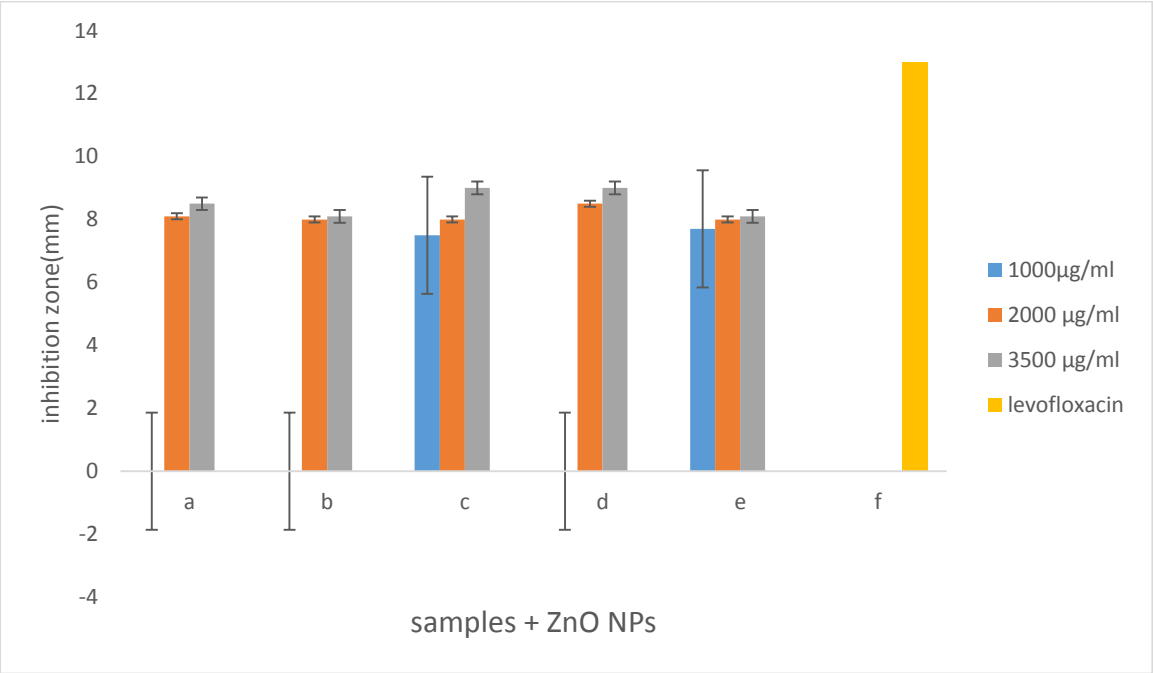

Figure 4.24: Antibacterial activity of zinc oxide nanoparticle against strain of *Escherichia coli species*

A:Zinc oxide nanoparticles synthesized by neem plant (*Azadirachta indica*)

B:Zinc oxide nanoparticles synthesized by Bitter leaf (*Vernonia amygdalina*)

C:Zinc oxide nanoparticles synthesized by Scent leaf (*Ocimum gratissimum*)

D:Zinc oxide nanoparticles synthesized by Moringa leaf (*Moringa oliefera*)

E:Zinc oxide nanoparticles synthesized by Ginger lily (*Costus afer*)

F:Standard levofloxacin sensitivity disc

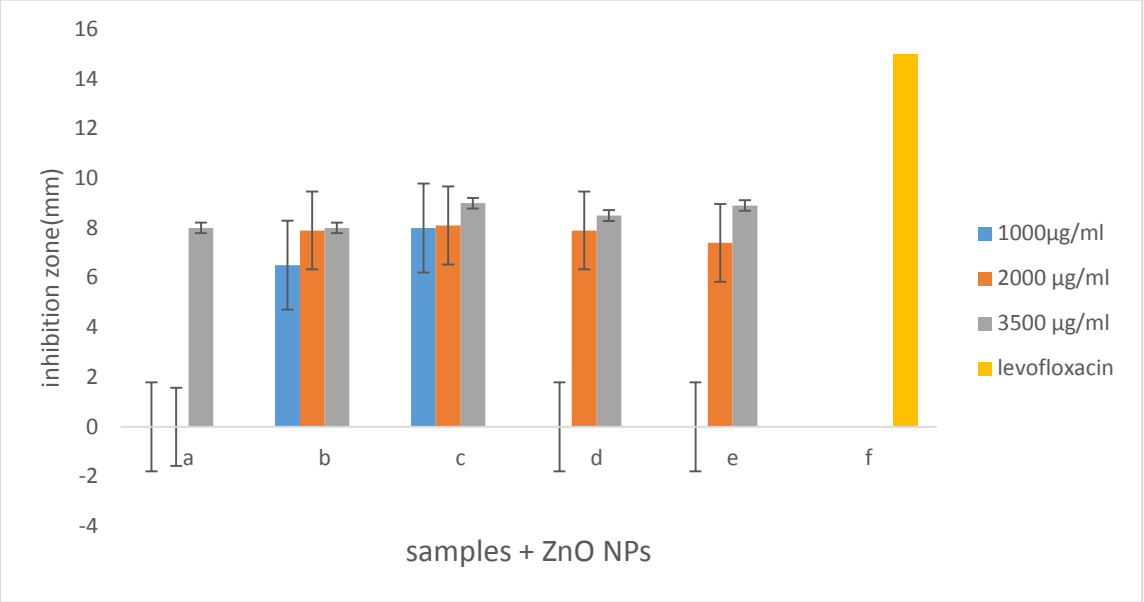

Figure 4.25: Antibacterial activity of zinc oxide nanoparticle against strain of *Klebsiella* spp

A:Zinc oxide nanoparticles synthesized by neem plant (*Azadirachta indica*)

B:Zinc oxide nanoparticles synthesized by Bitter leaf (*Vernonia amygdalina*)

C:Zinc oxide nanoparticles synthesized by Scent leaf (*Ocimum gratissimum*)

D:Zinc oxide nanoparticles synthesized by Moringa leaf (*Moringa oliefera*)

E:Zinc oxide nanoparticles synthesized by Ginger lily (*Costus afer*)

F:Standard levofloxacin sensitivity disc

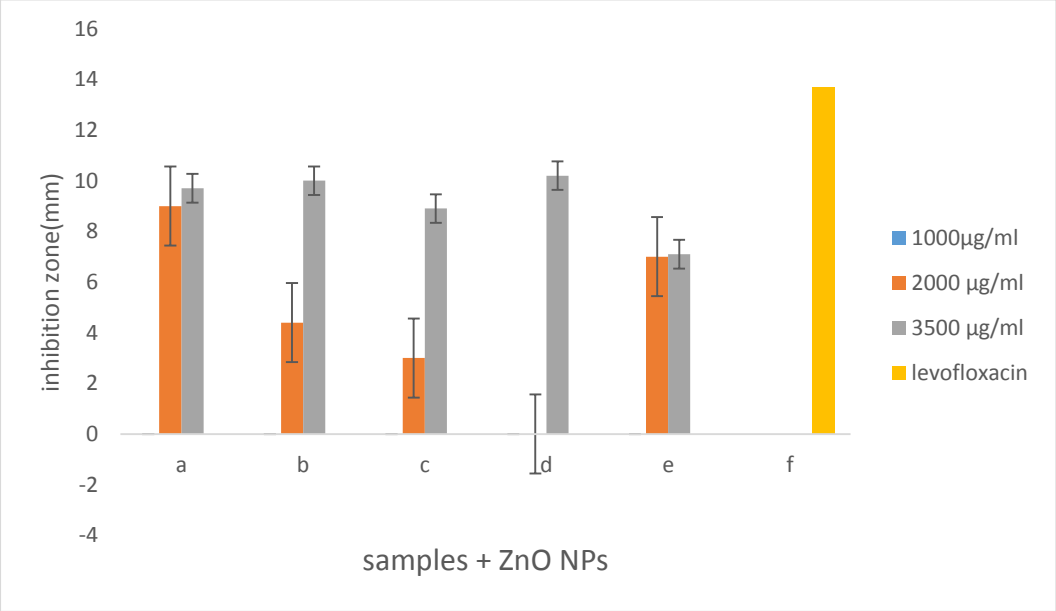

Figure 4.26: Antibacterial activity of zinc oxide nanoparticle against strain of *Pseudomonas* spp.

A: Zinc oxide nanoparticles synthesized by Neem plant (*Azadirachta indica*)

B:Zinc oxide nanoparticles synthesized by Bitter leaf (*Vernonia amygdalina*)

C:Zinc oxide nanoparticles synthesized by Scent leaf (*Ocimum gratissimum*)

D:Zinc oxide nanoparticles synthesized by Moringa leaf (*Moringa oliefera*)

E:Zinc oxide nanoparticles synthesized by Ginger lilly (*Costus afer*)

F:Standard levofloxacin sensitivity disc

Fig 4.27 shows the antibacterial activity of various green synthesized nanoparticles on *Proteus* spp. There was no zone of inhibition observed for all nanoparticle implanted discs as *Proteus* spp showed resistance.

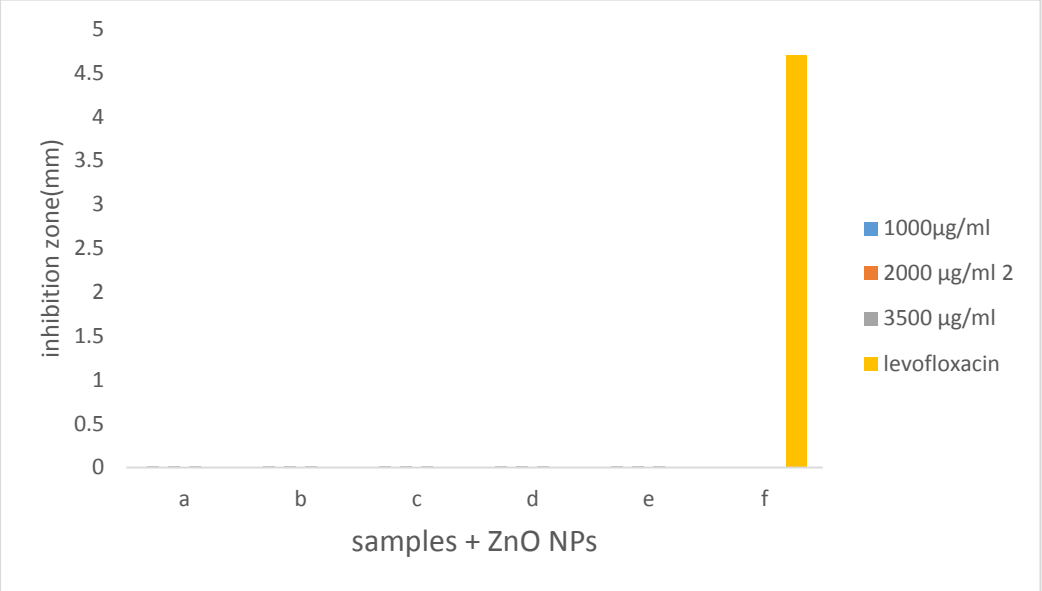

Figure 4.27: Antibacterial activity of zinc oxide nanoparticle against strain of *Proteus* spp

A:Zinc oxide particles synthesized by Neem plant (*Azadirachta indica*)

B:Zinc oxide particles synthesized by Bitter leaf (*Vernonia amygdalina*)

C:Zinc oxide particles synthesized by Scent leaf (*Ocimum gratissimum*)

D:Zinc oxide particles synthesized by Moringa leaf (*Moringa oliefera*)

E:Zinc oxide particles synthesized by Ginger lilly (*Costus afer*)

F: Standard levofloxacin sensitivity disc

4.3 DISCUSSION

This work focuses on the use of aqueous plant extract in zinc oxide synthesis/production process to yield safer and higher output of zinc oxide nanoparticles and the effect of zinc oxide nanoparticles on *Staphylococcus aureus, Staphylococcus epidermidis, klebisella* species, *Escherichia coli, Proteus* species, *Pseudomonas* species. The use of green plant extract as a capping agent and reducing agent has been gaining more grounds, it has been reported that phenolic species existing in plant extracts have revealed high antioxidant properties, which is an important characteristic for bioapplications (Arvanag *et al.*, 2019).

The Fourier Transform Infrared Spectroscopy result revealed peaks at > 3100 cm^{-1} which are related to OH species with co-adsorbed H_2O on ZnO surfaces. The characteristics bands at 2109.7 to 2117.1 cm^{-1} and at 1006.4 to 1051.1 cm^{-1} were attributed to the C-N vibrations (Solabomi *et al*., 2019). Aromatic C-H bending vibrations were observed at 1992.9 cm^{-1}, 1982.9 cm^{-1}, 1990.4 cm^{-1} and 1990.4 cm^{-1} for ZnO nanoparticles from neem, bitter leaf, moringa and ginger lily plant extracts respectively. At the characteristics band ranging from 1608.5 to 1671.1 cm^{-1} were attributed to the stretching vibration mode of C=O residues probably due to atmospheric moisture and CO_2 (Demissie *et al*., 2020), these can also be attributed to stretching in acetate groups, which further verifies the coverage state of ZnO colloidal nanoparticles (Divya *et al*., 2017). This band however was absent in the ZnO nanoparticles from ginger lily plant extracts. The characteristics peak at around 1576.7 and 1599 cm^{-1} was due to the C-C stretching aromatic ring, and the strong intensity at 1408.9 cm^{-1} and 1412.8 cm^{-1} are due to α-CH_2 bending vibrations of aldehydes and ketones (Demissie *et al*., 2020). The peak in the region of less than 900 cm^{-1} is assigned to Zn-O stretching vibration (Divya *et al*., 2017; Demissie *et al*., 2020), confirming ZnO NPs are synthesized using the different plant extract as a reducing and capping agent.

The X-Ray Diffractogram spectroscopy (XRD) shows the different synthesized nanoparticles which are in agreement with the previously reported work (Getie *et al*., 2017; Demissie *et al*., 2020). The sharpness of the diffraction peaks related to the ZnO structure indicates a polycrystalline nature of the nanoparticle. Furthermore, XRD spectra also showed that all the diffraction peaks fit well with the hexagonal wurtzite structure of ZnO NPs (Bouzouraa *et al*., 2016; Getie *et al*., 2017; Demissie *et al*., 2020). The findings for average crystallite size of the synthesized ZnO nanoparticles are presented also. The sizes were 661.55 nm, 449.80 nm, 357.74 nm, 206.15 nm and 591.96 nm for ZnO nanoparticles synthesized from neem plant, bitter leaf scent leaf, moringa leaf and ginger lily extracts respectively. These findings are in agreement with the study of Muthukumar *et al* (2015). The authors reported an average crystallite size in the range of 400 nm to 700 nm for a ZnO nanoparticle grown on copper substrate using electroplating method. However, lower average crystallite sizes were obtained for ZnO nanoparticles from leaves of *Lippia adoensis* (9-26.7 nm) (Demissie *et al*., 2020) and 30 nm for a ZnO nanoparticle prepared by chemical method (Meruvu *et al*., 2011).

Scanning electron microscopy and Energy Dispersive X-Ray spectroscopy (SEM-EDX) were also performed and the observations generally showed variable shapes with predominantly spherical and rectangular shapes in this study the particles are also found to be inclined together due to the presence of more capping agent that stabilizes the nanoparticles. Meruvu *et al* (2011) have reported similar results for ZnO nanoparticles synthesized by chemical methods.

The SEM for the ZnO nanoparticle produced from neem plant leaf and moringa leaf extracts in this study showed both nanorod and flake-type shapes in aggregated form. The aggregation/agglomeration may be caused due to polarity and electrostatic attraction of ZnO nanoparticles (Vijayakumar *et al.*, 2016).

The Energy Dispersive X-Ray spectroscopy of the samples obtained from the SEM-EDX analysis show that the sample prepared by the different plants leaf extract has pure ZnO phases The weight concentration of Zn in the different ZnO nanoparticles were 85.97, 70.84, 82.49, 87.53 and 76.89 % for neem, bitter leaf, scent leaf, moringa leaf and ginger lilly respectively. The findings corroborates with that reported for ZnO nanoparticle synthesized from leaf extract of *Lippia adoensis* (Koseret) (Demissie *et al*., 2020) and indicated that the reaction product is composed of high purity zinc nanoparticles.

The UV-Vis spectra for the synthesized ZnO nanoparticles are of strong absorbance. Strong absorbance was observed at 356 nm, 368 nm, 368 nm, 368 nm and 369 nm for ZnO nanoparticles synthesized from neem plant, bitter leaf, scent leaf, moringa leaf and ginger lily extracts respectively. The synthesized ZnO nanoparticles confirmed, in this study by the UV – vis absorption spectra, at the wavelength which is the characteristic wavelength coupled with the absence of any other absorbance peak in the spectra confirms that the synthesized products are pure ZnO nanoparticles (Salahuddin *et al*., 2015; Mohammadian *et al*., 2018; Demissie *et al*., 2020). These corroborates with ZnO nanoparticle synthesized from chamomile flower (*Matricaria chamomilla* L.), olive leaves (*Olea europaea*), and red tomato fruit (*Lycopersicon esculentum* M.) (Ogunyemi *et al*., 2019) and from leaves of *Lippia adoensis* (Demissie *et. al*., 2020). Furthermore, it is reported that the peak positions of UV-visible spectra are related with size of nanoparticles and blue shifted as the crystal size of the nanoparticles decreased (Pranjali *et al*., 2019).

The band gap are found to range from 5.38 to 5.55 eV which higher than those reported earlier (3.88 eV) (Ogunyemi *et al.,* 2019; Demissie *et al.,* 2020). The variation in band energies for the different ratios could be due to variation in average crystal size of the ZnO nanoparticles.

Microorganisms are known to be protected by a cell membrane covering them and through this membrane sufficient nutrient are transported (Jones *et al.,* 2008; Jayaseelan *et al.,* 2012). Zinc oxide nanoparticles, as an antibacterial agent, act with a series of mechanisms; in this way, cell membrane integrity loss (induced by disruption of the phospholipid bilayer) and oxidative stress (induced by reactive oxygen species generation which causes cell death by inhibiting) are two important events (Jones *et al*., 2008; Agarwal *et al.,* 2019). Zinc oxide and its related defects can be easily activated by UV and visible light, which leads to electron-hole pair generation (Shokrzadeh *et al*., 2009); the formed excitons could increase ROS concentration. Reactive oxygen species molecules could be superoxide, hydroxyl, singlet oxygen, and peroxide ions which are produced on the surface of nanoparticles and possess high electronegativity that can enhance the antimicrobial activity. For example, the generated H_2O_2 molecules can penetrate into the bacterial cell membrane inducing structural changes to membranes and hence disturbing nutrient/protein transport and causing bacteria death. OH radicals are negatively charged, and thus cannot penetrate the outer cell membrane of *E. coli*, which is also negatively charged, and remain in direct contact with the outer surface of the bacterium (Fernández *et al*., 2012; Singh *et al.,* 2016).

The activities of zinc oxide nanoparticles strongly depend on shape, size, powder concentration, specific surface area, zeta potential, and so on. For example, it is reported that zinc oxide nanoparticles with positive surface potential showed higher antimicrobial properties compared with zinc oxide nanoparticles of the same size but with negative surface potential (Arakha *et al.,* 2015). Furthermore, it is reported that small-sized nanoparticles can penetrate the bacterial membrane easily and spherically shaped zinc oxide nanoparticles release Zn^{+2} ions more effectively than rod-shaped ions (Peng *et al.,* 2011; Leung *et al.,* 2012).

Surface modifying reagent molecules result in differences in the release of Zn^{2+} ions and the production of reactive oxygen species (ROS). Moringa, scent leaf, bitter leaf, ginger lily and neem plant leaf extract contains enormous numbers of carbonyl, carboxyl, and hydroxyl groups in polyphenols and flavonoids (Shokrzadeh *et al.,* 2009; Mittal *et al.,* 2013; Liu *et al.,* 2016). These compounds present a wide range of biological activities and inflammatory and anticancer agents. Indeed, these compounds present a wide range of biological activities, and the presence of abundant hydroxyl and carbonyl groups is responsible for antibacterial applications (Mittal *et al.,* 2013; Luo *et al* 2016). The existence of these compounds in the extract and the surface helps Zinc oxide nanoparticles as observed in this study to adhere to the bacterial cell membranes. The chemical interaction between the extract molecules and zinc oxide nanoparticles enhance the reactivity of nanoparticles and improves penetration via bonding to the surface of the bacteria. Plant extract compounds attach to the surface of the bacteria and create new pathways near the surface for better transportation of or penetration by ions. For example, hydrogen in these compounds acts as both an oxidizing and a reducing agent (due to its two distinct oxidation states) which can easily form many bonds with other molecules (Wu *et al.,* 2015; Weng *et al.,* 2017).

This study shows that Moringa, scent leaf, bitter leaf, ginger lily and neem plant leaf increased the antibacterial effect of biosynthesized zinc oxide nanoparticles. In the research, zinc oxide nanoparticles (100–190 nm) were synthesized using Moringa, scent leaf, bitter leaf, ginger lily and neem plant leaf extract. The zone of their growth inhibition (6.5–11 mm) against *Staphylococcus aureus, Staphylococcus epidermidis, Klebisella* species, *Escherichia coli, Proteus* species, *Pseudomonas* species at different concentrations (1000-3500 μg/mL) varied based on the nature of the test bacteria.

However despite the novel properties of Moringa leaf, scent leaf, bitter leaf, ginger lily and neem plant, similar to many kinds of plants, its use in large amounts may exhibit toxicity as it

showed in *Sambucus ebulus* extract (Garrosa *et al.,* 2015). Briefly, it can be concluded that combining zinc oxide nanoparticles with Moringa leaf, scent leaf, bitter leaf, ginger lily and neem plant extract is a simple and safe approach for producing new materials with great potential for future biomedical and industrial applications.

CHAPTER FIVE

CONCLUSIONS AND RECOMENDATION

5.1 Conclusions

Green synthesis of metal and metal oxides nanoparticle, have been a highly attractive research area over the last decade. Numerous kinds of natural extracts have been employed as efficient resources for the synthesis and fabrication of materials, among them, plants extract has been proven to possess high efficiency as stabilizing and reducing agents for the synthesis of controlled materials .In this study, zinc oxide nanoparticles were successfully prepared through a green synthesis method using Moringa leaf, Scent leaf, Bitter leaf, Ginger lily and Neem plant leaf aqueous extract, which showed considerable properties. X-ray diffraction analysis confirmed the formation of a Zinc oxide hexagonal wurtzite structure. The UV-Visible spectrum of colloidal solutions had absorbance peaks at 356-369 nm. The Energy Dispersive X-ray spectroscopy (EDX) showed that the Zinc oxide nanoparticles of the five samples contain higher amount of Zn both in atomic concentration and in weight concentration. The prepared Zinc oxide nanoparticles exhibited high UV absorbance.

The prepared biosynthesized zinc oxide nanoparticles demonstrated efficient antibacterial effect, while surface modifying reagent molecules from the extract resulted in qualitative-subjected antibacterial activity, which may be due to the differences in the release of Zn^{2+} ions and the production of reactive oxygen species. The findings of this investigation demonstrated that biosynthesized zinc oxide nanoparticles possess promising potential in medical care, food packaging, and industrial applications as an alternative to chemical compounds.

5.2 Recommendation

People should be sensitized on the dangers associated with misuse and abuse of antibiotics. There should be an intensive and continuous monitoring of drugs that are released by the various companies. Health professionals should be directed in cases of antibiotic resistant species. Pharmaceuticals and health institution should adopt this study as it might be key to developing vaccines necessary to curb the menace caused by antibiotic resistant microorganisms. Also, the biosynthesis of metals and their oxides is likely to also be applied in the field of environmental remediation, food and cosmetic industries.

5.3 Contribution to knowledge

This study has successfully synthesized ZnO using aqueous plant leaf extract of *Azadirachta indica, Vernonia amygdalina, Ocimum gratissimum, Moringa oliefera* and *Costus afer.*

This study has confirmed the antimicrobial effect of the biosynthesized ZnO nanoparticle.

The study also revealed that at same concentration and volume of biosynthesis, sample 2(bitter leaf), sample 3(scent leaf) has higher amount in terms of quantity compared to other samples.

REFERENCES

Adams, L.K., Lyon, D.Y., & Alvarez, P.J.J. (2006). Comparative eco-toxicity of nanoscale $Ti0_2$, SiO_2, and ZnO water suspensions. *Water research*, 40, 3527-3532.

Adebayo-tayo, B., Adebayo, S., & Adebola, A. (2019). Green synthesis of silver nanoparticle using *Oscillatoria sp*. Extract, its antibacterial, antibiofilm potential and cytotoxicity activity. *Heliyon*, 5(10), Article e02250.

Agakwal, H., Menon, S., Venkat, K.S., Rajeskumar, S., David S.R., Lakshmi, T., & Deepak, N.V. (2019). Phyto-assisted synthesis of zinc oxide nanoparticles using *Cassia alata* and its antibacterial activity against *Eschericha coli*. *Biochemistry and biophysics Reports*, 17, 205-211

Anitha, R., Ramesh, K.V., Ravishankar, T.N., Sucheer, K.H., & Ramakrishnappa, T. (2018). Cytotoxicity, antibacterial and antifungal activities of ZnO nanoparticles prepared by the *Arthocurpus gomezianus* fruit mediated facile green compustion method. *Journal of science: advance materials and devices*. 3, 440-451.

Arakha, M., Saleem, M., Mallick, B.C., & Jha, S. (2015). The effects of interfacial potential on antimicrobial property of ZnO nanoparticle. *Scientific reports.* 5, 9578

Ashwini, J., Aswathy, T.R., & Achuthsankar, S.N. (2021). Green synthesis and characterization of zinc oxide nanoparticles using *Cayratia pedata* leaf extract. *Biochemistry* & *biophysics reports*, 26, 1-8

Ayandiran, D.A., Oluwafayoke, O., Okaro, G., Folasade, O.A., Olusola, N. M., Olumide, D.O., Mary, C.S., & Aderiike, G.A. (2018). Biosynthesis of Silver Nanoparticles using Almond Plant leaf extract and their Antibacterial Activity .*International Journal of Engineering Science* & *Computing,* 8(10), 19227-19231

Azizi, S., Ahmad, M.B., Namvar, F., & Mohamad, R. (2014). Green biosynthesis and characterization of zinc oxide nanoparticles using brown marine macroalga *Sargassum muticum* aqueous extract. *Materials Letters*, 116, 275-277.

Bernten, P., Park, C.Y., Rothen-Rutishauser, B., Tsuda, A., Sager, T.M., Molina, R.M., Donaghey, T.C., Alencar, A.M., Kasahara, D.I., Ericsson, T., Millet, E.J., Swenson, J., Tschumperlin, D.J., Butler, J.P., Brain, J.D., Fredberg, J.J., Gehr, P., & Zhou, E.H. (2010). Biomechanical effects of environmental and engineered particles on human airway smooth muscle cells. *Journal of the Royal Society Interface*, 7, S331-S340

Blessy baby Mathew (2014). A review on recent diseases caused by microbes, *Journal of Applied and Environmental Microbiology*, 2(4), 106-115

Bouzouraa, M.B., En Naciri, A., Moadhen, A., Rinnert, H., & Guendouz, M. (2016) Effects of silicon porosity on physical properties of zinc films. *Materials Chemistry & Physics, Elsevier*, 175, 233-240

Brayner, R., Ferari-lliou, R., Brivois, N., Djediat, S., Benedetti, M.F., & Fievet, F. (2006). Toxicological impact studies based on *Escherichia coli* bacteria in ultratine ZnO nanoparticle colodial medium. *Nano Letters*, 6, 866-870.

Cho, W.S., Duffin, R., Thielbeer, F., Bradley, M., Megson, I.L., Macnee, W., Poland, C.A., Tran, C.L., & Donaldson, K. (2012). Zeta potential and solubility to toxic ions as mechanisms of lung inflammation caused by metal/metal oxide nanoparticles. *Toxicology Sciences*, 126(2), 469–477.

Da Costa, J.P., Ana, V.G., João, P.L., Monteiro, O.C., Tito, T., & Maria Clara, C. (2013). Green synthesis of covellite nanocrystals using biologically generated sulfide: potential of bioremediated systems. *Journal of Environmental Management*, 128, 226-232.

Dada, A.O., Folahan, A.A., Fehintoluwa, E.D., Adunola, T.A., Micheal, O.B., Chidiogo, R.O., Adejumoke, A.I., Abimbola, P.O., Adeniyi, O., Kolawole, O.A., & Charles, O.A. (2019). Silver nanoparticle synthesis by *Acalypha wilkesiana* extract: phytochemical screening, characterization, influence of operational parameters, and preliminary antibacterial testing. *Heliyon*, 5(10), Article e02517

Dameron, C.T., Reese, R.N., Mehra, R.K., Kortan, A.R., Carrol, P.J., Sterigerwald, M.L., Bros, L.E., & Winge, D.R. (1989). Biosynthesis of cadmium sulphide quantum semiconductor crystallites. *Nature*, 338, 596-597.

De Berardis, B., Civitelli, G., Condello, M., Lista, P., Pozzi, R., & Arancia, G. (2010). Exposure to ZnO nanoparticles induces oxidative stress and cytotoxicology in

human colon carcinoma cells. *Toxicology & Applied Pharmacology*, 246(3), 116-127

Demissie, M.G., Sabir, F.K., Edossa, G.D., & Gonfa, B.A. (2020). Synthesis of Zinc Oxide Nanoparticles Using Leaf Extract of Lippia adoensis (Koseret) and Evaluation of Its Antibacterial Activity. *Journal of Chemistry*, 2020, Article 7459042

Dhanalakshmi, P.K., Azeez, R., Rekha, R., Poonkodi, S., & Thangaraju, N. (2012). Synthesis of silver nanoparticles using green and brown seaweeds. *Phykos*, 42(2), 39-45.

Divya, B.j., Suman, B., Venkataswamy, M., & Thyagaraju, K. (2017). A study of phytochemicals, functional groups and mineral composition of *Allium sativum* (Garlic) cloves. *International Journal of Current Pharmaceutical Research*, 9(3), 42-45

Dong, X., Potter, D., & Erkey, C. (2002). Synthesis of CuS nanoparticles in water in Carbon(iv)oxide microemulsions. *Industrial Engineering Chemistry*, 41, 4489-4493.

El-Rafie, H., El-Rafie, M., & Zahran, M. (2013). Green synthesis of silver nanoparticles using polysaccharides extracted from marine macro algae. *Carbohydrate Polymers*, 96, 403–410.

Elwy A. Mohamed (2020). Green synthesis of copper and copper oxide nanoparticles using the extract of seedless dates. *Heliyon*. 6(1), Article e03123.

Fernández, L., & Hancock, R.E.W. (2012). Adaptive and mutational resistance: Role of porins and efflux pumps in drug resistance. *Clinical Microbiology Reviews*, 25(4), 661-681

Florian, J. H., & Niederberger, .M. (2013). The fascinating world of nanoparticle research. *Materials Today*, 16, 1369-7021

Freestone, I., Meeks, N., Sax, M., & Higgitt, C. (2007). The Lycurgus cup - A Roman nanotechnology. *Gold bull*, 40, 270-277

Gade, A., Bonde, P.P., Ingle, A.P., Marcato, P., Duran, N., & Rai, M.K. (2008). Exploitation of *Asperigillus niger* for synthesis of silver nanoparticles. *Journal of Bio Based Materials & Bioenergy*, 2(3), 1-5.

Garagounis, I., Vasileois, K., Aglaia, S., Eirini, V., & Micheal, S. (2014). Electrochemical synthesis of ammonia in solid electrolyte cells. *Frontiers in Energy Research*, 2(1), 1-10

Garrosa, M., Tejero, J., Cordoba-Diaz, D., Jimenez, P., Quinto, E.J., Gayoso, M.J., & Girbes, T. (2015). Ebulin from dwarf elder (*Sambucus ebulus*): a mini review. *Toxins*, 7(3), 648-658

Gayathiri, E., Bharathi, B., & Priya, K. (2018). Study of the enumeration of twelve clinical important bacterial populations at 0.5 McFarland standard. *International Journal of Creative Research Thoughts,* 6(2), 880-893

George, S., Pokhrel, S., Xia, T., Gilbert, B., Ji, Z., Schowalter, M., Rosenauer, A., Damoiseaux, R., Bradley, K.A., Madler, L., & Nel, A.E. (2010). Use of a rapid cytotoxicity screening approach to engineer a safer zinc oxide nanoparticle through iron doping. *ACS Nano*, 4(1), 15-29.

Getie, S., Belay, A., Chandra Reddy, A.R., & Belay, Z. (2017). Synthesis and characterization of zinc oxide nanoparticles for antibacterial applications. *Journal of Nanomedicine and Nanotechnology,* S8, 004

Ghodake, G., & Lee, D.S. (2011). Biological synthesis of gold nanoparticles using the aqueous extract of the brown algae *Laminaria japonica*. *Journal of Nanoelectronics and Optoelectronics,* 6, 268–271

Godwin, A., Shri, K.M., and Balaji, M. (2015). nanoparticles and their applications- a mini review. *International Journal of Research in Engineering and Biosciences,* 3(5), 11-29

Hajipour, M. J., Fromm, K. M., Ashkarran, A. A., Parak, W. J., Aberasturi, D.J., Larramendi, .I.R., Rojo, T., Serpooshan, V., & Mahmoudi, M. (2012). Erratum: Antibacterial properties of nanoparticles .*Trends in Biotechnology*, 30, 499-511

Hangxun, X., Brad, W.Z., & Kenneth, S.S. (2013). Sonochemical synthesis of nanomaterials. *Chemical Society Reviews,* 42(7), 2555-2567

Happy, A., Venkat, K., & Rajeskvmar, S. (2017). A review on green synthesis of zinc oxide nanoparticles: An eco-friendly approach. *Resource efficient technologies,* 3, 406-413.

Hidayat, M.Y., Rosfarizan, M., Uswatun, H.Z., & Rahman, N.A. (2019). Microbial synthesis of zinc oxide nanoparticles and their potential application as an antimicrobial agent and a feed supplement: a review. *Journal of animal science & biotechnology*, 10, 57

Huang, C.C., Aronstam, R.S., Chen, D.R., & Huang, Y.W. (2010) Oxidative stress, calcium homeostasis, and altered gene expression in human lung epithelial cells exposed to ZnO nanoparticles. *Toxicology in Vitro*, 24(1), 45–55.

Hulla, J.E., Sahu, S.C., & Hayes, A.W. (2015). Nanotechnology: History and future. *Human and Experimental Toxicology*, 34(12), 1318-1321

Ibrahim, K., Khalid, S., & Idrees, K. (2019). Nanoparticles: Properties, applications and toxicities. *Arabian Journal of Chemistry*, 12, 908–931.

Iravani, S., Thota, S., & Crans D. (2018). Metal Nanoparticles: Synthesis and Applications in Pharmaceutical Sciences. *Wiley: New York, NY, USA*, 15–32.

Jha, A.K. & Prasad, K. (2010). Green synthesis of silver nanoparticles using cycas leaf. *International Journal of Green Nanotechnology: Physics & Chemistry*, 1(2), 110-117.

Joerger, R., Klaus, T. & Granqvist, G.G. (2000). Biologically produced silver-Carbon composite materials for optically functional thin-film coatings. *Advance materials Research*, 12(6), 407-409.

Jones, N., Ray, B.K.T., & Manna, A.C. (2008). Antibacterial activity of ZnO nanoparticle suspensions on a broad spectrum of microorganisms. *FEMS Microbiology Letter*, 279, 71–76

Kalabegishvili, T., Kirkesali, E., & Rcheulishvili, A. (2012). Synthesis of Gold Nanoparticles by Blue-Green Algae *Spirulina Platensis. Frank Lab. of Neutron Physics: Dubna, Russia*.

Kannan R.R.R., Arumugam, R., Ramya D., Manivannan K. & Anantharaman P. (2013). Green synthesis of silver nanoparticles using marine macroalga *Chaetomorpha linum*. *Applied Nanoscience*, 3, 229-233.

Kashyap, P.L., Kumar, S., Srivastava, A.K., & Snarima, A.K., (2013). Myconanotechnology in agriculture: a perspective. *World Journal of Microbiology & Biotechnology*, 29(2), 191-207.

Kelly, S.A., Havrilla, C.M., Brady, T.C., Abramo, K.H., & Levin E.D. (1998). Oxidative stress in toxicology; established mammalian and emerging piscine model systems. *Environ Health Perspective*, 106, 375-384.

Khadeeja, P., Viktoria, B., & Lalita, L. (2016). Green synthesis of nanoparticles: Their advantages and disadvantages. *AIP Confrence Proceeding*, 1724, 020048

Khairia, M. A. (2017). Cadmium removal from aqueous solution by green synthesis zero valent silver nanoparticles with Benjamina leaves extract. *Egyptian Journal of Aquatic Research*, 43, 269-274.

Khalil, M.M., Ismail, E.H., El-Baghdady, K.Z., & Mohamed, D. (2014). Green synthesis of silver nanoparticles using olive leaf extract and its antibacterial activity. *Arabian Journal of Chemistry*. 7, 1131–1139.

Khan, A.U., Khan, M., Malik, N., Cho, M.H., & Khan, M.M. (2019). Recent progress of algae and blue–green algae-assisted synthesis of gold nanoparticles for various applications. *Bioprocess & Biosystems Engineering*, 42, 1–15.

Khwaja, S.S., Aziz, R., Tajuddin, & Azamal, H. (2018). Properties of zinc oxide nanoparticles and their activity against microbes. *Nanoscale Research Letters*, 13(1), 141

Knoll, A.W., Pires, D., Coulembier, O., Dubois, P., Hedrick, J.L., Frommer, J., & Duerig, U. (2010). Probe-Based 3-D Nanolithography Using Self-Amplified Depolymerization Polymers. *Advanced Materials*, 22, 3361-3365.

Kocbek, P., Teskac, K., Kreft, M.E., & Kristl, J. (2010). Toxicological aspects of long-term treatment of keratinocytes with ZnO and TiO_2 nanoparticles. *Small*, 6(17), 1908–1917.

Kowshik, M., Ashtaputre, S., Kharrazi, S., Vogel, W., Urban, J., Kulkarni, S.K., & Paknikar, K.M. (2003) Extracellular synthesis of silver nanoparticles by a silver-tolerant yeast strain MKY3. *Nanotechnology*, 14(1), 95-100.

Kumar, D., and Kalita, P.(2017) Reducing Postharvest Losses during Storage of Grain Crops to Strengthen Food Security in Developing Countries. *Foods*. 6(1):8.

Kumar-Krishnan, S., Prokhorov, E., Hernández-Iturriaga, M., Mota-Morales, J.D., Vázquez-Lepe, M., Kovalenko, Y., Sanchez, I.C., & Luna-Bárcenas, G. (2015). Chitosan/silver nanocomposites: Synergistic antibacterial action of silver nanoparticles and silver ions. *European Polymer Journal*, 67, 242-251.

Kushnerova, N., Fomenko, S., Sprygin, V., Kushnerova, T., Khotimchenko, Y.S., Kondrat'eva, E., & Drugova, L. (2010). An extract from the brown alga *Laminaria japonica*: A promising stress-protective preparation. *Russian Journal of Marine Biology*, 36, 209-214.

Laerentz, L., Ample, F., Yu, H., Hecht, S., Joachim, C., & Grill, L. (2009). Conductance of a Single Conjugated Polymer as a Continuous Function of Its Length. *Science*, 323, 1193-1197.

Lakshimipriya, G., Kruthi, D., & Devarai, S.K. (2016). *Moringa oleifera*: a review on nutritive importance and its medicinal application. *Food Science & Human Wellness*, 5, 49-56

Lenz, A.G., Karg, E., Lentner, B.,Dittrich, V., Brandenberger, C., Rothen-Rutishauser, B., Schulz, H., Ferron, G.A., & Schmid, O. (2009). A dose-controlled system for air-liquid interface cell exposure and application to zinc oxide nanoparticles. *Particle & Fibre Toxicology*, 6, 32.

Leung, Y., Chan, C., Alan Man Ching, N.G., Chan, H.T., Chiang, M., Djruisic, A., Ng, Y., Jim, W., Guo, M., Leung, F., Chan, W., & Au, D. (2012). Antibacterial activity of ZnO nanoparticles with a modified surface under ambient illumination. *Nanotechnology*, 23(47), 475703

Li, X., Xv, H., Xhen, Z., & Chen, G. (2016). Biosynthesis of nanoparticles by microorganisms and their applications. *Journal of Nanomaterials*, 2011(8): 1-16.

Liu, B., Xie, J., Lee, J., Ting, Y., & Chen, J.P. (2005). Optimization of high-yield biological synthesis of single-crystalline gold nanoplates. *The Journal of Physics & Chemistry B*, 109, 15256-15263.

Liu, D., Zhou, W., & Wu, J. (2016). CuO-CeO2/ZSM-5 composites for reactive adsorption of hydrogen sulphide at high temperature. *The Canadian Journal of Chemical Engineering*, 94(12), 2276-2281

Lovine, J, Cho, S.J., Winnik, F.M., & Dusica, M. (2005). Unmodified cadmium telluride quality dot induce reactive oxygen species formation leading to multiple orgaraelle damage and cell death. *Chemistry and Biology*, 12(11), 1227-1234.

Madhiyazhagan, P., Murugan, K., Kumar, A.N., Nataraj, T., Dinesh, D., Panneerselvam, C., Subramaniam, J., Kumar, P.M., Suresh, U., & Roni, M. (2015). *Sargassum muticum*-synthesized silver nanoparticles: An effective control tool against mosquito vectors and bacterial pathogens. *Parasitology Research*, 114, 4305-4317.

Mahmoud, M.B. (2016). Nanotechnology in wastewater treatment; influence of nanomaterial on microbial systems. *International Journal of Current Microbiology Appllied Science*, 5, 713-726.

Matinise, N., Fuku, X.G., Kaviyarasu, K., Mejediva, N., & Maaza, M. (2017). ZnO Nanoparticle via *Moringa oleifera* green synthesis: physical properties & mechanism of formation. *Applied Surface Science*, 406, 339-347

Meruvu, H., Vangalapati, M., Chippada, S., & Bammidi, S. (2011). Synthesis and characterization of zinc oxide nanoparticles and its antimicrobial activity against *Bacillus subtilis* and *Escherichia coli. Rasayan Journal of Chemistry*, 4(1), 217-222

Meyer, K., Rajanahalli, P., Ahamed, M., Rowe, J.J., & Hong, Y. (2011). ZnO nanoparticles induce apoptosis in human dermal fibroblasts via p53 and p38 pathways. *Toxicology In Vitro.* 25(8), 1721–1726

Miroslav, pohanka (2019). Current trends in the biosensors for biological warfare agents assay. *Materials,* 12, 2303

Mittal, A., Muthukumar, S., Bhakya, S., Kumar, T.S., & Rao, M.V. (2015). Biosynthesis, characterization and antibacterial effect of plant –mediated silver nanoparticles using Ceropegiathwaitesii-an endemic species. *Industrial Crops & Products*, 63, 119-124

Mittal, A.K., Christi, Y., & Banerjee, U. (2013). Systhesis of metallic nanoparticles using plant extracts. *Biotechnology Advances,* 31(2), 346-356

Moabiemand, G., Barbara, N.N., Demel, T., & Oluwatoyin, D.K. (2013). Ethno-Vertinary practices amongst livestock farmers in Ngamiland District, Bostwana. *African Journal of Traditional Complementary and Alternative Medicines*, 10(3), 490-502

Moghaddam, K.M. (2010). An introduction to microbial metal nanoparticle preparation method. *Journal of Young Investigators*, 19(19), 1-7.

Mohammadian, M., Zarrin, E. & Sara, H. (2018). Green and chemical synthesis of zinc oxide nanoparticles & size evaluation by UV-vis spectroscopy. *Journal of Nanomedicine Research*, 7(1), 00175

Mohammadinejad, R., Shavani, A., Raie, D. Sangeetha, J., Soleimani, M., Shokrian, S., Thangadorai, D., Hospet, R., Popoola, J., Arzani, A., Gomez-lim, M., Iravani, S., & Varma, R., (2019). Plant molecular farming: production of metallic nanoparticles and therapeutics proteins using green factories. *Green Chemistry*, 21(8), 1845-1865.

Mohanpuria, P., Rana, N.K., & Yadav, S.K. (2008). Biosynthesis of nanoparticles: technological concepts and future applications. *Journal of Nanoparticle Research*, 10, 507-517.

Mokhtari, N., Daneshpajouh, S., Sayedbagheri, S., Attashdehghum, Res Abdi, K., Sarkar, S., Minaian, S. & Shahversi, H.R. (2009). Biological synthesis of very small silver nanoparticles by culture supernatant of *Klebsiella pneumonia*: the effect of visible-light irradiation and the liquid mixing process. *Materials Research Bulletin*, 44(6), 1415-1421.

Mourato, A., Gadauho, M., Lino, A.R., & Tenreiro, R. (2011). Biosynthesis of crystalline silver & Gold nanoparticles by Extremophilic yeasts. *Bioinorganic Chemistry & Applications*, Article 546074.

Mukherjee, P., Senapati, S., Mandal, D., Ahmad, A., Khan, M.I., Kumar, R., & Sastry, M. (2002). Extracellular synthesis of gold nanoparticles by the fungus *Fusarium oxysporum*. *Chembiochem*. 3, 461-463.

Mukherjee, S., Das, G., & Ramesh, A. (2019). A biocompatible nanocomposite tailored to endure the gastric ninche renders effective *in vitro* elimination of intestinal pathogenic bacteria and supports adhesion of beneficial bacteria. *ACS Applied Biomaterials*, 2, 3225-3233.

Murugesan, S., Bhuvaneswari, S., & Sivamurugan, V. (2017). Green synthesis, characterization of silver nanoparticles of a marine red alga *Spyridia fusiformis* & their antibacterial activity. *International Journal of Pharmacy & Pharmaceutical Sciences*, 9, 192-197.

Muthuraman, P., & Doo, H.K. (2015). In vitro toxicity of zinc oxide nanoparticles: a review. *Journal of Nanoparticle Research*, 7,158

Nair, B., & Pradeep, T. (2002). Coalescence of nanoclosters and formation of submicron crystallites assisted by *Lactobacillus* strains. *Crystal Growth & Design*, 2(4), 293-298.

Nazanin, R., Richard, H., Roya, K., & Rainer, S. (2013). Zinc and its importance for human health: an integrated review. *Journal of Research in Medical Science*, 18(2), 144-157

Novoselov, K.S., Geim, A.K., Morozov, S.V., Jiang, D., Zhang, Y., Dubonos, S.V., Grigorieva, I.V., & Firsov, A.A. (2004). Electric field effect in atomically thin carbon films. *Science*, 306, 666–669.

Ogunyemi, S.O., Abdallah, Y., Zhang, M., Hong, X., Ibrahim, E., Masum, M.I., Hossain, A., Li, B. & Fouad, H. (2019). Green synthesis of zinc oxide nanoparticles using different plant extracts and their antibacterial activity against *Xanthomonas oryzea* pv. oryzae. *Artificial cells, Nanomedicine & Biotechnology,* 47, 341-352

Olabemiyo, O.M., Waheed, A.A., Okunlola, D.S., Akinwale, D.R., Adeyinka, G.C., Adeniji, T.W., & Akintelu, S.A. (2021). Green synthesis, characterization and preliminary antimicrobial study of nanoparticles using extract of stem bark of *Annona senegalensis*. *Nanoplus: Science & Technology of Nanomaterials,* 1, 3-78

Oyeniyi, Y.J., & Mumuni, A.M. (2021). Formulation development of an herbal hand sanitizer containing *Moringa oleifera* silver nanoparticles. *Nanoplus: Science & Technology of Nanomaterials,* 1, 3-78

Palaniyandi, V., Govindarajan, V.K., Venkadapathi, J., Jayabrata, D., & Raman, P. (2016). Bio-inspired green nanoparticles: Synthesis, mechanism and antibacterial application. *Toxicology Research,* 32(2), 95-102

Palomaki, J., Karisola, P., Pylkkanen, L., Savolainen, K., & Alenius, H. (2010). Engineered nanomaterials cause cytotoxicity and activation on mouse antigen presenting cells. *Toxicology,* 267(1-3), 125-131

Parial, D., & Pal, R. (2015). Biosynthesis of monodisperse gold nanoparticles by green alga Rhizoclonium and associated bischemical changes. *Journal of Applied Phycology*, 27(2), 975-984.

Pati, R., Mehta, RK., Mohanty, S., Padhi, A., Sengopta, M., Vasseeharan, B., Goswami, C., & Sonawane, A. (2014). Topical application of zinc oxide nanoparticels reduces bacterial skin infection in mice and exhibit antibacterial activity by inducing oxidative stress response and cell membrane disintegration in macrophages. *Nanomedicine: Nanotechnology, Biology & Medicine*, 10(6), 1195-1208.

Peng, X., Palma, S., Fisher, N.S., & Wong, S.S. (2011). Effects of morphology of ZnO nanostructures on their toxicity to marine algae. *Aquatic Toxicology,* 102, 186-196

Petersen, P., Tikhomirov, G., & Qian, L. (2018). Information-based autonomous reconfiguration in systems of interacting DNA nanostructures. *Nature Communications*. 9, 5362.

Piner, R.D., Zhu, J., Xu, F., Hong, S., & Mirkin, C.A. (1999). "Dip-Pen" nanolithography. *Science,* 283, 661–663.

Prakash, J., Vignesh, K., Anusuya, T., Ramachandran, C., Sudha, Rani R., Momna, R., Imran, K., Fazie, E., Deog-Hwan, O., & Devanandvenkatasubbu, G. (2019). Application of nanoparticles in food preservation and food processing. *Journal of Food Hygiene & Safety*, 34(4), 317-324

Pranjali, P.M., Pooja, M.P., Manohar, B., Pratiksh, P., Bhagyashi, S.T., Abhay, P., & Raghvendra, A.B. (2019). Biofilm formation to inhibition: Role of zinc oxide-based nanoparticles. *Materials Science and Engineering: C.* 108, 110319

Prasad, K., Tha, A.K., & Kulkarni, A.R. (2007). Lactobacillus assisted synthesis of titanium nanoparticles. *Nanoscale Research Letters*, 2(5), 248-250.

Prasad, V.K.V., Subba Rao Kambala, V., & Naidu, R. (2011). A critical review on biogenic silver nanoparticles and their antimicrobial activity corr. *Journal of Nanoscience & Nanotechnology*. 7(4), 531-544.

Prathna, T.C., Mathew, L., Chandrasekaran, N., Ashok, M.R., & Amitav., M. (2010). Biomimetic synthesis of nanoparticles; science, technology and applicability. *Biomimetics learning Nature,* 10, 1-20.

Priyadharshini, R.I., Prasannaraj, G., Geetha, N., & Venkatachalam, P. (2014). Microwave-mediated extracellular synthesis of metallic silver and zinc oxide nanoparticles using macro-algae (*Gracilaria edulis*) extracts and its anticancer activity against human PC3 cell lines. *Applied Biochemitry & Biotechnology*. 174(8), 2777–2790.

Rai, M., Yadav, A., Bridge, P., & Gade, A. (2009). Myconanotechnology: a new and emerging science in applied mycology. *CAB International publishers, New York*, 258-267.

Rajeshkumar, S., Kannan, C., & Annadurai, G. (2012). Synthesis and characterization of antimicrobial silver nanoparticles using marine brown seaweed *Padina tetrastromatica*. *Drug Invention Today*, 4, 511–513.

Rajeskumar, S., & Rinitha, G. (2018). Nanostructural characterization of antimicrobial and antioxidant copper nanoparticles synthesized using novel *Persea Americana* seeds. *Opennano*, 3, 18-27

Rajeskumar, S., Mlarkodi, C., Gnanajobitha, G., Paulkomar, K., Vanaja, M., & Kanan, C. (2013) Seaweed mediated synthesis of Gold nanoparticles using *Turbinaria conodies* and its characterization. *Journal of Nanostructure in Chemistry*. 3(44), 2-7.

Ramakritinan, C., Shankar, S., Anand, M., & Kumaraguru, A. (2020). Biosynthesis of silver, gold and bimetallic alloy (Ag: Au) Nanoparticles from green alga, *Lyngpya* sp. *In Proceedings of the 3rd National Conference on Nanaomaterials and Nanotechnology, Lucknow, India,* 21–23 December, 174–187

Rao, P.S., Mantri, V.A., & Ganesan, K. (2007). Mineral composition of edible seaweed *Porphyra vietnamensis*. *Food Chemistry*. 102, 215–218.

Rikans, L.E., & Hornbrook, K.R. (1997). Lipid peroxidation, antioxidant protection and Aging. *Biochimica et Biophyssica Acta*, 1362, 116-127.

Ruman, P., Kadarkarai, M., Angelo, C., & Giovanni, B. (2017). *Saponaria offinalis*-synthesized silver nanocrystals as effective biopesticides and oviposition inhibition against *Tetranychus urticae* Koch. *Industral Crops and Products*, 97, 338-344.

Sabir, S., Muhammad, A., & Sunbal, K.C. (2014). Zinc oxide nanoparticles for revolutionizing agriculture: synthesis and applications. *The Scientific World Journal*, Article 925494.

Saiqa, I., Shakeel, A., Ahmad, M. & Swami, B.L. (2016). Green synthesis of silver nanoparticles using *Azadirachta indica* aqueous leaf extract. *Journal of Radiation Research and Applied Sciences*, 9, 1-7

Salahuddin, N.A., El-Kemary, M., & Ibrahim, E.M. (2015). Synthesis and characterization of ZnONPs via precipitation method: effects of annealing temperature on particle size. Journal of *Nanoscience and Nanotechnology*, 5(4), 82-88

Samer, B., Muhammad, A., Tiziano, T., Macro, C., & Flavio, R. (2020). The history of nanoscience and nanotechnology: from chemical-physical applications in nanomedicine. *Molecules,* 25, 112

Sangeetha, G., Rajeshwari, S., & Venekatesh, R. (2012). Green synthesis ZnO nanoparticles against bacterial and fungal pathogens. *Progress in Natural Science: Materials International*, 22, 693-700

Santhoshkumar, J., Venkat, S., & Rajeskumar, S. (2017). Synthesis of zinc oxide nanoparticles using plant leaf extract against urinary tract infection pathogen. *Resource-Efficient Technologies*, 3, 459-465

Sara, Z., Asma, A., Mohammad, U.J., Saima, M., Mohammad, H.S., Sidra, A., Rahat, A., Khalid, A.A., Fahad, A., Zubair, A., & Shahid, M. (2020). Eco-friendly synthesis of antibacterial zinc nanoparticles using *Sesanium indium* L. extract. *Journal of king Saud University-Science*, 32, 1116-1122

Sathish, B., & Satyanarayana, T. (2018) A review on Characterization techniques of Nanomaterials. *International Journal of Engineering, Science and Mathematics,* 7(1), 169-175

Satyanarayana1, T. & Reddy, S.S. (2018). A Review on Chemical and Physical Synthesis Methods of Nanomaterials. *International Journal for Research in Applied Science & Engineering Technology*, 6, 2321-9653

Sawani, J., Shoji, S., Lgarashi, H., Hashimoto, A., Kokugan, T., Shinmizu, M., & Kojima, H. (1998). Hydrogen peroxide as an antibacterial factor in Zinc oxide power slurry. *Journal of Fermentation & Bioengineering*, 86, 521-522.

Seshadri, S., Saranya, K., & Kowshik, M. (2011). Green synthesis of lead sulfide nanoparticles by the lead resistant marine yeast, *Rhodosporidium diobovatum*. *Biotechnology Progress,* 27(5), 1464-1469.

Shahram, S.K., Hamed, T., & Mojdeh, J. (2021) Coexistence of virulence factors and efflux pump genes in clinical isolates of *Pseudomonas aeruginosa*: analysis of biofilm-forming strains from Iran. *International Journal of Microbiology*, Article 5557361

Shao, Y., Jin, Y., & Dong, S. (2004). Synthesis of gold nanoparticles by Aspartate reduction of Gold Chloride. *Chemical Communications (Cambridge, England)*, 10, 1004-1105.

Sharad, S. Sankhe. (*2017*). Green Synthesis of ZnO Nanoparticles Using Leaves of *Trachyspermum ammi* and *Citrus aurantifolia***.** *International Journal for Research in Applied Science & Engineering Technology,* 8, 2321-9653

Sharma, N., Pinnaka, A.K., Raje, M., Ashish, F., Bhattacharyya, M.S., & Choudory, A.R. (2012). Exploitation of marine bacteria for production of gold nanoparticles. *Microbial Cell Factories,* 11(1), 86

Sharmila, D. R., & Gayathri, R. (2014). Green synthesis of zinc oxide nanoparticles by using *Hibiscus rosa-sinensi*. *International Journal of Current Engineering and Technology*, 4(1), 1137

Shokrzadeh, M., Saeedi Saravi, S.S., & Mirzayi, M. (2009). Cytotoxic effects of ethyl acetate extract on *Sambucus ebulus* copared with etopo-side on normal and cancer cell lines *Pharmacognosy Magazine,* 5(20), 316-319

Shuaixuan, Y., Zhenru, G., Polycarp, C. O., Preston, C., Cyren, R., Feng, He., and Jie, H. (2022). Green synthesis of nanoparticles: Current developments and limitations, *Environmental Technology & Innovation*, 26: 102336.

Siavash Iravani (2014). Bacteria in Nanoparticle synthesis: current status and future prospects. *International Scorlarly Research Notices,* Article 359316.

Siddhant, J., & Mohan, S.M. (2017). Medicinal plant leaf extract and pure flavonoid mediated green synthesis of silver nanoparticles and their enhanced antibacterial property. *Scientific report,* 7, 15867

Siddiqi, K.S., Rahman, A., & Husen, A. (2018). Properties of Zinc Oxide Nanoparticles and Their Activity Against Microbes. *Nanoscale Research Letters*, 13, 141

Singaravelu, G., Arockiamary, J., Kumar, V.G., & Govindaraju, K.A. (2007). Novel extracellular synthesis of monodisperse gold nanoparticles using marine alga, *Sargassum wightii* Greville. *Colloids & Surfaces B: Biointerfaces,* 57, 97-101.

Singh, A., Gautam, P.K., Verma, A., Singh, V., Shivapriya, P.M., Shivalkar, S., Sahoo, A. K., & Samanta, S.K. (2020). Green synthesis of metallic nanoparticles as effective alternatives to treat antibiotics resistant bacterial infections: A review. *Biotechnology Reports*, 25, Article e00427

Singh, B.N., Prateeksha, D., Upreti, D.K., Singh, B.R., Defoirdt, T., Gupta, V.K., De Souza, A.O., Singh, H.B., Barreira, I.C., Ferreria, I.C., & Vahabi, K. (2016). Bactericidal, quorum quenching and anti-biofilm nanofactories: A new ninche for nanotechnologists. *Critical Reviews in Biotechnology,* 37, 1-6

Singh, J., Dutta, T., Kim, KH. Kim, K., Rawat, M., Samddar, P., & Kuma P. (2018). Green synthesis of metals and their oxide nanoparticles: applications for environmental remediation. *Journal of Nanobiotechnology*, 16, 84

Singh, M., Kalaivani, R., Manikandan, S., Sangeetha, N., & Kumaraguru, A. (2013). Facile green synthesis of variable metallic gold nanoparticle using *Padina gymnospora*, a brown marine macroalga. *Applied Nanoscience*, 3, 145-151.